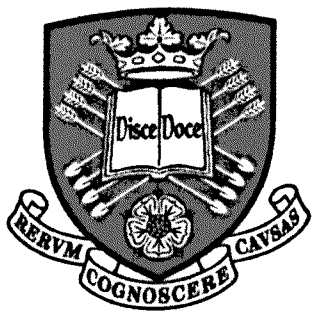

The University Of Sheffield.

DYNAMIC MODELLING AND CONTROL OF A FLEXIBLE MANOEUVRING SYSTEM

by

Fareg Mohamed Aldbrez

A thesis submitted to the University of Sheffield for the degree of
Doctor of Philosophy

Department of Automatic Control and Systems Engineering
The University of Sheffield
Mappin Street
Sheffield, S1 3JD
UK

February 2007

ABSTRACT

In this research a twin rotor multi-input multi-output system (TRMS), which is a laboratory platform with 2 degrees of freedom (DOF) is considered. Although, the TRMS does not fly, it has a striking similarity with a helicopter, such as system nonlinearities and cross-coupled modes. Therefore, the TRMS can be perceived as an unconventional and complex "air vehicle" that poses formidable challenges in modelling, control design and analysis, and implementation. These issues constitute the scope of this research.

Linear and nonlinear models for the vertical movement of the TRMS are obtained via system identification techniques using black-box modelling. The approach yields input-output models without a priori defined model structure or specific parameter settings reflecting any physical attributes of the system. Firstly, linear parametric models, characterising the TRMS in its hovering operation mode, are obtained using the potential of recursive least squares (RLS) estimation and genetic algorithms (GAs). Further, a nonlinear model using multi-layer perceptron (MLP) neural networks (NNs) is obtained. Such a high fidelity nonlinear model is often required for nonlinear system simulation studies and is commonly employed in the aerospace industry. Both time and frequency domain analyses are utilised to investigate and develop confidence in the models obtained. The frequency domain verification method is a useful tool in the validation of extracted parametric models. It allows high-fidelity verification of dynamic characteristics over a frequency range of interest. The resulting models are utilized in designing controllers for low frequency vibration suppression, development of suitable feedback control laws for set-point tracking, and design of augmented feedforward and feedback control schemes for both vibration suppression and set-point tracking performance. The modelling approaches presented here are shown to be suitable for modelling complex new generation air vehicles, whose flight mechanics are not well understood.

Modelling of the TRMS revealed the presence of resonance modes, which are responsible for inducing unwanted vibrations in the system. Command shaping

control strategies are developed to reduce motion and uneven mass induced vibrations, produced by the main rotor during the vertical movement around the lateral axis of the TRMS rig. 2-impulse, 3-impulse and 4-impulse sequence input shapers and low-pass and band-stop digital filters are developed to shape the command signals such that the resonance modes are not overly excited. The effectiveness of this concept is then demonstrated in both simulation and real-time experimental environments in terms of level of vibration reduction using power spectral density profiles of the system response.

Combinations of intelligent and conventional techniques are commonly used the control of complex dynamic systems. Such hybrid schemes have proved to be efficient and can overcome the deficiencies of conventional and intelligent controllers alone. The current study is confined to the development of two forms of hybrid control schemes that combine fuzzy control and conventional PID compensator for input tracking performance. The two hybrid control strategies comprising conventional PD control plus PID compensator and PD-type fuzzy control plus PID compensator are developed and implemented for set-point tracking control of the vertical movement of the TRMS rig. It is observed that the hybrid control schemes are superior to other feedback control strategies namely, PID compensator, pure PD-type and PI-type fuzzy controllers in terms of time domain system behaviour.

This research also witnesses investigations into the development of an augmented feedforward and feedback control scheme (AFFCS) for the control of rigid body motion and vibration suppression of the TRMS. The main goal of this framework is to satisfy performance objectives in terms of robust command tracking, fast system response and minimum residual vibration. The developed control strategies have been designed and implemented within both simulation and real-time environments of the TRMS rig. The employed control strategies are shown to demonstrate acceptable performances. The obtained results show that much improved tracking is achieved on positive and negative cycles of the reference signal, as compared to that without any control action. The system performance with the feedback controller is significantly improved when the feedforward control component is added. This leads to the conclusion that augmenting feedback control with feedforward method can lead to more practical and accurate control of flexible systems such as the TRMS.

ACKNOWLEDGEMENT

All praise and glory are due to Almighty Allah, the sole Lord of the universe, Whose mercy and blessings have been bestowed constantly upon the author. Peace and blessings be upon His final messenger Mohammad.

I would like to express my deepest gratitude to my supervisor Dr. M. Osman Tokhi for his affectionate supervision, assistance, motivation and encouragement throughout this work. His friendly approach and unbound patience have left a deep impression upon me.

It gives me great pleasure to appreciate and thank my fellow research colleagues for their help and support in this work. My thanks go to Dr. Zaharuddin Mohamed, Dr. M. Abbod, Mohd. Shafiul Alam, Mohd. Saiful Huq, Md. Zain, Rasha Massud, Hector Marin-Reyes and Omar Shaebi. Their technical discussion and encouragement have been highly beneficial to my work.

I would also like to thank the departmental staff, specially, Mr. C. Bacon, Mr. I. Durkacz, Ms. R. Beech, Ms. A. Satur, Ms. A. Ashe, Ms. A. Kisby, Mr. D. Fox, Mr. P. Staniforth and Mr. A. Price for their support.

My heartiest thanks also to all of my teachers and colleagues throughout my primary-university education for their love and respect, specially, those who tried to keep me motivated by contacting me through phone and emails from time to time.

The financial support of the Ministry of Higher Education in Libya is gratefully acknowledged. I also appreciate and thank Mr. Jamal Al-Miladi, Asanoussi Emhmed and other colleagues at the department of Culture Affairs of the Libyan Embassy in London for their administrative support throughout my study.

Finally, I am indebted and thankful to my day-to-day sacrifice, love and patients my wife Mariam and three daughters Eman, Noor Ulhuda and Fatma Azzahara. I am also deeply indebted and thankful to my mother Fatema Aljehawi, my brother Abdallah, my sisters Salha and Aisha and all other family members, relatives and friends for their prayers and loving support.

LIST OF FIGURES

LIST OF TABLES

CONTENTS

CHAPTER 1

INTRODUCTION

1.1 Background

Recent developments in sensor technology, data processing hardware, and software algorithms have made the use of robotic aircraft or uninhabited aerial vehicles (UAVs) a highly feasible approach to achieve a variety of aerial mission objectives at lower risk and cost. Research interest in UAVs has increased importance in recent years. Unmanned air vehicle means that a human is not onboard actively piloting or directing the aircraft. The control functions are either on-board or off-board (computer or remote pilot). There is a broad spectrum of UAVs, differing in size, type, capabilities and complexity. They range from the piezo electrically actuated flying insect that attempts to mechanically emulate the flapping wing motion of an insect and Micro-UAVs, which are as small as 15 cm and weigh just 90 g (Harvey, 1997), to the USAF Unmanned Combat Aircraft (UCAV) and Global Hawk (Warwick, 2000).

Unmanned autonomous aerial vehicles have been found indispensable for various applications where human intervention is considered difficult or dangerous. UAV technology has the potential for use in many applications such as aerial surveys, meteorological data collection, autonomous target identification, close-up inspection of power lines and bridges, terrain surveying, cinematography and aerial mapping, surveillance, law enforcement and border patrol and oceanography. Additionally, the UAV provides an inexpensive and efficient experimental platform for flight control and planning research. Carnegie-Mellon University have tested an unmanned helicopter in the Arctic to examine Haughton Crater's rock and conducted other experiments to asses the crater and its environs. This UAV was designed to create three dimensional maps using lasers and satellite data for further geological studies (Long, 1999). Aerosonde's robotic aircraft was developed primarily for meteorological and environmental reconnaissance over oceanic and remote areas and in harsh environments (http:// www.aerosonde.com). It has been flight tested across

the Atlantic ocean and Alaska for use in environment related research. In short, they are expected to carry out difficult and dangerous tasks. The advantages outlined above have led to a burst of activity in this arena. It is important to note that there are few operational UAVs and fewer still available for academic research; most current UAVs have been developed for military applications.

The significant features of these endeavours have included the introduction of innovative design, fascinating structural materials and sophisticated control paradigms. This is a striking departure from the classical systems engineering philosophy. The assimilation of the above in systems development has led to systems, which are sophisticated, accurate and robust. For instance, soft computing techniques such as neural networks (NNs), fuzzy logic (FL), and genetic algorithms (GAs), have been employed to address a range of engineering issues, such as modelling, optimisation, control, guidance, and fault-diagnosis. These advances have also come at a cost and the penalties imposed are complex systems with little historical data, no exhaustive literature or proven track record. An unconventional system configuration means that considerable efforts are required to develop new mathematical models, especially in case of air vehicles. In flexible or elastic structures the added complexity of the control problem is due to the inherently lightly damped nature of the structure, which causes vibration in the system. Control of modern systems with flexible modes is rather daunting and necessitates knowledge of a broad range of control methodologies.

1.2 Research developments

The vast majority of modern systems incorporate the latest light weight material, smart sensors and complex control paradigms, in order to facilitate characteristics such as greater payload capability for a given structure, high manoeuvrability and a fast speed of response. Therefore, system design, modelling and control design and analysis of such systems are non-trivial and entail multi-disciplinary expertise from domains such as aerodynamics, control, structures, sensors and electronic hardware.

The current research focuses on challenges associated with contemporary systems in terms of:

1) Modelling and model analysis.

2) Control design, analysis and implementation.

1.2.1 Soft computing techniques for modelling and control

Suitable plant models are always required for the ensuing control design and analysis. After the design process, the most daunting task is to develop a working model. Construction of a mathematical model that perfectly describes the dynamics of a physical system using traditional analytical method is generally possible for simple systems. However, with the increasingly complex nature of systems with complex dynamics and highly non-linear behaviour, modelling of such systems based on first principle rules is often a formidable and undesirable task (Ljung and Söderström, 1983). Thus, the utility of mathematical modelling to fairly complex plants is limited. On the other hand, system identification, which is an experimental technique used for obtaining mathematical model of a dynamic system based on observed input and output data, has proven to be an excellent tool to model complex processes such as aerospace structures where it is not possible to obtain reasonable models using only physical insight (Ljung, 1987). Generally, the procedure of identification entails a matching between the system output and an estimated output. In the process of identification a suitable model is developed that exhibits the same input/output characteristics as the controlled plant (Tokhi and Leitch, 1992). Once a model of the physical system is obtained, it can be used for solving various problems such as, to control the physical system or predict its behaviour under different operating conditions.

Important applications of system identification are visible in areas that require higher accuracy of the mathematical model for simulation, validation, control system design and handling qualities such as aerospace applications (Vandersteen *et al.*, 1996; Ahmad *et al.*, 2002). It provides an accurate, rapid and reliable approach for defining design specifications and for validating control systems. System identification, used to construct a model to represent a given system, plays an important role in system analysis, control and prediction. Identification of systems

has drawn a great deal of interest because of the increasing need in estimating the behaviour of a system with partially known dynamics. Especially in the areas of control, pattern recognition and even in stock markets the system of interest needs to be known to some extend.

In many cases when it is difficult to obtain a model structure for a system using traditional system identification approaches, soft computing techniques may be used to describe the system in the best possible way (Elanayar and Yung, 1994). Genetic algorithms (GAs), neural networks (NNs), fuzzy logic (FL), and neuro-fuzzy inference system (ANFIS) are forms of soft computing techniques commonly used for system identification and modelling. They are excellent in pattern recognition and in determining models that best represent the behaviour of non-linear systems that might be difficult to obtain using traditional approaches (Roberts *et al.*, 2003; Shaheed, 2000; Sowerby *et al.*, 2005). The following subsections highlight the applications of NN, FL and GA techniques in the area of modelling and control.

1.2.1.1 Neural networks

Neural networks offer many advantages over traditional ones especially in terms of flexibility and hardware realisation (Ljung and Sjöberg, 1992). The application of NNs has attracted significant attention in several disciplines, such as signal processing, identification and control. Neural networks possess an inherent nonlinear structure suitable for mapping complex characteristics, learning and optimization (Hornik *9*, 1989; Rumelhart and McClelland, 1986; Widrow and Laher, 1990). These features have recently been shown to have considerable potential for modelling and control of nonlinear dynamic systems (Miller *et al.*, 1990; Narendra and Parthasarathy, 1990 and 1991; Thapa *et al.*, 2000). This fundamental link of NNs to nonlinear system representation, together with the availability of reliable and inexpensive computing hardware, has resulted in a tremendous growth of research and development in the area. The limitation of many of the conventional control schemes for nonlinear systems is another important reason for the interest in neural designs (Miller *et al.*, 1990).

Mistry and Nair (1994) considered real-time neural identification and control designs using multi-layer perceptron (MLP) feedforward networks and reported

implementation results using a single-input single-output (SISO) hardware example case study with both time-varying and time-invariant load dynamics. The obtained results illustrated that neural designs are shown to be experimentally viable for on-line identification and control. Dynamic neural schemes were also found to consistently perform much better as compared to the static schemes. Reduced order linear observers were also being investigated for use in dynamic schemes for the time-invariant load case to improve convergence and learning features as compared to the static cases (Mistry *et al.*, 1996). Henriques *et al.* (1999) applied a combination of a modified recurrent Elman network with a truncated backpropagation through time (BTT) algorithm for modelling non-linear plants. This approach has proved through experiments on a laboratory plant, to be a feasible alternative for real-time identification. In this context, given the adaptive features revealed by the Elman networks has also implied their ability for modeling any kind of non-linearities in the form of non-linear state space representation. Dynamic recurrent neural networks (DNNs) are bringing a valuable added-value to the control field and particularly to those strategies using an explicit model of the plant to be controlled. Efe and Kaynak (2000) have reported identification of robotic manipulators using NNs and ANFIS. Arai *et al.* (1994) have reported modelling and trajectory control of flexible plate structures using NNs and Sharma (2000) has reported NNs for dynamic modelling and control of a flexible manipulator.

The first application of NNs to control systems was developed in the mid-1980s. Models of dynamic systems and their inverses have immediate utility in control. In the literature on neural networks, architectures for the control and identification of a large number of control structures have been proposed and used (Miller *et al.*, 1990; Narendra and Parthasarathy, 1990). Artificial NNs, which have the ability to approximate general continuous nonlinear functions, are also ideal for the adaptive flight control application (Hornik *et al.*, 1989; Sanner and Slotine, 1992).

One advantage of the NN over simple lookup table approaches is the reduced amount of memory and computation time required. In addition, the NN can provide interpolation between training points with no additional computational effort. Furthermore, experience has shown that NNs function as highly nonlinear adaptive

control elements and offer distinct advantages over more conventional linear parameter adaptive controllers in achieving desired performance.

The literature includes numerous applications of NN to flight control systems. Applications in which NN are used to control super-manoeuvrable aircraft are described by Baker and Farrel (1991), and by Steck and Rokhaz (1992). Survey papers commenting on the role of NN technology in flight control system design have been contributed by Werbos (1995) and Steinberg (1994). Examples of applications to helicopters and tilt-rotors aircraft may be found in (Jiang *et al.*, 1996; Leitner *et al.*, 1997; Rysdyk and Calise, 1998; Rysdyk *et al.*, 1997). Baker and Farrel (1991) motivated and described an approach for the design and development of a learning augmented flight control system for high performance aircraft. Troudet *et al.*, (1991) designed a model following neuro-controller for integrated airframe linearized model of a modern fighter aircraft. Calise (1996) presented an on-line adaptive architecture that employed an NN to compensate for inversion error present when feedback linearization methods are employed to control a dynamic process (fighter aircraft). A stable weight adjustment rule for the NN was presented, and they used on-line adaptation approach and employed concepts from (Sanner and Slotine, 1992), wherein the dynamics are linear in the control variable. Kaneshige and Gundy-Burlet (2001) presented an Integrated Neural Flight and Propulsion Control System (INFPCS), which used an NN based approach for applying alternate sources of control power in the presence of damage or failures. Under normal operating conditions, the system utilized conventional flight control surfaces. Neural networks were used to provide consistent handling qualities across flight conditions and for different aircraft configurations. Under damage or failure conditions, the system utilized unconventional flight control surface allocations, along with integrated propulsion control, when additional control power was necessary for achieving desired flight control performance. In that case, NNs were used to adapt to changes in aircraft dynamics and control allocation schemes. The neural flight control architecture was based upon the augmented model inversion controller, developed by Rysdyk and Calise (1998). This direct adaptive tracking dynamic inverse controller integrates feedback linearization theory with both pre-trained and on-line learning NNs. Piloted simulation studies were performed at NASA Ames Research Centre on a commercial transport aircraft simulator. The obtained results demonstrated the

potential for improving handling qualities and significantly increasing survivability rates under various simulated failure conditions. Of significant importance here is the fact that this system can operate without emergency or backup flight control mode operations. An additional advantage is that this system can utilize, but does not require, fault detection and isolation information or explicit parameter identification.

1.2.1.2 Fuzzy logic

Conventional control system design is predominantly based upon the development of mathematical models, which attempt to describe the dynamic behaviour of the system in question using typically, differential equations. Many such methods of system design have been developed over time, including three-term Proportional, Integral, Derivative control (PID control), root-locus design, state-space, Nyquist, Bode and optimal control offering a variety of ways in which good controller design may be achieved (Passino and Yurkovich, 1998; Smuts, 2002).

Due to the continuously developing automation systems and more demanding control performance requirements, conventional control methods are not always adequate. On the other hand, practical control problems are usually imprecise and the input-output relations of the system may be uncertain and they can be changed by unknown external disturbances. New schemes are, thus, needed to solve such problems. Increased mathematical complexity required for conventional modelling techniques thus led to the application of intelligent control techniques such as neural networks, fuzzy logic and genetic algorithms to support control systems design and optimization. The use of fuzzy logic controllers has steadily grown among industrial users (Lopez-Toribio *et al.*, 2000; Omerdic and Roberts, 2003).

Most of classical design mythologies such as Nyquist, Bode, state-space, optimal control, root locus, H_∞ and μ-analysis are based on assumptions that the process is linear and stationary and hence is represented by a finite dimensional constant coefficient linear model. Hence, such methods do not suit complex systems well because few of those represent uncertainty in process knowledge or complexity in design. But, in the real world many industrial processes are highly nonlinear and complex. As the complexity of a system increases, quantitative analysis and precision become more difficult. The control of such complex and nonlinear

processes has been approached in recent years using fuzzy logic techniques. During the past several years, fuzzy control has emerged as one of the most active and powerful areas of research in applications of such complex and real world systems.

Since the introduction of the theory of fuzzy sets by Zadeh in 1965, and the industrial application of the first fuzzy controller by Mamdani in 1974, fuzzy systems have assumed a major role in engineering systems and consumer products. Theoretical results (Choi *et al.*, 2000; Driankov *et al.*, 1996; Hu *et al.*, 2001; Lee, 1990; Lin and Lee, 1996) and applications (Jain *et al.*, 1999; Cohen *et al.*, 2002; Kumbla and Jamshidi, 1994; Von Altrock, 1995) are presented continuously. A reason for this significant role is that fuzzy logic provides a flexible and powerful alternative to construct controllers, supervisory blocks, computing units and compensation systems in different application areas (Driankov *et al.*, 1996). With fuzzy sets very nonlinear control actions can be formed easily. The transparency of fuzzy rules and the locality of parameters are helpful in the design and maintenance of systems (Jager, 1995). Therefore, preliminary results can be obtained within a short development period.

Fuzzy systems are indicating good promise in consumer products, industrial and commercial systems, and decision support systems. The term "fuzzy" refers to the ability of dealing with imprecise or vague inputs. Instead of using complex mathematical equations, FL uses linguistic descriptions to define the relationship between the input information and the output action. In engineering systems, FL provides a convenient and user-friendly front-end to develop control programs, helping designers to concentrate on the functional objectives, not on the mathematics.

FLC has been successfully applied in the control of various physical processes (Jnifene and Andrews, 2005; Lai and Lin, 2003; Pedrycz, 1991; Sugeno, 1985). Most commercial fuzzy products are rule-based systems that receive current information in the feedback loop from the device as it operates and control the operation of a mechanical or other device (Simoes and Friedhofer, 1997; Simoes and Franceschetti, 1999).

Application of fuzzy logic control (FLC) in the domain of PID control has been, in general, used to augment existing PID controller operation or replacement of

PID by FL controller (Bandyopadhyay *et al.*, 2001; Hu *et al.*, 2001; Karr, 1991; Li, 1998). Increased technology sophistication, and use of microprocessors have enabled the development of fuzzy-PID hybrid systems, where FLC is used to adaptively tune the parameters of conventional PID controllers (Bandyopadhyay *et al.*, 2001), and replacement of PID controller with FL controller (Karr, 1991). Visioli (2001) used FLC to implement supervisory control by auto-tuning PID controller gains in order to adapt/optimize system performance of the controller in response to changing operating conditions. Fuzzy controllers have also been used in industrial and research applications where their use has conferred improved system performance, or where a mathematical process model is intractable.

1.2.1.3 Genetic algorithms

Genetic algorithms (GAs) are search algorithms that are based on the mechanics of natural selection and natural genetics (Goldberg, 1989). They perform a global, random, parallel search for an optimal solution using simple computations. Starting with an initial population of genetic structures, genetic inheritance operations based on selection, mating, and mutation are performed to generate "offspring" that compete for survival to make up the next generation of population structures. The benefit of this technique is that it searches for a solution from a broad spectrum of possible solutions, rather than restrict the search to a narrow domain where the results would be normally expected (Fleming and Purshouse, 2002). Genetic algorithms try to perform an intelligent search for a solution from a nearly infinite number of possible solutions.

The application of GA to black-box and grey-box model identification has received considerable interest since the seminal paper by Kristinsson and Dumont (1992). The authors applied GA to the system identification of both continuous- and discrete-time systems. The technique employed can be used in online as well as off-line applications. The GA was used to directly identify poles and zeros, or to obtain the values of physical parameters. The cost function used was the error between the estimated and actual output over a window of data, which consisted of the current input–output pair and the previous 30 samples. For each sample point, the population was evolved for a further three generations. Kristinsson and Dumont reported

comparable or better results to well-known techniques, but noted the high computational expense incurred.

GA has been extensively applied to the off-line design of controllers. It has been used to obtain controller parameters (for various classes of controller), or controller structure, or occasionally both. GA has also been combined with fuzzy and neural controllers to form an intelligent control scheme. An early use of GA was as an alternative means of tuning proportional-integral-derivative (PID) controllers. Oliveira *et al.* (1991) used a standard GA to determine initial estimates for the values of PID parameters. They applied their methodology to a variety of classes of linear time-invariant (LTI) systems, encompassing minimum phase, non-minimum phase, and unstable systems. They improved the efficiency of their algorithm by identifying ancestral (already-assessed) chromosomes and avoiding re-evaluation of these. Wang and Kwok (1994) tailored an evolutionary algorithm (EA) using inversion and pre-selection 'micro-operators' to PID controller tuning. They stressed the benefit of flexibility with regard to cost function (there being no requirement for mathematical tractability) and, in particular, alluded to the concept of Pareto-optimality (providing the potential to simultaneously address multiple objectives, such as transient performance and disturbance rejection). In an independent enquiry, Porter and Jones (1992) proposed a GA-based technique as a simple, generic, method of tuning digital PID controllers.

Vlachos *et al.* (1999) applied GA to the tuning of decentralised proportional-integral (PI) controllers for multivariable processes. Controller performance was defined in terms of time-domain bounds on the closed-loop responses for both reference following and loop interactions. This approach afforded good visualisation of the performance of potential solutions.

Onnen *et al.* (1997) applied GA to the determination of an optimal control sequence in model-based predictive control (MBPC). Particular attention was paid to MBPC for non-linear systems with input constraints. Specialised genetic coding and operators were developed with the aim of preventing the generation of infeasible solutions. The resulting scheme was applied to a simulated batch-fed fermenter, with favourable results reported (compared to the traditional branch-and-bound method) for long control horizons.

A further approach to controller design using GA is applying the methodology indirectly. In such a scheme, the GA manipulates input parameters to an established controller design process, which in turn produces the final controller. The linear quadratic Gaussian (LQG) method and the H-infinity control scheme have both been utilised in this manner. GA has also been successfully applied directly in the field of H-infinity control. In this approach, the actual controller is designed via GA. Recognising the difficulty in implementing unconstrained H-infinity controllers, in which the order of the controller is much higher than that of the plant, Chen and Cheng (1998) proposed a structure specified H-infinity controller. GA was used to search for good solutions within the admissible domain of controller parameters (obtained via the Routh-Hurwitz stability criterion).

1.2.2 Command shaping techniques for vibration control

Control of flexible structures requires the design of a stable feedback control system. In addition to stability, certain performance measures are also integrated into the design. For very rapid motions of a flexible system, a satisfactory feedback controller may prove difficult to design. Augmenting the feedback control system with a feedforward control method (i.e. command shaping algorithm) can facilitate the controller design, or enable the attainment of better performance.

Although command shaping for vibration reduction is an old idea (Smith, 1958), the field has been invigorated by the notion that the technique can be used successfully even when there is large uncertainty in the system parameters (Cutforth and Pao, 2000; Kozak *et al.*, 2003; Pao, 2000; Shan *et al.*, 2005). A feedforward approach, known as input shaping, has been successfully applied for controlling flexible structures and computer-controlled machines. Input shaping is implemented by convolving a sequence of impulses, an input shaper, with a desired system command to produce a shaped input that is then used to drive the system. The popularity of input shaping is partly due to its simplicity and its ability to be used with arbitrary actuator commands in real time. Further, since input shapers reside outside of the feedback loop, they are compatible with closed loop vibration reduction schemes.

The effectiveness of input shaping has been demonstrated on many different types of systems and many papers have been published on input shaping since its original presentation (Singer and Seering, 1990). Methods for increasing the robustness to modelling errors have been presented (Singer and Seering, 1992; Singhose *et al.*, 1994). Input shaping was shown to be effective on multi-mode systems (Mohamed and Tokhi, 2002; Singh and Vadali, 1995). Methods for using input shaping with on-off actuators have also been developed (Liu and Wie, 1992; Singhose *et al.*, 1996a).

Due to its ease of implementation and robustness to modelling errors, input shaping has been implemented on applications ranging from precision machinery to large gantry cranes. It has been used to improve the throughput of a wafer handling robot (Rappole *et al.*, 1994). Input shaping has also been used to improve the measurement repeatability of coordinate measuring machines (Jones and Ulsoy, 1994; Seth *et al.*, 1993; Singhose *et al.*, 1996b). A large gantry crane operating in a nuclear environment was equipped with input shaping to enable swing-free operation and precise payload positioning (Singer *et al.*, 1997).

Input shaping was a major component of an experiment in flexible system control, which flew on the Space Shuttle Endeavor (Tuttle and Seering, 1996). Input shaping was combined with a post-manoeuvre damping controller to improve large angle slewing (Hillsley and Yurkovich, 1993). Input shaping has been investigated as a means of reducing residual vibrations of long reach manipulators (Magee and Book, 1995) for handling hazardous waste, and it has also been used for reducing sloshing in an open container of liquid while being carried by a robot arm (Feddema *et al.*, 1997). Mohamed and Tokhi (2002) presented experimental investigations into the development of feedforward control strategies for vibration control of a flexible manipulator using input shaping and low-pass and band-stop techniques. Effects of using a higher number of impulses and filter orders have also been investigated and a significant reduction in the system vibrations has been achieved with these control strategies.

Singhose and Pao (1997) compared input shaping to the time optimal flexible body control for rest-to-rest motion. Several types of input shaping have been compared with robust and non-robust time optimal flexible body control. The methods were compared in terms of speed, robustness to modelling errors, transient

deflection, high mode excitation, and ease of implementation. The negative shapers provide an attractive alternative for achieving rapid responses.

1.3 Aims and objectives of the research

This research focuses on the development of novel modelling and control techniques for input tracking and vibration suppression in the vertical movement of a multi-input multi-output twin rotor system (TRMS). The work comprises several components, each of which is carried out systematically with associated objectives, given as follows:

1) Dynamic modelling of the vertical movement of the TRMS plant using both conventional (RLS) and intelligent black box (GA and NN) system identification techniques, with the view to obtain an accurate model representing the actual system.

2) Assessment of the performance of the developed models characterising the behaviour of the TRMS in terms of accuracy and computational requirements. This is accomplished by validating the simulation results with experiments.

3) Development and performance evaluation of feedforward control methods based on input shaping and filtering techniques for vibration suppression of the TRMS rig. Three forms of input shaper (with two, three and four impulse sequences) and low-pass and band-stop digital filters are designed and implemented on the TRMS rig based on the natural frequency and damping ratio of the TRMS. A comparative assessment and evaluation of performance of the designed command shaping techniques is carried out through simulation and real-time exercises.

4) Development and realisation of feedback control methods including nonlinear hybrid control scheme for tracking performance. This is accomplished by implementing the developed control strategies in both simulation and real-time environments.

5) Investigation into the development of augmented control schemes consisting of feedforward and feedback controllers for input tracking and vibration suppression of the TRMS. Three different forms of augmented controllers are developed and evaluated on the TRMS rig through both simulation and real-time experiments.

1.4 Motivation

The motivation for this work stems from the fact that the TRMS behaviour in certain aspects resembles that of a helicopter. The TRMS, described in Chapter 2 in detail, is a laboratory set-up designed for control experiments by Feedback Instruments Ltd. (1996). Although, the TRMS does not fly it has a striking similarity with a helicopter, such as system nonlinearities and cross-coupled modes. The TRMS, therefore, can be perceived as an unconventional and complex air vehicle with a flexible main body. These system characteristics present formidable challenges in modelling and control design, analysis and implementation. From the control point of view it typifies a high-order non-linear system with significant cross-coupling.

The hovering property of the TRMS rig is the main area of interest in this work. Station keeping (i.e. hovering) is vital for a variety of flight missions such as load delivery, air-sea rescue etc. Yet maintaining a station is one of the most difficult problems in helicopter flight because in this mode the dynamically unstable helicopter is flying at near zero forward speed. Although, the TRMS rig reference point is fixed, it still resembles a helicopter by being highly non-linear with strongly coupled modes. Such a plant is thus a good benchmark problem to test and explore modern identification and control methodologies. The experimental set-up simulates similar problems and challenges encountered in real systems. These include complex dynamics leading to both parametric and dynamic uncertainty, unmeasurable states, sensor and actuator noise, saturation and quantization, bandwidth limitations and delays.

The presence of flexible dynamics in the TRMS is an additional motivating factor for this research. There is an immense interest in design, development, modelling and control of flexible systems, due to their utility in a multitude of applications, as discussed briefly in Section 1.2.

1.5 Thesis outline

The organisation of the thesis reflects the sequence of steps taken in the development of dynamic modelling and control schemes for the TRMS platform. A brief outline of contents of the thesis is given as follows:

Chapter 2 describes the TRMS experimental test bed. A brief description of the rig, necessary instrumentation, hardware and software are presented. The TRMS is used as an experimental platform throughout this work.

Chapters 3 and 4 present the development of linear and nonlinear dynamic models for the vertical movement of the TRMS rig, respectively. Chapter 3 presents development of linear models using RLS and GA identification techniques. Rigid and flexible modes are accounted for in the modelling exercise. Rigorous time and frequency domain tests are employed to validate the identified models. Chapter 4 describes the nonlinear system identification technique for modelling the vertical movement of the TRMS using MLPNN. The extracted model is also verified using several time and frequency domain tests including one-step-ahead (OSA) prediction of the system output, correlation tests and time domain cross validation tests. The rationale for obtaining a high fidelity dynamic model is that such a model is often required for assessing the performance of control design and system analysis.

The development of command shaping feedforward control strategies for vibration control of the vertical movement of the TRMS rig using input shaping and filtering techniques is presented in Chapter 5. The residual vibrations in flexible systems are normally due to their fast motion. Three forms of input shapers (with two, three and four impulse sequences) and low-pass and band-stop digital filters are designed and used for pre-processing the desired input to the system. The feedforward control techniques are designed on the basis of natural frequency and damping ratio of the TRMS system. The goal of the open-loop control is to shape the input signal so as to avoid excitation of residual vibrations during and at the end of the system manoeuvre. Performances of the developed controllers are assessed in terms of level of vibration reduction at the natural frequencies. This is accomplished by comparing the system response to that with the unshaped input signal in both simulation and real-time experiments. The advantage of this method is that it is not

necessary to change the feedback control law in order to attenuate system's vibration.

Chapter 6 investigates the development and realization of hybrid feedback control schemes that combine conventional PID compensator and fuzzy controller for tracking performance. The motivation of combining both controllers is to enhance the control performance during transient and steady states. The performances of the proposed feedback control methods are evaluated on the TRMS plant within both simulations and real-time experiments. The controllers are shown to exhibit good tracking capabilities.

Chapter 7 presents investigations into the development and realisation of an augmented feedforward and feedback control scheme (AFFCS) for input tracking and vibration suppression of the vertical movement in the TRMS rig. A 4-impulse input shaper, representing the feedforward control component, is designed and employed for pre-processing the command input. It is combined with three feedback controllers to form three different augmented control strategies. The motivation that stem from the augmentation process is to obtain good tacking performance with minimum system's residual vibrations. Such designed control mechanism that combines both feedforward and feedback controller is a practical approach and desirable for fast manoeuvring systems with rapidly changing command input.

Chapter 8 concludes the thesis with notable remarks and achievements. Future possible research directions are also outlined in this chapter.

1.6 Contributions

The main contributions of this research are highlighted in the following subsections:

1.6.1 Dynamic modelling of the vertical movement of the TRMS rig

This work involves dynamic modelling of the vertical movement of the TRMS using linear and nonlinear black box system identification techniques. The extracted linear models using RLS and GA parametric approaches are employed to detect system resonance modes for subsequent control design. It has been demonstrated that the

black-box modelling approach, utilised in this work, is suitable for modelling a class of unconventional air vehicles, whose flight dynamics are not well understood or difficult to model from first principles.

The work further includes nonlinear modelling of the TRMS utilising MLP NNs. The modelling concept provides an attractive alternative to model new generation UAVs with significant nonlinearities. Such a high fidelity nonlinear model is often required for gauging the performance of control design and analyses. The linear and nonlinear modelling exercises are carried out to include rigid as well as flexible modes of the system.

1.6.2 Open loop vibration control using command shaping techniques

This work involves development and realization of feedforward control strategies based on command shaping techniques for vibration control of the TRMS rig. The control techniques are designed on the basis of natural frequency and damping ratio of the TRMS system and their performances are evaluated in simulation and real-time experimental environments in terms of level of vibration reduction at the main system's resonant mode. This is accomplished by comparing the system response to that with the raw input in simulation and real-time experiments using power spectral density profiles. Command shaping methods developed in this investigation are shown to be effective in reducing motion-induced vibration in flexible manoeuvring systems where the fast motion without oscillation is desirable.

1.6.3 Nonlinear hybrid feedback control laws for tracking performance

This work involves development and implementation of different combinations of feedback control strategies, including nonlinear hybrid control scheme, for set-point tracking performance. Two forms of novel hybrid control are developed and realized for the control of the TRMS rig in hovering mode. The first proposed hybrid control scheme consists of a conventional PD controller augmented with PID compensator (PDPID). While the second nonlinear hybrid control scheme, referred to as (FPDPID), comprises PD-type FLC augmented with PID compensator. In both cases, the novelty is claimed based on the structure of the hybrid control scheme,

which is designed in such a way that the output of the first controller (i.e. PD controller or FPD-type FLC) is fed to the proportional gain of the augmented PID compensator. The performances of the two proposed nonlinear hybrid control strategies (PDPID and FPDPID) are compared with PID compensator and pure PD-type and PI-type fuzzy controllers in terms of set-point tracking.

1.6.4 Augmented control scheme for input tracking and vibration suppression

This includes development and implementation of augmented feedforward and feedback control scheme (AFFCS) for vibration attenuation as well robust tracking performance, and demonstration of the suitability of integrated feedforward and feedback method to tackle the dual problem of vibration reduction and command tracking in the system through a comparative performance assessment study. The augmented control scheme developed in this research is shown to be adequate for tackling both problems (i.e. input tracking and vibration suppression) simultaneously. Therefore, such control strategy is ideal for flexible manipulators and flexible aircrafts.

1.7 List of publications

Technical papers arising from this research, which are either published, accepted or under review are listed in the following subsections.

1.7.1 Journal papers

Aldebrez, F. M. and Tokhi, M. O. Vibration control of flexible manoeuvring systems using command shaping techniques, *Journal of Low Frequency*, (Submitted in 2007).

Aldebrez, F. M. and Tokhi, M. O. Augmented control scheme for input tracking and vibration suppression of flexible manoeuvring system, *Proceedings of IMechE-I: Journal of Systems and Control Engineering*, (Submitted in 2007).

Tokhi, M. O., Md Zain, M. Z., Alam, M. S., Aldebrez, F. M., Mohd Hashim, S. Z. and Mat Darus, I. Z. Genetic algorithm optimisation and control system design of flexible structure, *Journal of Intelligent Systems*, special issue on "Cybernetic systems: Fuzzy, neural and evolutionary computing approaches" (To appear).

Aldebrez, F. M. and Tokhi, M. O. (2004). Vibration control of pitch movement using command shaping techniques: experimental investigation, *Journal of Systems Science*, **29**, (2), pp. 129-143.

1.7.2 Conference papers

Aldebrez, F. M., Alam, M. S. and Tokhi, M. O. (2006). Design of hybrid control schemes for tracking performance of a flexible manoeuvring system, *3rd AUS International Symposium on Mechatronics (AUS-ISM06)*, Sharjah, UAE, 18-20 April 2006.

Aldebrez, F. M., Alam, M. S. and Tokhi, M. O. (2005). Hybrid control scheme for tracking performance of a flexible system, *Proceedings of CLAWAR-2005: 8th International Conference on Climbing and Walking Robots CLAWAR 2005 & Introductory Mobile Robotics Workshop*, London, UK, 12-15 September 2005, pp. 543-550.

Tokhi, M. O., Aldebrez, F. M. and Alam, M. S. (2005). Real-time vibration control of a flexible structure using an augmented feedforward and feedback scheme, *Twelfth International Congress on Sound and Vibration (ICSV12)*, Lisbon, Purtugal, 11-14 July, 2005.

Aldebrez, F. M., Alam, M. S. and Tokhi, M. O. (2005). Input-shaping with GA-tuned PID for target tracking and vibration reduction, *Joint 2005 International Symposium on Intelligent Control & 13th Mediterranean Conference on Control and Automation (2005 ISIC-MED)*, Limassol, Cyprus, 27-29 June 2005.

Alam, M. S., Aldebrez, F. M., Tokhi, M. O. and Ahmad, F. (2004). Augmented feedforward and feedback control scheme for input tracking and vibration control, *International Conference on Computer and Information Technology (ICCIT04)*, Dhaka, Bangladesh, December 2004.

Aldebrez, F. M., Alam, M. S., Tokhi, M. O. and Shaheed, M. H. (2004). Genetic modelling and vibration control of a twin rotor system, *UKACC International Conference on Control-2004*, Bath, UK, 6-9 September 2004.

Tokhi, M. O., Alam, M. S. and Aldebrez, F. M. (2004). Adaptive IIR filtering techniques for dynamic modelling of a twin rotor system, *7th Biennial Conference on Engineering Systems Design and Analysis (ESDA04)*, Manchester, UK, 19-22 July 2004.

Alam, M. S., Aldebrez, F. M. and Tokhi, M. O. (2004). System identification of a twin rotor multi-input multi-output system using adaptive filters with pseudo random binary input, *Eleventh International Congress on Sound and Vibration (ICSV11)*, St. Petersburg, Russia, 13-15 July 2004.

Aldebrez, F. M., Mat Darus, I. Z. and Tokhi, M. O. (2004). Dynamic modelling of a twin rotor system in hovering position, *First International Symposium on Control, Communications and Signal Processing (ISCCSP04)*, Hammamet, Tunisia, 21-24 March 2004.

Aldebrez, F. M., Tokhi, M. O., Mohamed, Z. and Ahmad, M. S. (2003). Vibration control of pitch movement using command shaping techniques, *9th IEEE International Conference on Emerging Technologies and Factory Automation (ETFA03)*, Lisbon, Portugal, 16-19 September 2003.

Aldebrez, F. M. and Tokhi, M. O. (2003). Vibration control of pitch movement using command shaping techniques: experimental investigation, *Sixteenth International Conference on Systems Engineering (ICSE'03)*, Coventry, UK, 9-11 September 2003.

CHAPTER 2

THE TWIN ROTOR MULTI-INPUT MULTI-OUTPUT SYSTEM EXPERIMENTAL SETUP

2.1 Introduction

There is a small but growing body of literature on laboratory platforms to simulate complex aircraft manoeuvres and to investigate different control paradigms. A multi-modal approach to robust controller design is illustrated for a 2 DOF laboratory aircraft model, developed to model the behaviour of a vertical-take-off aircraft by Werner and Meister (1999). In this work, the Linear Matrix Inequality (LMI) formulation in conjunction with convex programming for robust command tracking and disturbance rejection in normal operation as well as in failure mode is employed. This platform is quite similar to the twin rotor multi-input multi-output system (TRMS). It has roll and yaw movement where as the TRMS has pitch and yaw motion.

A radio controlled (RC) model helicopter is adopted as a platform by Morris *et al.* (1994) to study various modern identification and robust control synthesis techniques. The helicopter is mounted on a 3 DOF wrist which in turn is connected to a 3 DOF stand. This experimental set up is perceived as the hover mode. Stabilising LQG and H-∞, controllers with set-point tracking are designed and compared for the RC helicopter. The Caltech ducted fan flight control experiment is designed to represent the dynamics of either a Harrier in hover mode or a thrust vectored aircraft such as the USAF F18-HARV or X-31 in forward flight (Van Nieuwstadt and Murray, 1998). A comparison of several different linear and nonlinear controllers was performed by Kantner *et al.* (1995) on the same rig. The Georgia Tech model helicopter and NRL's foldable UAV and VTOL UAV (Sivashankar *et al.*, 1994) fall under the small experimental platform category. These platforms are thus, ideal test-bench for modelling, design and control research.

This chapter presents a general description of the TRMS platform considered in this research. The details of the physical description and system operation as well as the hardware and software aspects of the TRMS are explained. Important considerations that are essential for conducting the experiments are also highlighted.

2.2 Description of the TRMS experimental set-up

The TRMS is a laboratory platform designed for control experiments by Feedback Instruments Ltd (Feedback Instruments Ltd., 1996). The schematic diagram of the TRMS is shown in Figure 2.1. Its behaviour in certain aspects resembles that of a helicopter. For instance, like a helicopter there is a strong cross-coupling between the main rotor and the tail rotor. As such the TRMS can be considered a static test rig for an air vehicle. These platforms are often employed to test the suitability of different control methods for these systems.

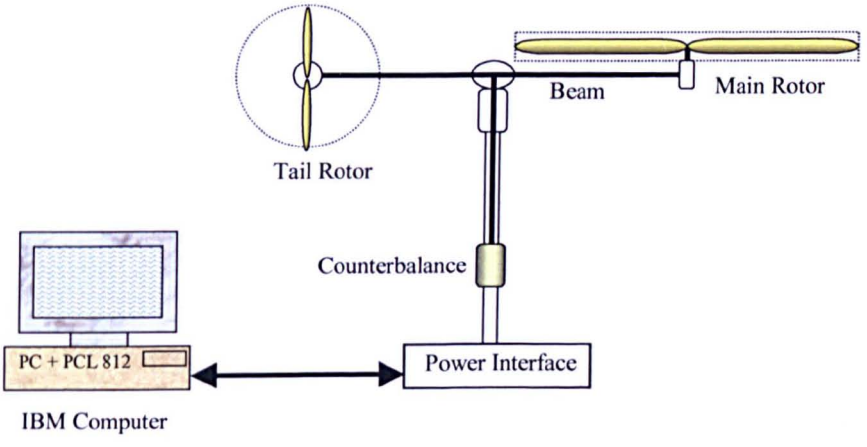

Figure 2.1: Schematic diagram of the TRMS

The TRMS consists of a beam pivoted on its base in such a way that it can rotate freely in both the horizontal and vertical planes. At both ends of the beam there are two rotors, the main and tail rotors, driven by DC motors. As shown in Figure 2.2, the rotation of the main rotor produces a lifting force allowing the beam to rise vertically making a rotation around *pitch axis*. This vertical movement of the

beam makes an elevation angle (θ) with respect to pitch plane. While, the tail rotor which is smaller than the main rotor is used to make the beam turn left or right around *yaw axis* producing a rotational angle (φ). A counterbalance arm with a weight at its end is fixed to the beam at the pivot. The state of the beam is described by four process variables: horizontal and vertical angles measured by position sensors fitted at the pivot, and two corresponding angular velocities. Two additional state variables are the angular velocities of the rotors, measured by tacho-generators coupled with the driving DC motors. Either or both axes of rotation can be locked by means of two locking screws, provided for physically restricting the horizontal or vertical plane TRMS rotation. Thus, the system permits both 1 and 2 DOF experiments.

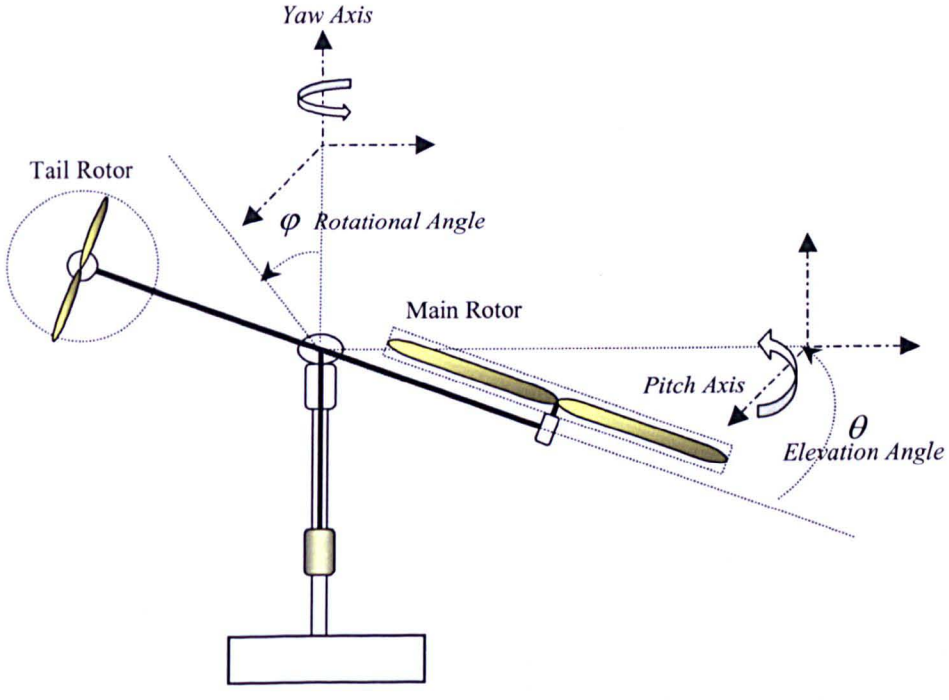

Figure 2.2: Configuration of the 2DOF movements of the TRMS

In a normal helicopter, changing the angle of attack of the blades controls the aerodynamic force. However, the TRMS is constructed in such a way that the angle of attack is fixed. In this case, the aerodynamic force is controlled by varying the speed of the DC motors. Therefore, the control inputs are supply voltages of the DC

motors. A change in the voltage value results in a change of the rotational speed of the propeller, which in turn results in a change of the corresponding position of the beam (Feedback Instruments Ltd., 1996). The input voltage is limited to ±10 volts.

Rotation of a propeller produces an angular momentum, which according to the law of conservation of angular momentum, must be compensated by the remaining body of the TRMS. This results in the interaction between two planes of motion. This interaction directly influences the velocity of the beam in both planes. The coupling effect between the two channels may be accounted for by representing the dynamics of the TRMS by the multivariable transfer-function model given in Figure 2.3. In this figure, the input signals $u_1(s)$ and $u_2(s)$ represent voltage inputs to the main rotor and tail rotor respectively. The outputs $y_1(s)$ and $y_2(s)$ represent the elevation and rotational angles (θ and φ) around pitch and yaw axes, respectively. A similar coupling exists in a real helicopter. The coupling between various channels or planes of motion therefore makes the modelling and control problems challenging in such systems.

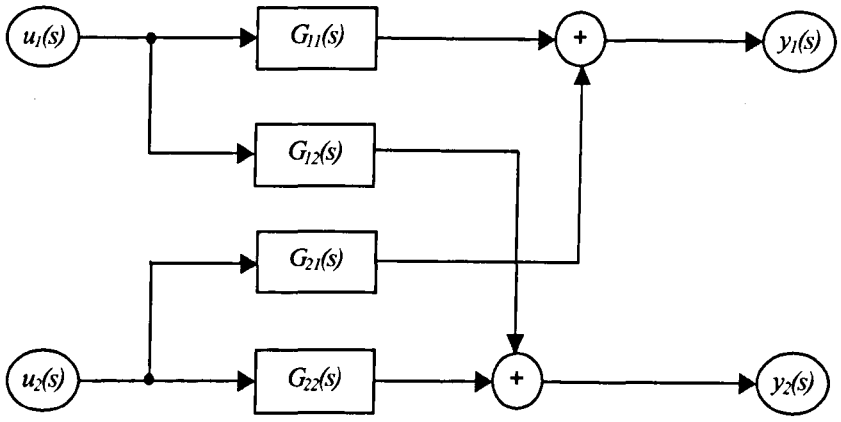

Figure 2.3: Coupled MIMO transfer function model

2.3 The TRMS hardware and software description

An IBM-PC compatible computer is used for real-time control of the TRMS. The computer is supplied with an interface board (PCL-812), which is a high performance, high speed, and multi-function data acquisition card for IBM PC/XT/AT and compatible computers. Figure 2.4 shows details of the hardware and

software configuration of the control system for the TRMS. The control software for the TRMS consists of:

- Real-time kernel (RTK).
- The TRMS toolbox.

2.3.1 Real-time kernel (RTK)

The real-time kernel (RTK) provides a mechanism of real-time measurements and control of the TRMS in the WINDOWS environment. It is implemented by dynamic linked library (DLL) and contains measurement procedures, digital filters, data acquisition buffer, built-in control algorithms, software to control system actuators and a MATLAB-to-RTK interface. The RTK controls flow of all signals to and from the TRMS. It contains functions for performing analogue-to-digital and digital-to-analogue conversions. The RTK DLL library is excited by time interrupts. The main part of the RTK is executed during interrupt time. In summary, the RTK contains all the functions that are required for feedback control and data acquisition in real time. Examples of control algorithms are embedded in the RTK including open-loop, PID and state-space control. It is possible to tune the parameters of the controller without emphasis on analytical model. Such an approach to the control problem seems to be reasonable, if a well-defined model of the TRMS is not available. These controller parameters are functions of error signals, that is the difference between the desired and actual TRMS beam positions and angular velocities. Selection of control algorithms and tuning of their parameters is done by means of the communication software, as shown in Figure 2.4, from the MATLAB environment.

The communication interface is also used for configuration of real-time kernel parameters, e.g. setting of the sampling period for experiments or encoder resetting at the beginning of each new experiment. Time history of experiments is collected in a cyclic buffer. The data can be transferred to the MATLAB workspace using the communication interface.

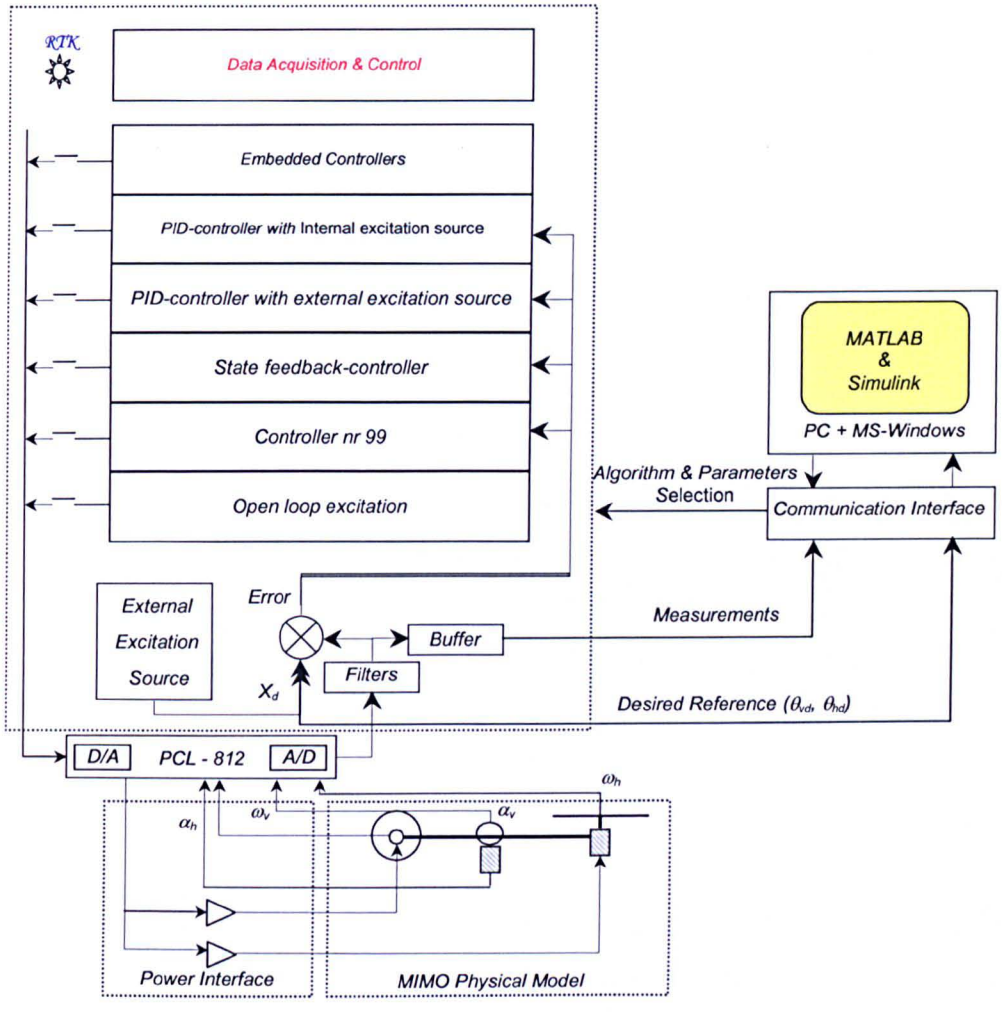

Figure 2.4: Hardware and software configuration of the TRMS

2.3.2 The TRMS toolbox

The TRMS toolbox is a collection of m-functions and C-coded DLL-files that extend the MATLAB environment in order to address TRMS modelling and real-time control problems. On-line data flow between the RTK and toolbox functions is performed by the communication interface. The TRMS toolbox, using MATLAB matrix functions and Simulink utilities, provides the user with functions specialised for real-time control of the twin rotor system. This toolbox is an open system. This approach by its nature makes basic functions of the toolbox available to the user. It empowers the user to create a system of his own, add new control algorithms to it, or further customise it to satisfy his requirements better.

There are 34 toolbox functions. The functions are divided into the four following categories according to the specific roles performed:

- *Hardware:* functions in this category are used to obtain and set the base address of PCL-812 interface board. A function is also available to reset the encoders at the beginning of each experiment.
- *Data acquisition:* includes functions that are employed to set the sampling time, acquire the sampling interval and retrieve the time histories of various measurements.
- *Software:* loading and unloading of the RTK to and from the memory are carried out by functions in this category.
- *Control:* the job of assigning different control parameters for various in-built control algorithms is mainly achieved by invoking functions in this category.

2.4 TRMS experimentation

The hovering property of the TRMS is the main area of interest in this work. Hovering or station keeping is vital for a variety of flight missions such as load delivery and air-sea rescue operations. Therefore, throughout this research the experimentations for system modelling and control design exercises are carried out with the TRMS beam in a flat horizontal position representing the hovering mode, as illustrated in Figure 2.5.

For carrying out the experiments with the TRMS, three main issues are carefully considered during this research; level of input signal, sampling time and environmental conditions. The level of input signal is selected in this research so that the signal does not drive the TRMS out of its linear operating range. For the identification of the discrete time models, the sampling time has to be selected before starting the experiments. The sampling time depends on the final application and the intended accuracy of the resulting model. The model can easily exhibit high order behaviour if the sampling period is chosen too short. On the other hand, if the sampling period is too large, the model looks like a constant or multiple integrators and its dynamic representation would be inaccurate. It has been observed that, the

TRMS is very sensitive to atmospheric disturbances. A slight gust of wind can affect its dynamic behaviour. Therefore, care has been taken to conduct experiments with minimal environmental influence. If necessary experiments are repeated for several times until "true" responses are obtained, and the results presented throughout the thesis represent the latter.

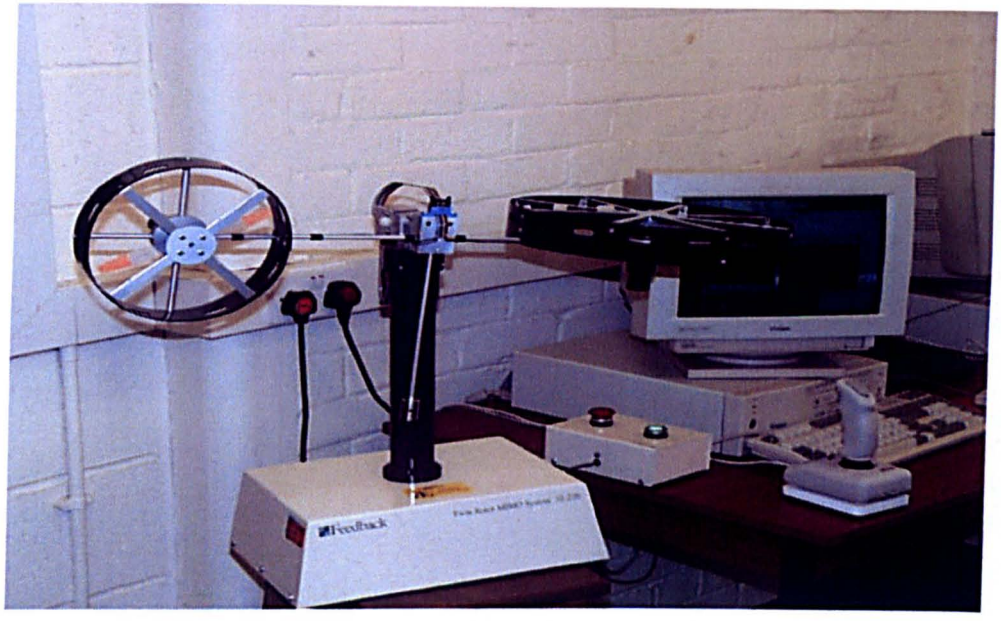

Figure 2.5: The TRMS in hovering mode

2.5 Summary

A general description of the TRMS considered for this research has been presented. The system consists of a main beam and measuring devices. The beam is pivoted on its base such that it can rotate freely in horizontal and vertical planes. Details of hardware and software configurations have also been presented. The PC communicates with the TRMS rig via MATLAB-Simulink environment. Important considerations while conducting experiments with the TRMS have been highlighted.

CHAPTER 3

PARAMETRIC MODELLING OF THE TWIN ROTOR FLEXIBLE STRUCTURE

3.1 Introduction

Construction of a mathematical model that perfectly describes the dynamics of a physical system using traditional analytical methods is generally possible for simple systems. The model obtained using this approach is generally derived from first principles and employing many simplifications and assumptions. However, with the increasingly complex nature of systems with complex dynamics and highly non-linear behaviour, modelling of such systems based on first principle rules is often a formidable and undesirable task (Ljung and Söderström, 1983). Moreover, these important dynamics and disturbances acting on the system if not accounted for may yield a poor system model. Thus, the utility of mathematical modelling to fairly complex plants is limited. On the other hand, system identification has proven to be an excellent tool to model complex processes where it is not possible to obtain reasonable models using only physical insight (Ljung, 1987). It is an experimental technique used for obtaining mathematical model of a dynamic system based on observed input and output data.

Important applications of system identification are visible in areas that require higher accuracy of the mathematical model for simulation, validation, control system design and handling qualities such as aerospace applications (Vandersteen *et al.*, 1996; Ahmad *et al.*, 2002). It provides an accurate, rapid and reliable approach for defining design specifications and for validating control systems. System identification, used to construct a model to represent a given system, plays an important role in system analysis, control and prediction. Identification of systems has drawn a great deal of interest because of the increasing need in estimating the behaviour of a system with partially known dynamics. Especially in the areas of

control, pattern recognition and even in stock markets the system of interest needs to be known to some extend.

Generally, the procedure of identification entails a matching between the system output and an estimated output, as shown in Figure 3.1, where $u(t)$ and $y(t)$ are system input and output respectively, $e(t)$ is disturbance, $\hat{y}(t)$ is the estimated or predicted output and $\varepsilon(t)$ is the modelling or prediction error. In the process of identification a suitable model is developed that exhibits the same input/output characteristics as the controlled plant (Tokhi and Leitch, 1992). Once a model of the physical system is obtained, it can be used for solving various problems such as, to control the physical system or predict its behaviour under different operating conditions.

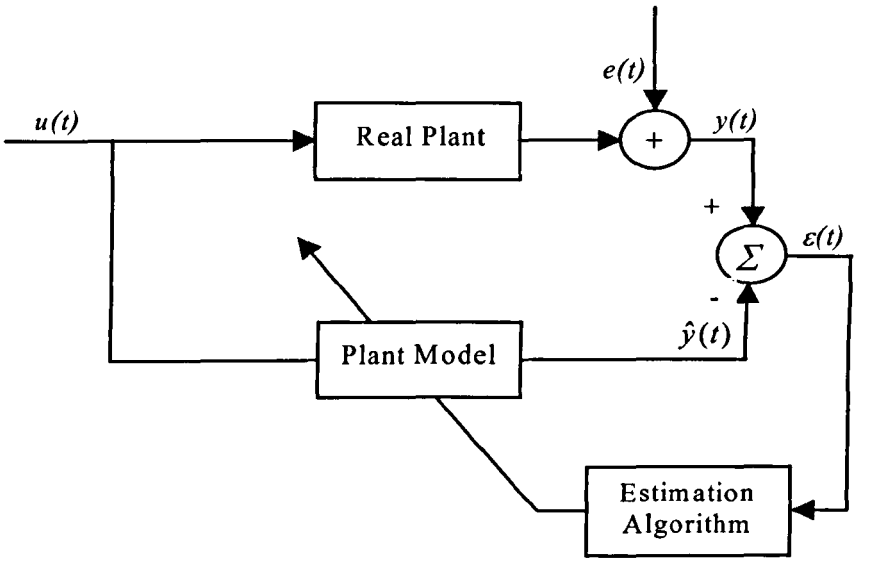

Figure 3.1: Schematic diagram of the identification process

The process of system identification technique for estimating a mathematical model that characterises the behaviour of a dynamic system can be summarized in four steps, shown in Figure 3.2. The process begins by conducting some preliminary experiments on the actual system to examine its behaviour and identify its resonance modes and operating conditions. This stage is done by applying an excitation signal and extracting the corresponding system response. The selection of the type and characteristics of plant excitation signal is important in the system identification process (Billings and Voon, 1995). The most popular excitation signals are pseudo

random binary sequence (PRBS), random gaussian sequence (RGS), finite step sequence (FSS), and switched step (SS) or bang-bang step (BBS) signals (Ahmad, 2001). The excitation signal and the counterpart system response are referred as observed input and output data, respectively. These data are later used to construct the system model in the identification process. Data quality and consistency are critical to the identification process. Excessively noisy data may lead to identification of an incorrect model. Preliminary checks of data quality and consistency can ensure that sources of error are minimised.

When the model is obtained it is required to verify whether the model is adequate by carrying out few validation tests including correlation tests, using error function, estimation and testing data. If the result of the test is not satisfied or inadequate then, the process of identification has to be repeated until some level of satisfaction is achieved.

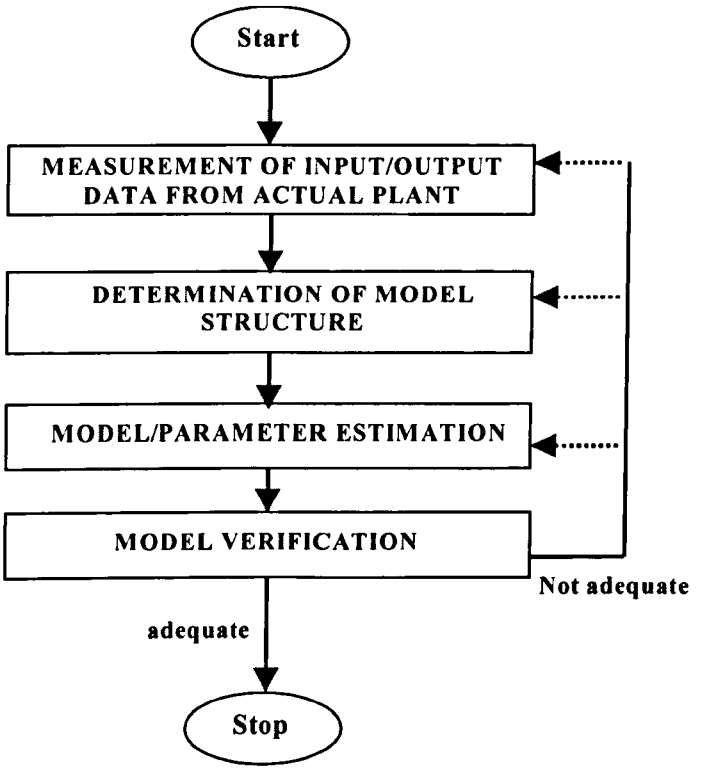

Figure 3.2: System identification procedure

This chapter addresses the parametric modelling of the TRMS, described in Chapter 2, using recursive-least squares (RLS) and genetic algorithm (GA)

identification techniques. The objective of the identification process is to obtain a dynamic model of the lateral axis (vertical movement) of the TRMS with its main beam (body) in a flat horizontal position representing the hovering mode. In other words, the aim of the identification experiments is to get a satisfactory model of the pitch plane (elevation angle) dynamics without any prior system knowledge related to the physical system.

The extracted model is later used in this thesis for low frequency vibration suppression (Chapter 5), design of suitable feedback control laws for disturbance rejection and set-point tracking (Chapter 6) and augmented feedforward and feedback control scheme for vibration suppression and tracking performance (Chapter 7).

3.2 Parametric modelling

Parametric estimation is one of the two major classes of system identification technique (Shaheed and Tokhi, 2002). In parametric modelling, the identification process is defined as a process of parameter estimation of the required model characterising a plant/system. The primary interest lies in the identification of low frequency (0-3 Hz) dynamic modes of the TRMS. This range is assumed to be good enough for high fidelity modelling of the TRMS (Ahmad *et al.*, 2002). Parametric modelling of the TRMS is carried out in this investigation by minimising the prediction error between the actual output and the predicted output (elevation angle). With the view to find an accurate model of the system a comparative assessment of the RLS and GA methods is carried out in the parametric dynamic modelling of the systems.

3.2.1 Recursive least squares

Adaptive algorithms such as RLS estimation are able to provide a complete model of a system based on known parameters and previous history of inputs and outputs. The RLS algorithm is based on least square (LS) estimation method and uses an iterative refinement technique to continuously tune estimated parameters using knowledge of some existing parameters as well as information obtained from the continuous

operation of the system (Billings, 2001). While LS provides a best-fit estimate for a set of recorded data, the RLS algorithm creates a continuous estimate for a set of unknown system parameters. The RLS algorithm is given by the following set of equations at iteration *(i)*:

$$\hat{\theta}(i) = \hat{\theta}(i\text{-}1) + K(i)\,E(i) \tag{3.1}$$

$$K(i) = \frac{\lambda^{-1} P(i\text{-}1)\,x(i)}{1 + \lambda^{-1} x(i)^T P(i-1)\,x(i)} \tag{3.2}$$

$$P(i) = \lambda^{-1} P(i-1) - \lambda^{-1} K(i)\,x(i)^T P(i-1) \tag{3.3}$$

$$E(i) = y(i) - x(i)^T \hat{\theta}(i\text{-}1) \tag{3.4}$$

A diagrammatic representation of the RLS algorithm is given in Figure 3.3, which describes the relationship between the regression vector $x(i)$, the unknown parameter vector $\hat{\theta}(i)$ and the system output $y(i)$. At each iteration *(i)* of the algorithm, a new estimate $\hat{\theta}(i)$ is calculated based on the recent values $x(i)$ and $y(i)$. The system output $y(i)$ is one time step behind the input $x(i)$ and the parameter vector $\hat{\theta}(i)$. λ is defined as the forgetting factor used to help the algorithm converge to the global minimum. The convergence of the algorithm is determined by the magnitude of the modelling error $E(i)$ reaching a minimum or by the estimated set of parameters reaching a steady level. The concept of forgetting factor is such that older information is gradually discarded in favour of the most recent information or giving less weight to older data and more weight to recent data (Haykin, 1986; Ljung and Söderström, 1983). However, the use of a forgetting factor could cause the predicted values of parameters to fluctuate rather than converge to a certain value. The level of fluctuation depends on the value of λ (the smaller the value the bigger the fluctuation in the parameter values). Values commonly used in practice lie between 0.95 and 1 (Ljung and Söderström, 1983). In this investigation it was noted that good results are obtained when λ was set to 0.96. The computational cost of the RLS algorithm may be reduced by defining:

$$J(i) = \lambda^{-1} P(i-1)\, x(i) \tag{3.5}$$

Hence, equations (3.2) and (3.3) can be simplified as

$$K(i) = \left[1 + x(i)^T J(i)\right]^{-1} J(i) \tag{3.6}$$

$$P(i) = \lambda^{-1} P(i-1) - K(i)\, J(i)^T \tag{3.7}$$

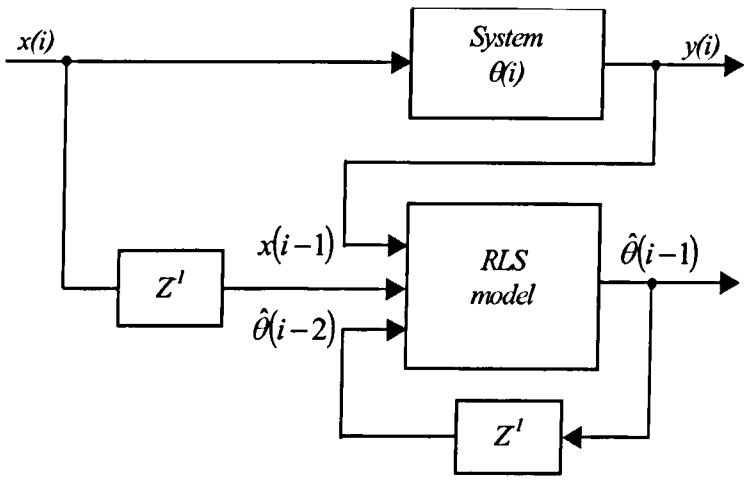

Figure 3.3: Diagrammatic representation of the RLS algorithm

3.2.2 Genetic algorithms

Genetic algorithms (GAs), introduced and studied by Holland (1975) and his students at the University of Michigan, are search algorithms that are based on the mechanics of natural selection and natural genetics (Goldberg, 1989). They perform a global, random, parallel search for an optimal solution using simple computations. Starting with an initial population of genetic structures, genetic inheritance operations based on selection, mating, and mutation are performed to generate "offspring" that compete for survival to make up the next generation of population structures.

The concepts in the theory of evolution have been translated into algorithms to search for solutions to problems in a more 'natural' way. First, different possible

solutions to a problem are created. These solutions are then tested for their performance. Among all possible solutions, a fraction of the good solutions is selected, and the others are eliminated 'survival of the fittest' (Efe and Kaynak, 2000). The selected solutions undergo the processes of reproduction, crossover, and mutation to create a new generation of possible solutions (which are expected to perform better than the previous generation). This process of production of a new generation and its evaluation is repeated until there is convergence within a generation. The benefit of this technique is that it searches for a solution from a broad spectrum of possible solutions, rather than restrict the search to a narrow domain where the results would be normally expected (Fleming and Purshouse, 2002). Genetic algorithms try to perform an intelligent search for a solution from a nearly infinite number of possible solutions.

3.2.2.1 GA operation

In the last years GA has been found as a very powerful method for the solution of engineering problems (Efe and Kaynak, 2000; Fleming and Purshouse, 2002). The algorithm searches the solution in the whole searching region, and as GA is not a gradient search method, it suffers less from problems due to local minima (Chipperfield and Fleming, 1994). Therefore, this method has more chances to find the global solution of the problem than other methods. GA is a stochastic search method and operates on a population of potential solutions applying the principle of survival of the fittest to produce better and better approximations to a solution (Goldberg, 1989).

The operating mechanism of GA is illustrated in Figure 3.4 (Patterson, 1996). At the beginning of the computation a number of individuals (the population) are randomly initialized from a range defined by the user. Each element of the population is mapped onto a set of strings (the chromosome) to be manipulated by the genetic operators. The performance of each member of the population is assessed through an objective function imposed by the problem. If the optimization criteria are not met, the creation of a new generation starts.

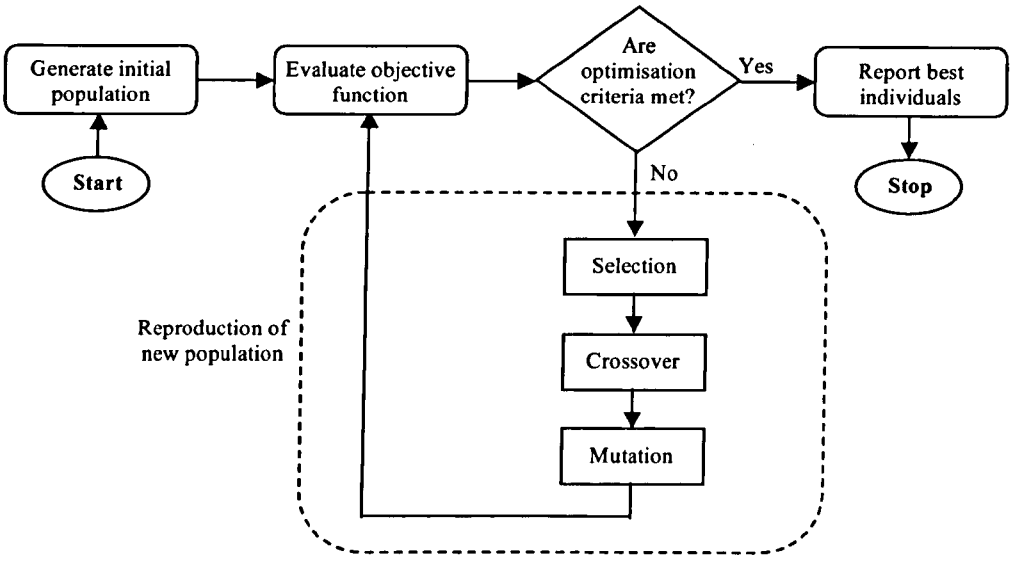

Figure 3.4: Flow chart of basic GA operation

This establishes the basis for selection of pairs of individuals that will be mated together during the reproduction process in which genetic operators such as crossover and mutation are used to produce a new population of individuals (offspring) by manipulating the "genetic information" usually called genes, possessed by the members (parents) of the current population. After manipulation by the crossover and mutation operators, the objective function is evaluated, a fitness value assigned to each individual and individuals selected for mating according to their fitness, and so the process continues through subsequent generations. In this way, the average performance of individuals in a population is expected to increase, as good individuals are preserved and breed with one another and the less fit individuals die out. The GA search continues until one of the optimisation criteria is satisfied (e.g., a certain number of generations completed or when a particular point in the search space is reached).

3.2.2.2 Major elements of genetic algorithms

The simple operating principles of GA described above cannot be directly applied to solve every engineering problem. In fact, each problem has its own nature, which is quite unique to it and thus to apply GA, an engineering insight to the problem is required to be studied and considered. There are many factors and operational modes

that need to be introduced and reorganised to alter the structure of a GA to suit the requirement of a particular problem to be solved. Some elements of the modified GA are discussed below.

3.2.2.3 Population representation and initialisation

As mentioned earlier, GA operates simultaneously on a set of potential solutions. The members of the population are called individuals/chromosomes and their number could be as high as 100 or more and as low as 10, depending upon the nature of the problem and type of GA. Very small populations, as small as 10 individuals, are usually used by micro GA with a restrictive reproduction and replacement strategy in an attempt to satisfy real-time execution requirements (Chipperfield *et al.*, 1994).

The classical approach of representing chromosomes in the GA is that of the normal binary string. In this case, each decision variable in the parameter set is encoded as a binary string and these are concatenated to form a chromosome. The use of gray coding is claimed to provide slightly better results than normal binary representation (Fleming and Purshouse, 2002). This type of coding is extensively used by researchers. However, there is also an increasing interest in alternative encoding strategies, such as integer and real-valued representations. A number of practical problems have been solved by using real-coded GA despite the opinion that a real-coded GA would not necessarily yield good results in some situations.

3.2.2.4 Objective function and fitness value

The objective function is the main link between the GA and the problem to be solved. It evaluates the performance of each chromosome in the problem domain and helps in selecting the best ones for further reproduction. It takes chromosomes as input and produces a value (objective value) as a measure of how individuals have performed in the problem domain. In the case of a minimisation problem, the most fit individuals will have the lowest numerical value of the associated objective function. The objective values vary from problem to problem, and to maintain

uniformity over various problem domains, the objective value is re-scaled to a fitness value by different processes (Goldberg, 1989).

3.2.2.5 Selection

An effective parent selection mechanism is necessary to generate good offspring. Selection is the process of determining the number of times a particular individual is chosen for reproduction and, thus, the number of offspring that an individual will produce. Roulette wheel selection mechanisms are currently used due to their simplicity of implementation. However, other selection mechanisms such as stochastic universal sampling and ranking have gained some considerable interest in recent years (Fleming and Purshouse, 2002).

3.2.2.6 Crossover and mutation

Crossover and mutation are the two fundamental genetic operators. Crossover is used for producing new chromosomes in the GA. It takes two chromosomes and swaps part of their genetic information to produce new chromosomes. The swapping points are randomly chosen. The simplest form of crossover is that of single-point crossover as shown in Figure 3.5. Here, at the crossover point, the portions of the parent strings P_1 and P_2 are swapped to produce the new offspring strings O_1 and O_2. There are many other forms of crossover such as: multi-point crossover, uniform crossover, intermediate recombination, and line recombination, have been proposed and are being utilised.

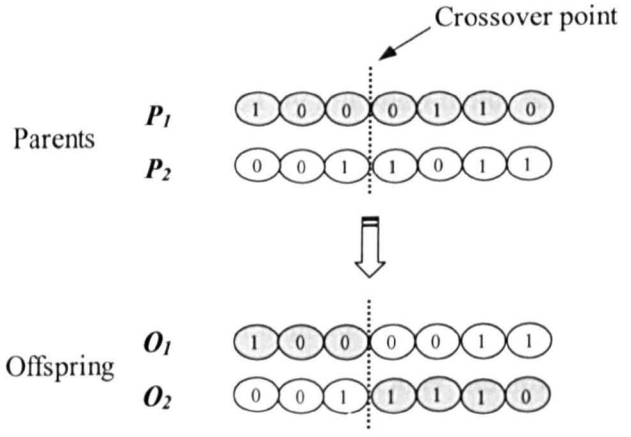

Figure 3.5: Single-point crossover operation

In natural evolution, mutation is a random process where one allele of a gene is replaced by another to produce a new genetic structure. In a GA, mutation is randomly applied with low probability, typically in the range 0.001 and 0.01, and modifies elements in the chromosomes. Usually considered as a background operator, the role of mutation is often seen as providing a guarantee that the probability of searching any given string will never be zero and acting as a safety net to recover good genetic material that may be lost through the action of selection and crossover (Goldberg, 1989). Thus, mutation is an important operator, which helps the algorithm to escape from trapping in the local minima of the fitness function, and it seeks to explore other areas of the search space in order to find a global maximum or minimum of the fitness.

The effect of mutation on a binary string is illustrated in Figure 3.6 for a 10-bit chromosome representing a real value with a mutation point of 5. Here, binary mutation flips the value of the bit at the loci selected to be the mutation point. Given that mutation is generally applied uniformly to an entire population of strings, it is possible that a given binary string may be mutated at more than one point.

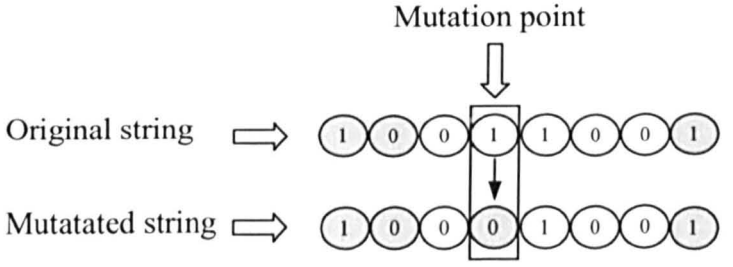

Figure 3.6: Binary mutation operation

Since the modification introduced by mutation is not related to any previous chromosome structure in the population, new structures are formed to increase the search space. Various types of mutation operations have been proposed and applied with GAs. A mutation operator for the real-coded GA that uses a non-linear term for the distribution of the range of mutation applied to gene values has been introduced by Muhlenbein and Schlierkamp-Voosen (1993). Other mutation operations such as

trade mutation and reorder mutation have raised considerable interest for specific problem domains.

3.2.2.7 Reinsertion

A number of strategies have been developed as to how and which individuals of the new generation will replace the individuals of the old generation. One of the mechanisms, called generation replacement, replaces the individuals in the current population by the offspring (Fleming and Purshouse, 2002). The major drawback of this procedure is that the best individuals of the old generation may fail to reproduce offspring in the next generation. Thus, elitist strategy is adopted where one, or a few, of the best individuals are carried forward in the succeeding generation. When selecting which members of the old population should be replaced, the most apparent strategy is to replace the least fit members. This further asserts that replacing the least fit members effectively implements an elitist strategy as the most fit will probabilistically survive through successive generations. The speed of dominance of a population by a super chromosome may be increased in the case of elitist strategy but on balance it appears to improve the performance (Man *et al.*, 1996). Another strategy is to create fewer numbers of offspring than the size of the original population and then replace a part of the individuals in the original population by the newly generated offspring. Usually the worst chromosomes are replaced with the new chromosomes. An important feature of not creating more offspring than the current population size at each generation is that the generation computational time is reduced, most dramatically in the case of the steady state GA, and that the memory requirements are smaller as fewer new individuals need to be stored while offspring are produced (Chipperfield *et al.*, 1994). A direct replacement of the parents by the corresponding offspring is also addressed in the literature (Man *et al.*, 1996).

3.2.2.8 Probability rate setting

The probability rate setting for crossover and mutation is an important factor in achieving good performance. Increasing the crossover probability rate introduces more diversity among the individuals of a population at the possible cost of

disruption of good chromosomes. In contrast, a sharp rise of mutation probability rate would turn the genetic search into random search but helps reintroduce lost genetic information (Man *et al.*, 1996). A linear variation in crossover and mutation probability rate, with decreasing crossover rate during the run while mutation rate increases, has been suggested by Davis (1985). More arguments in favour of dynamic variations, depending upon the spread of fitness, have been made by Booker (1987).

3.2.2.9 Termination of GA search process

Because the GA is a stochastic search method, it is difficult to formally specify convergence criteria. As the fitness of a population may remain static for a number of generations before a superior individual is found, the application of conventional termination criteria becomes problematic. A common practice is to terminate the GA after a prespecified number of generations and then test the quality of the best members of the population against the problem definition. If no acceptable solutions are found, the GA may be restarted or a fresh search initiated.

3.2.2.10 Search cycle of GA

GA differs substantially from traditional search and optimization methods. Several significant attractive features of GA, as compared to other conventional search techniques, include the following (Chipperfield *et al.*, 1994; Goldberg, 1989):

- GA search process uses discontinuous objective functions.
- GA searches a population of points in parallel, not a single point. It also searches from one population of solutions to another, rather than from individual to individual.
- GA uses probabilistic transition rules, not deterministic ones.
- It works on an encoding of the control variables, rather than the variables themselves.
- It provides a number of potential solutions and the choice of the final solution is left to the user.

All these advantageous features have made the GA easy to realise, implement and apply in solving practical problems. In this particular work, the parameters of the TRMS model are identified with a pool of population as the potential parameters and through the working mechanism of GA and adopting the objective function, the best parameters are obtained within the population of the last generation. However, GA is not without its own challenges. Much care must be taken to produce an effective search algorithm and the methodology suffers from computational inefficiency. Application to real-time and safety-critical systems is highly limited at present.

3.3 Model validation

Whichever model formulation or identification algorithm is implemented, it is important to test that the identified model adequately describes the data set (Billings and Voon, 1995). In practice, the model of the system will be unknown and the detection of an inadequate fit is more challenging.

3.3.1 One step ahead prediction

A common measure of predictive accuracy used in control and system identification is to compute the one-step-ahead (OSA) prediction of the system output (Shaheed, 2000). This approach is adopted in this work and expressed as:

$$\hat{y}(t) = f\left[u(t), u(t-1), \ldots, u(t-n_u), y(t-1), \ldots, y(t-n_y)\right] \tag{3.8}$$

where $f(.)$ is a linear function, $u(t)$ and $y(t)$ are the input and output respectively. The residual or prediction is the difference between the measured output and the predicted output, given by:

$$\varepsilon(t-1) = y(t) - \hat{y}(t) \tag{3.9}$$

Often $\hat{y}(t)$ will be a relatively good prediction of $y(t)$ over the estimation set even if the model is biased because the model was estimated by minimizing the prediction errors.

3.3.2 Correlation tests

A more convincing method of model validation is to use correlation tests. These tests not only give information on the quality of the model structures being investigated but also indicate bias to noise. If a model is adequate then the residuals or prediction errors $\varepsilon(t)$ should be unpredictable from all linear and nonlinear combinations of past inputs and outputs. The derivation of simple tests that can detect these conditions is complex, but it can be shown that the following conditions should hold (Billings and Voon, 1995; Shaheed and Tokhi, 2002):

$$\phi_{\varepsilon\varepsilon}(\tau) = E[\varepsilon(t-\tau)\varepsilon(t)] = \delta(\tau) \tag{3.10}$$

$$\phi_{u\varepsilon}(\tau) = E[u(t-\tau)\varepsilon(t)] = 0 \quad \forall\tau \tag{3.11}$$

$$\phi_{u^2\varepsilon}(\tau) = E[(u^2(t-\tau) - \bar{u}^2(t))\varepsilon(t)] = 0 \quad \forall\tau \tag{3.12}$$

$$\phi_{u^2\varepsilon^2}(\tau) = E[(u^2(t-\tau) - \bar{u}^2(t))\varepsilon^2(t)] = 0 \quad \forall\tau \tag{3.13}$$

$$\phi_{\varepsilon(\varepsilon u)}(\tau) = E[\varepsilon(t)\varepsilon(t-1-\tau)u(t-1-\tau)] = 0 \quad \tau \geq 0 \tag{3.14}$$

where, $\phi_{\varepsilon\varepsilon}(\tau)$, the auto-correlation of the residuals in equation (3.10) should be an impulse, and $\phi_{u\varepsilon}(\tau)$, the cross-correlation between the input $u(t)$ and residuals $\varepsilon(t)$ should ideally be zero. Ideally the model validity tests should detect all the deficiencies in the algorithm performance including bias due to internal noise. The cause of the bias will however be different for different assignments of input set. Consequently the full five tests defined by equations (3.10 - 3.14) should be satisfied if *u(.)'s* and *y(.)'s* are used as the input sets. Unfortunately, it is easy to show that these tests provide misleading and false results if the system is non-linear.

Correlation function between two sequences $\psi_1(t)$ and $\psi_2(t)$ is given by:

$$\hat{\phi}_{\psi_1\psi_2}(\tau) = \frac{\sum_{t=1}^{N-\tau} \psi_1(t)\psi_2(t+\tau)}{\sqrt{\sum_{t=1}^{N} \psi_1^{\,2}(t) \sum_{t=1}^{N} \psi_2^{\,2}(t)}} \tag{3.15}$$

In practice normalised correlations are computed. Normalisation ensures that all the correlation functions lie in the range $-1 \leq \hat{\phi}_{\psi_1\psi_2}(\tau) \leq 1$ irrespective of the signal strengths. The correlation will never be exactly zero for all lags and the 95% confidence band defined as $1.96/\sqrt{N}$ is used to indicate if the estimated correlation is significant or not, where N is the data length. Therefore, if the correlation function is within the confidence interval the model is regarded as adequate.

The OSA prediction and MPO tests are normally used to determine the model validity in the case of non-linear modelling (Shaheed, 2000). Estimation set and test set could be used in the cases of both linear and non-linear modelling. Among the five correlation tests, equations (3.10) and (3.11) are generally used to determine model validity in the case of linear modelling whereas all five equations (3.10) - (3.14) are used in the case of non-linear modelling.

In this type of investigation, it is always advantageous to apply pre-processing transformations to the input data before it is presented to the model. In order to fit the model, the relative magnitude of the input variables has to be reduced; which will lead to convergence. One common form of pre-processing is implemented here, which is linear rescaling of the input variables. Linear transformation is applied to rearrange for all the inputs to have similar values. This is usually done by retreating each of the input variables independently and calculating the mean $\bar{x}_i$ and variance $\sigma^2{}_i$ for each variable with respect to the presented data set (Billings and Voon, 1986, 1995; Bishop, 1995; Shaheed and Tokhi, 2002):

$$\bar{x}_i = \frac{1}{N}\sum_{n=1}^{N} x_i{}^n \tag{3.16}$$

$$\sigma^2{}_i = \frac{1}{N-1}\sum_{n=1}^{N}\left(x_i{}^n - \bar{x}_i\right)^2 \tag{3.17}$$

where, $n = 1,\ldots,N$ labels the patterns. Thus, a set of rescaled variables is defined by:

$$x^n{}_i = \frac{x^n{}_i - \bar{x}_i}{\sigma_i} \tag{3.18}$$

The transformed variables given by $\bar{x}_i^n$ have zero mean and unit standard deviation over the transformed data set. It was observed that with rescaled variables, the results obtained were better.

3.4 Implementation and results

The TRMS set-up is very sensitive to the atmospheric disturbances; hence, it was ensured that the identification experiments are conducted in calm air. The test signal was designed separately and read from the workspace in the MATLAB\Simulink environment. This is analogous to automation of the test signal, which ensures the experiments to be sufficiently controlled, be repeatable, and guarantees the desired spectral content.

The body resonance modes of the TRMS lie in a low frequency range of 0-3 Hz, while the main rotor dynamics are at significantly higher frequencies (Ahmad *et al.*, 2002). The excitation signal represents voltage input to the main rotor and the output signal represents the elevation angle (pitch angle) in radians. During experimentation, the yaw plane that represents the horizontal movement is physically locked, allowing only vertical plane motion. Trim configuration for the identification experiments was steady-state horizontal position of the beam of the TRMS.

3.4.1 Excitation signals

To investigate variations in the detected vibration modes of the TRMS, modelling exercise is carried out based on the actual system response to the applied excitation signal. A pseudo-random binary signal (PRBS), covering the dynamic range of interest of the TRMS flexible system is used as an excitation signal. For comparison purposes, the system is also modelled with a random gaussian signal (RGS) excitation signal.

The system was excited with PRBS and RGS signals of 10 Hz bandwidth for the duration of 120 sec. The two utilized excitation signals (PRBS and RGS) and their corresponding power spectral density plots are depicted in Figures 3.7 and 3.8,

respectively. The magnitude of the excitation signal was selected so that it does not drive the TRMS out of its linear operating range.

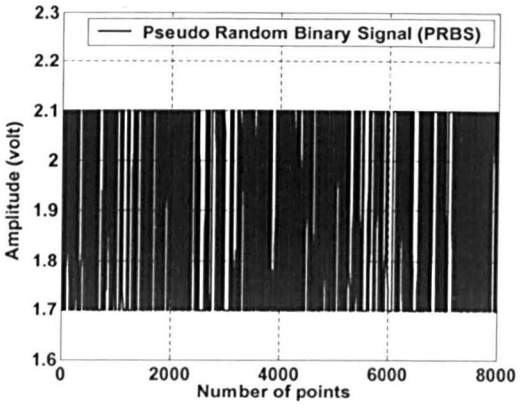

(a) Input signal (PRBS)

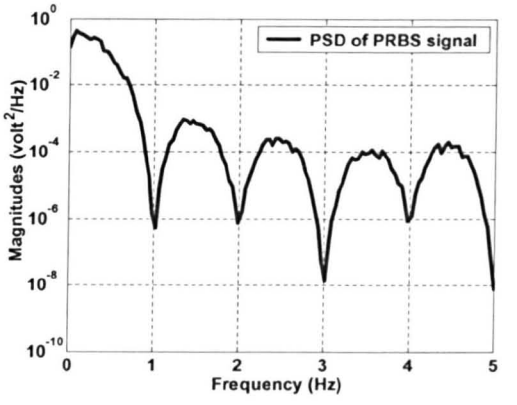

(b) Power spectral density plot of input (PRBS)

Figure 3.7: Pseudo random binary signal (PRBS)

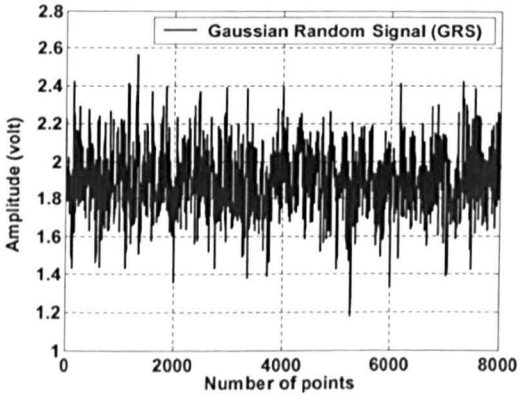

(c) Input signal (RGS)

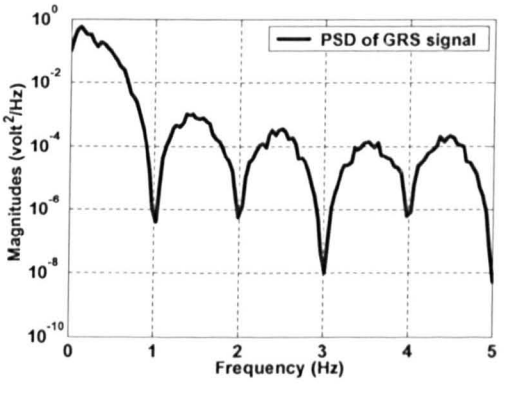

(d) Power spectral density plot of input (RGS)

Figure 3.8: Random gaussian signal (RGS)

The measured data was sampled and recorded on a PC using the real-time kernel (RTK) software (discussed in Chapter 2). Data quality and consistency are crucial to the identification. Excessively noisy or kinematically inconsistent data may lead to identification of an incorrect model. Preliminary checks of data quality and consistency can ensure that these sources of error are minimised. Moreover, in

order to ensure accurate identification application of each signal was repeated many times until a desired undisturbed response was obtained.

To overcome the problem of obtaining a biased model, the observed input and output data are divided into two data sets, referred as; estimation data and validation data sets. The estimation set is fed into the algorithm to develop a model. The model usually tracks the system output well and converges to a target error value. However, the validation data, which is different from the estimation data set, is presented to the developed model to verify its performance against the actual data. The optimisation function utilised is the mean-squared error (MSE) between the actual output $y(n)$ of the system and the estimated output $\hat{y}(n)$.

3.4.2 Model structure

The first step involved in the identification exercise, whether it is parametric or non-parametric, is to select the model structure. In this work, an auto-regressive with exogenous input (ARX) model structure was considered for parametric estimation using RLS and GA. This type of model structure is given as:

$$y(t)+a_1 y(t-1)+\ldots+a_{n_a} y(t-n_a)=b_1 u(t-1)+\ldots+b_{n_b} u(t-n_b)+e(t) \tag{3.19}$$

where a_i and b_i are the parameters to be identified. In this investigation, parametric identification using RLS and GA techniques is considered and their performances are presented and discussed in the subsequent sections.

3.4.3 Parametric modelling using RLS estimation

In the RLS estimation, from all attempted model orders ranging from 4 to 10, the best result was achieved with an order 4 and forgetting factor λ set to 0.96. The results are shown in Figures 3.9 - 3.12. Figures 3.9 and 3.10 show the performance of RLS estimation with distributed PRBS input and the corresponding correlation test results, respectively. Figures 3.11 and 3.12 show RLS estimation profile with RGS and its corresponding correlation test results, respectively. With both excitation signals the RLS estimation recorded a good tracking performance as shown in

Figures 3.9 and 3.11. It is also noted in Figures 3.9(d) and 3.11(d) that the RLS algorithm achieved satisfactory MSE levels of 5.62320×10^{-5} and 2.22431×10^{-4} with RGS and PRBS inputs, respectively. The main dominant mode of vibration of the TRMS found from the spectral density plots of the predicted output of the model was 0.35156 Hz as shown in Figures 3.9(e) and 3.11(e). Results of the corresponding correlation tests are shown in Figures 3.10 and 3.12 for the RLS based model using PRBS and RGS inputs, respectively, which in most cases are within the 95% confidence levels. These results thus confirm the adequacy of the obtained model.

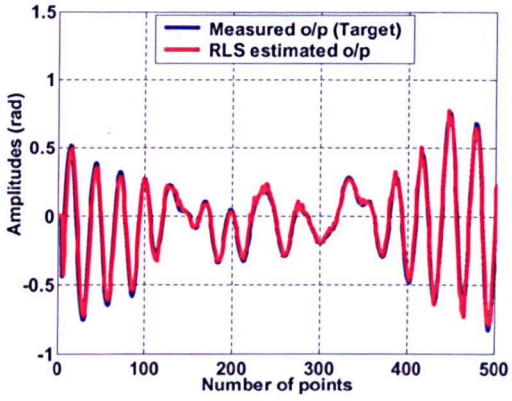

(a) Actual and predicted output (First 500 points)

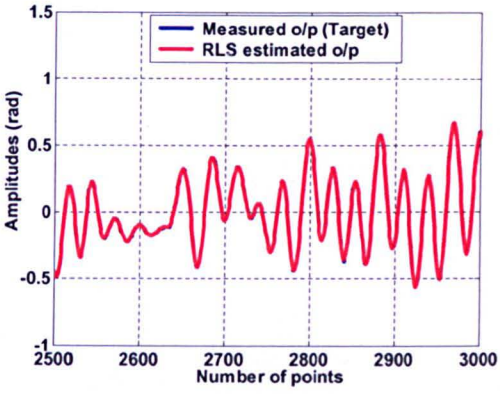

(b) Actual and predicted output (Last 500 points)

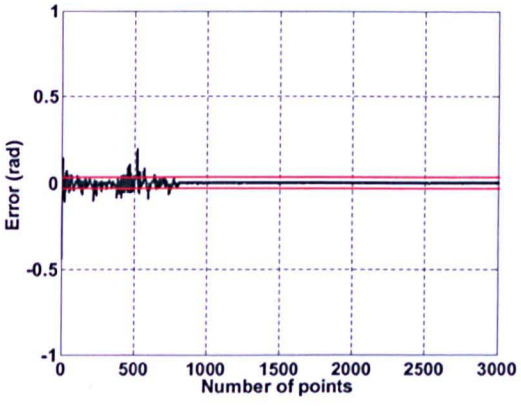

(c) Error between actual and predicted output

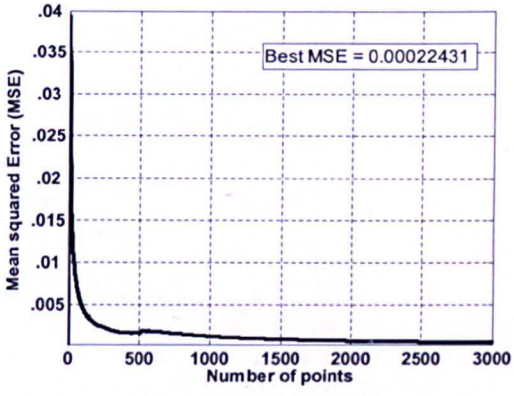

(d) Convergence of error

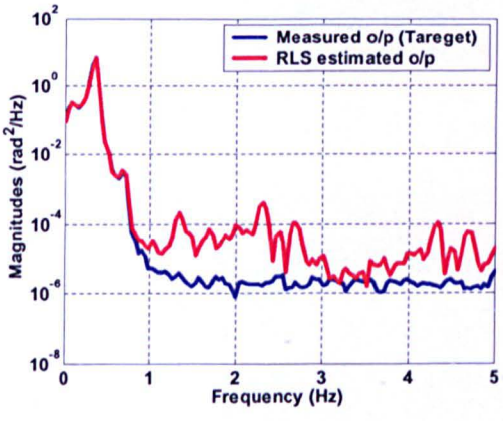

(e) Spectral density of actual and predicted output

Figure 3.9: RLS estimation with PRBS input

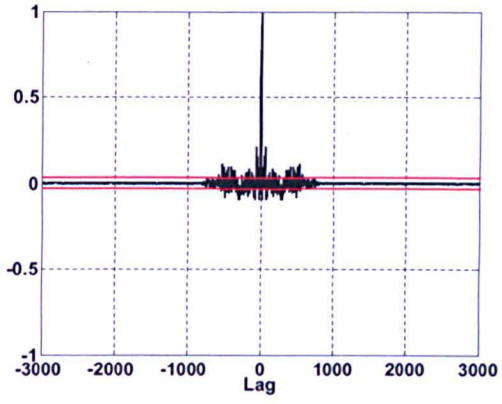

(a) Auto-correlation of residuals

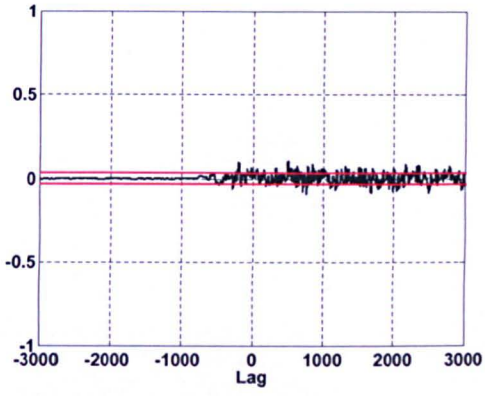

(b) Cross-correlation of input and residuals

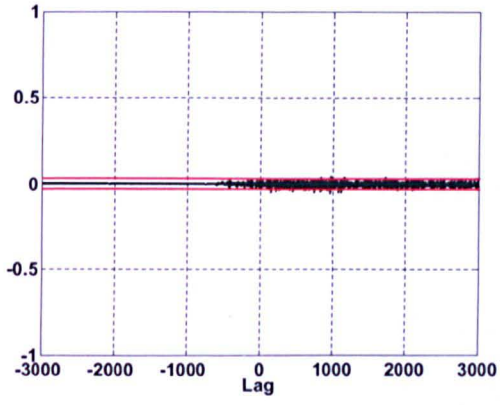

(c) Cross-correlation of input square and residuals

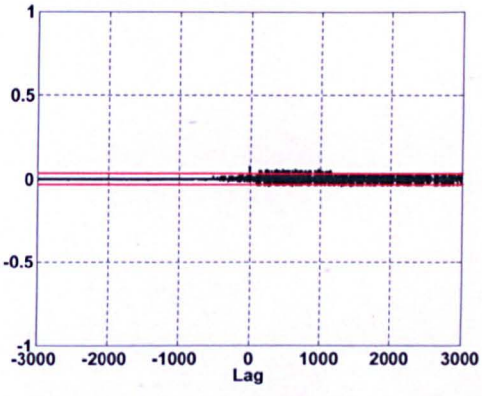

(d) Cross-correlation of input square and residuals square

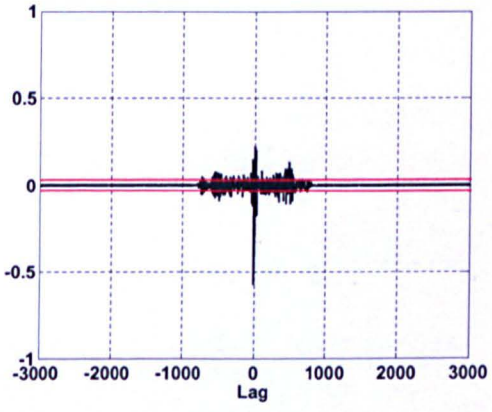

*(e) Cross-correlation of residuals and (input * residuals)*

Figure 3.10: Correlation tests of RLS model with PRBS input

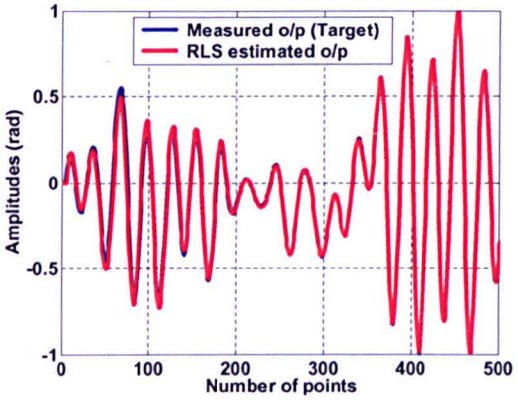

(a) Actual and predicted output (First 500 points)

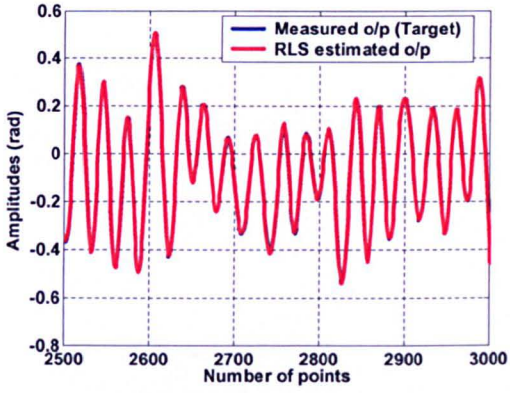

(b) Actual and predicted output (Last 500 points)

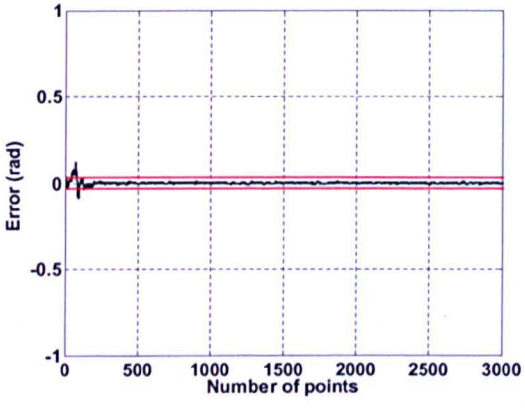

(c) Error between actual and predicted output

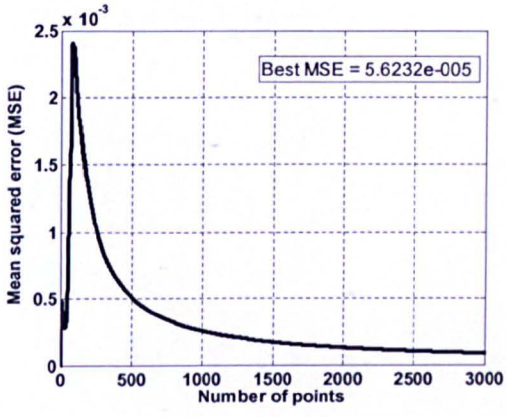

(d) Convergence of error

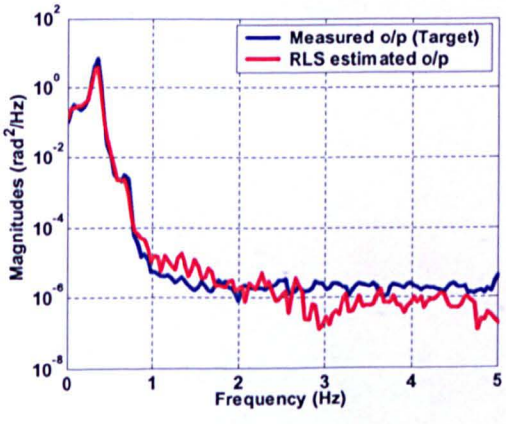

(e) Spectral density of actual and predicted output

Figure 3.11: RLS estimation with random input signal

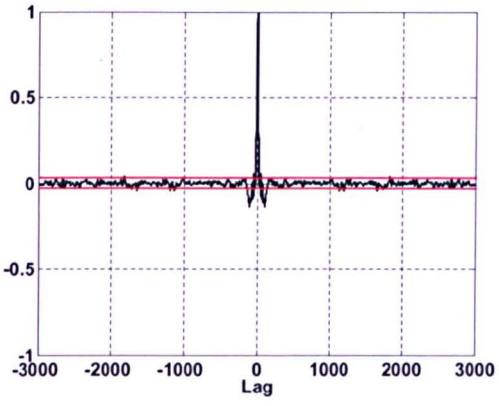

(a) Auto-correlation of residuals

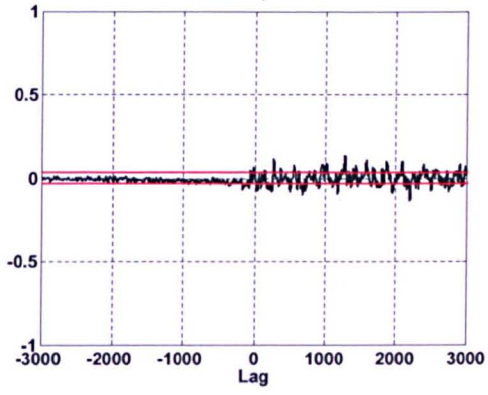

(b) Cross-correlation of input and residuals

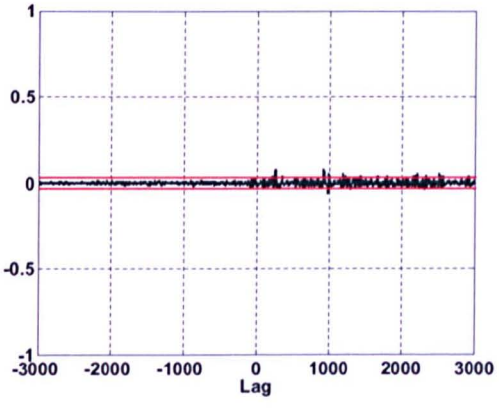

(c) Cross-correlation of input square and residuals

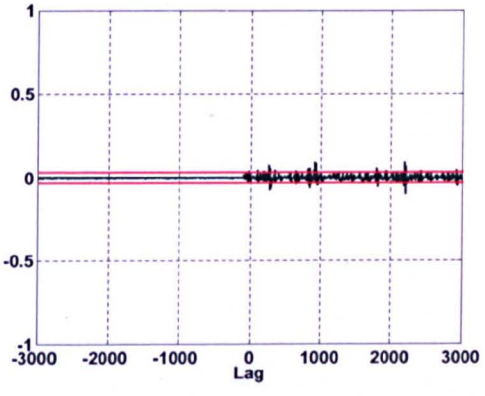

(d) Cross-correlation of input square and residuals square

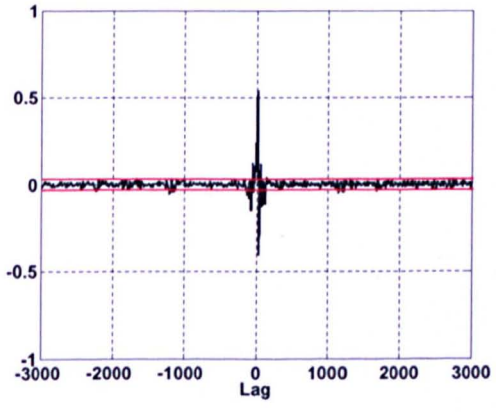

*(e) Cross-correlation of residuals and (input * residuals)*

Figure 3.12: Correlation tests of RLS model with random input

3.4.4 Parametric modelling using GA

In this investigation, randomly selected parameters are optimised for different, arbitrarily chosen order to fit to the system by applying the working mechanism of GA as explained earlier. In identifying the parameters of the model the MSE between the actual output $y(i)$ and the predicted output $\hat{y}(i)$ is adopted as the objective function of GA optimisation and given below:

$$f(x)=\frac{1}{N}\sum_{i=1}^{N}|y(i)-\hat{y}(i)|^2 \tag{3.20}$$

where N is the number of input/output data points. With the fitness function given above, the global search technique of the GA is utilised to obtain the best parameters among all attempted orders for the system, ranging from 4 to 10. Satisfactory results were achieved with order 4 and the following set of parameters; generation gap as 0.8, crossover rate as 0.67 and mutation rate as 0.001. The parameters of the model were represented by real strings with the GA convergence considered with 50 individuals over 100 generations.

The results of GA modelling exercise are shown in Figures 3.13 - 3.16. Figures 3.13 and 3.14 show the performance of GA prediction with distributed PRBS input and the corresponding correlation test results, respectively. Figures 3.15 and 3.16 show the GA prediction profile with RGS and its corresponding correlation test results, respectively. Figures 3.13(c) and 3.15(c) show the algorithm convergence for estimation data, and the simulated output with the best parameter set in both time and frequency domains. The algorithm achieved the best MSE levels of 1.0553×10^{-6} and 1.6660×10^{-6} in the 100^{th} generation using RGS and PRBS inputs, respectively.

Similar to RLS estimation, the main resonant mode was found from the GA predicted output at 0.35156 Hz. Results of the corresponding correlation tests are shown in Figures 3.14 and 3.16 for the GA based model using PRBS and RGS inputs, which in most cases are within the 95% confidence levels. These thus confirm the adequacy of the model. From the modelling exercises carried out, it is observed that with the correct parameters chosen for RLS and GAs, both can estimate the system well and manage to locate resonance frequencies of the system.

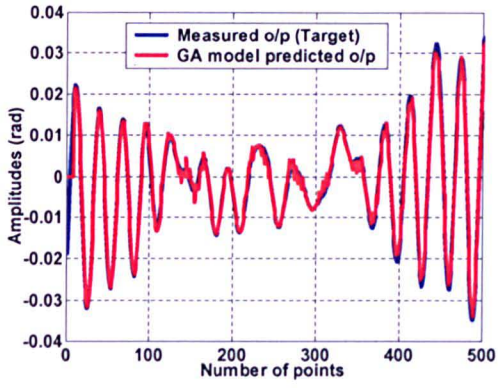

(a) Actual and predicted output (First 500 points)

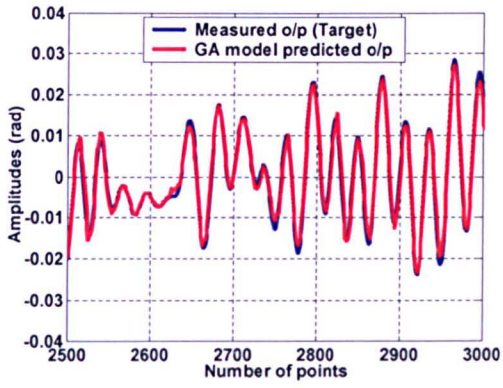

(b) Actual and predicted output (Last 500 points)

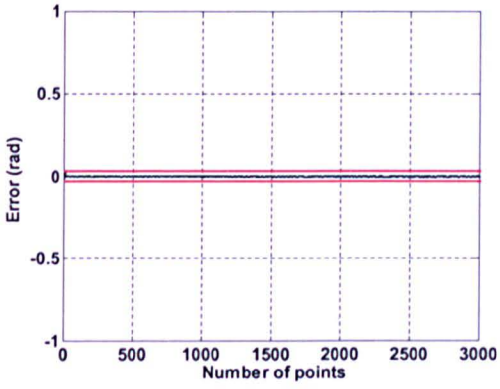

(c) Error between actual and predicted output

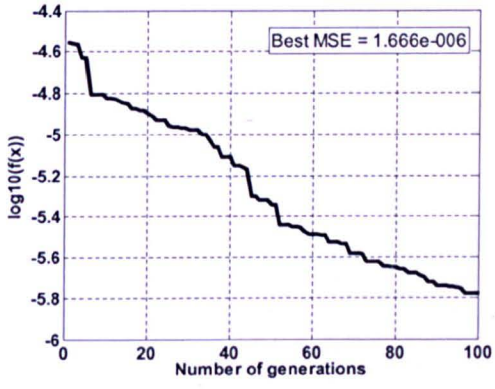

(d) Convergence of error

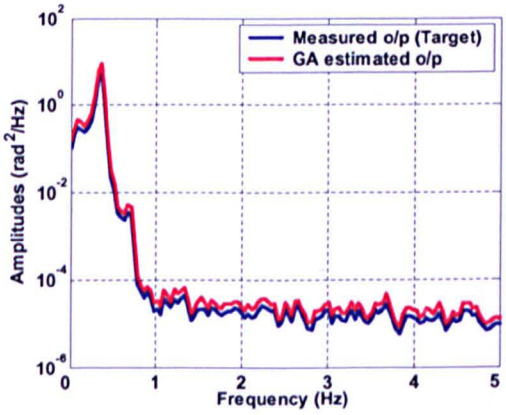

(e) Spectral density of actual and predicted output

Figure 3.13: GA prediction with PRBS input

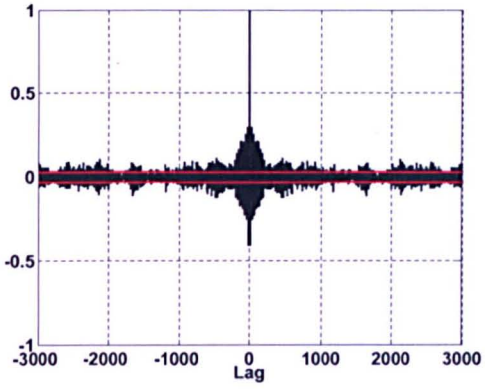

(a) Auto-correlation of residuals

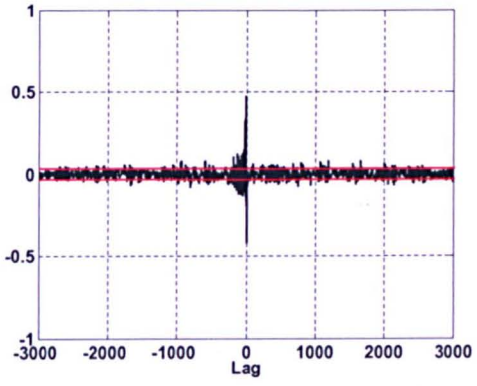

(b) Cross-correlation of input and residuals

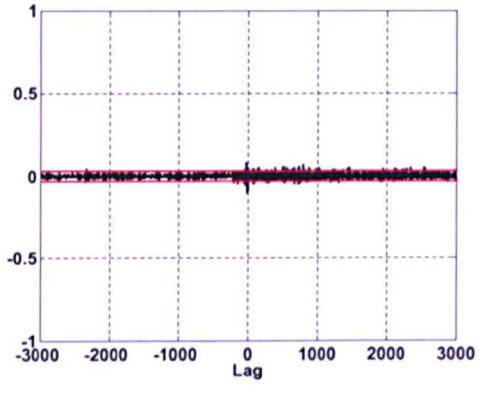

(c) Cross-correlation of input square and residuals

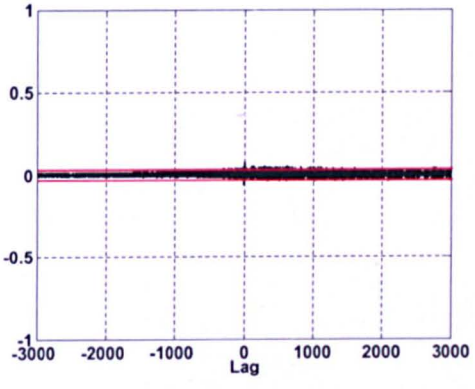

(d) Cross-correlation of input square and residuals square

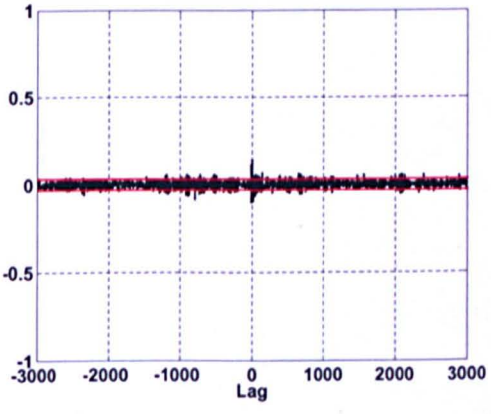

*(e) Cross-correlation of residuals and (input * residuals)*

Figure 3.14: Correlation tests of GA model with PRBS input

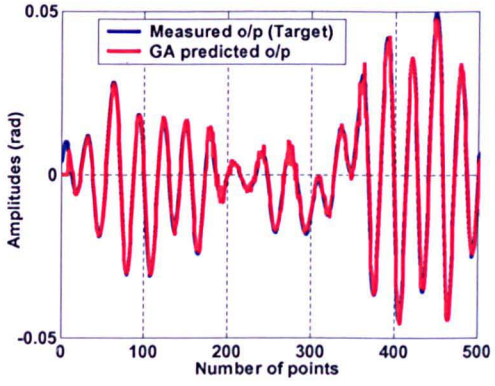

(a) Actual and predicted output (First 500 points)

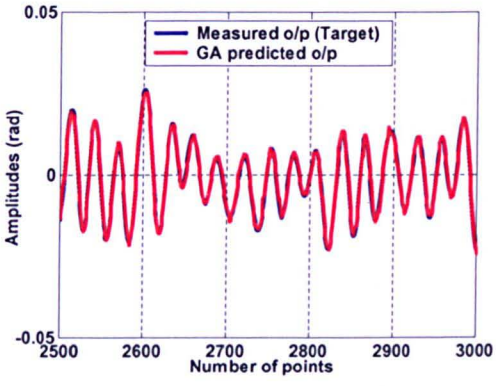

(b) Actual and predicted output (Last 500 points)

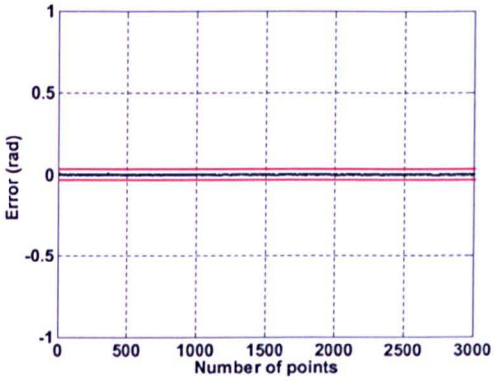

(c) Error between actual and predicted output

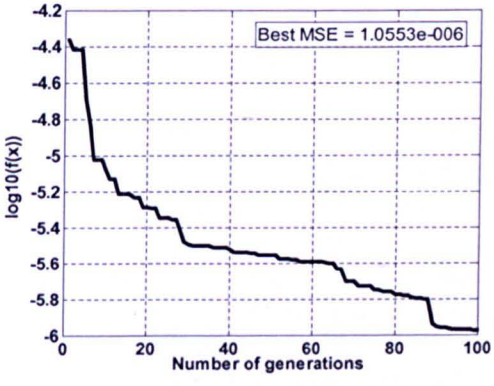

(d) Convergence of error

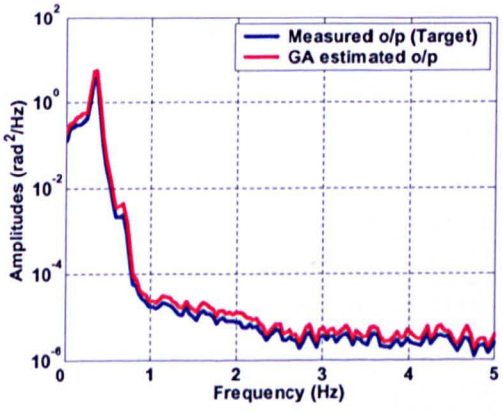

(e) Spectral density of actual and predicted output

Figure 3.15: GA prediction with random input

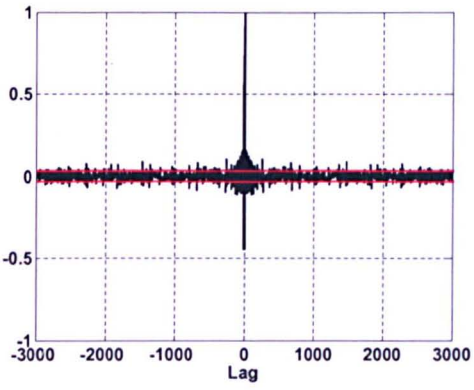

(a) Auto-correlation of residuals

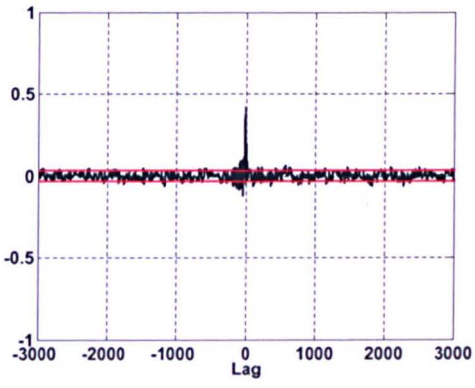

(b) Cross-correlation of input and residuals

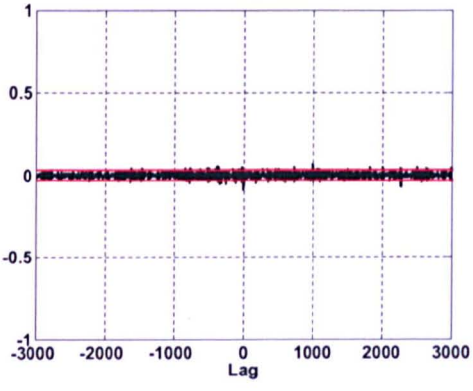

(c) Cross-correlation of input square and residuals

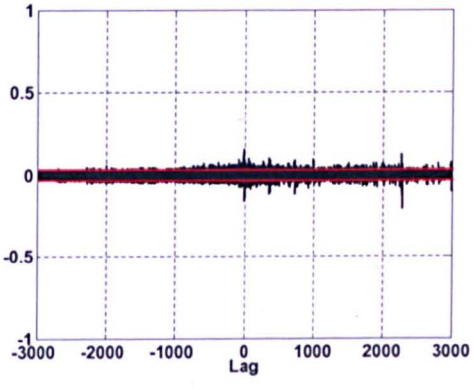

(d) Cross-correlation of input square and residuals square

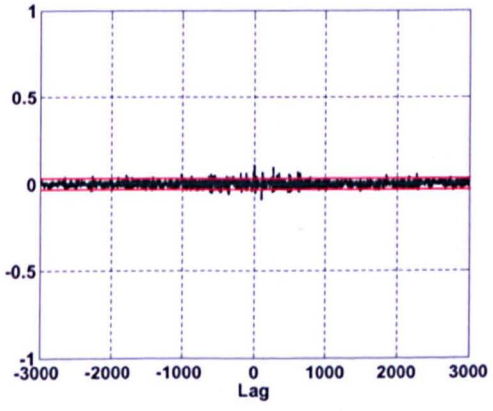

*(e) Cross-correlation of residuals and (input * residuals)*

Figure 3.16: Correlation tests of GA model with random input

3.5 Comparative assessment

Comparative performance of parametric modelling using RLS and GA techniques in terms of detecting the main resonance mode of the system and minimizing the error (MSE) between the actual and model outputs is assessed in this section. The quantities representing this comparative assessment are summarised in Table 3.1. It can be seen that the employed techniques have been able to detect the main resonant mode of the system successfully. GA based parametric modelling technique gives better approximation to the system response compared to RLS technique, as the GA uses a global search process in finding the parameters. It was also noted with the correlation tests that the GA performed better than RLS. However, a major advantage of the RLS is that the algorithm is simple. Also, the execution time of the RLS based algorithm was shorter than that of GA technique with the same computing platform. However, high performance computing techniques could provide appropriate solutions for the real-time implementation of the GA based identification.

Table 3.1: Performance of the employed parametric modelling methods

Parametric Modelling Technique	Mean-squared error (MSE)		Main resonant mode (Hz)	
	PRBS input	RGS input	PRBS input	RGS input
RLS Estimation	2.243E-004	5.623E-005	0.35156	0.35156
GA Prediction	1.666E-006	1.666E-006	0.35156	0.35156

3.6 Summary

Linear system identification, using the potential of RLS and GA techniques, has been investigated for parametric modelling of the TRMS in hovering operation. The aim of the identification experiments is to get a satisfactory model of pitch plane dynamics (elevation angle).

Good excitation was achieved from 0-5 Hz, which includes all the important rigid body and flexible modes of the system. It has been found that the significant system modes lie in the 0-1 Hz bandwidth. Both RLS and GA performed very well in detecting the main resonance mode (0.35156 Hz) of the system and their performances were quite comparable.

Both time and frequency domain analyses have been utilised to assess and develop confidence in the models obtained. The frequency domain verification method is a useful tool in the validation of extracted parametric models. It allows high-fidelity verification of dynamic characteristics over a frequency range of interest.

The extracted models have predicted the system behaviour well. It is presumed that the resulting models will be utilized in the succeeding chapters in designing controllers for low frequency vibration suppression (Chapter 5), development of suitable feedback control laws for set-point tracking and disturbance rejection (Chapter 6), and design of augmented feedforward and feedback control scheme for both vibration suppression and tracking performance (Chapter 7). Accordingly, the modelling approach presented is suitable for a certain class of new generation air vehicles, whose flight mechanics are not well understood.

CHAPTER 4

NONLINEAR MODELLING OF THE TWIN ROTOR SYSTEM USING MULTI-LAYER PERCEPTRON NEURAL NETWORKS

4.1 Introduction

In many cases when it is difficult to obtain a model structure for a system using traditional system identification approaches, intelligent techniques may be used to describe the system in the best possible way (Elanayar and Yung, 1994). Genetic algorithm (GA), neural network (NN), fuzzy logic (FL), and neuro-fuzzy inference system (ANFIS) are intelligent techniques commonly used for system identification and modelling. Their excellent pattern recognition capability, in determining models that best represent the behaviour of non-linear systems that might be difficult to obtain using traditional approaches (Elanayar and Yung, 1994; Shaheed, 2000).

NN approach offers many advantages over traditional ones especially in terms of flexibility and hardware realisation (Ljung and Sjöberg, 1992). The technique is quite efficient in modelling non-linear systems or if the system possesses nonlinearities to any degree. Recently NNs have become an attractive tool for use in constructing models of non-linear processes. This is because NNs have an inherent ability to learn and approximate non-linear functions. This therefore provides a possible way of modelling non-linear processes effectively (Irwin *et al.*, 1995; Thapa *et al.*, 2000).

The work in this chapter is devoted to exploration the potential of NNs in non-linear modelling exercise to characterise the behaviour of the TRMS. A black-box system identification technique based on multi-layer perceptron NN (MLPNN) is utilized to model the TRMS in its hovering operation, with neither a priori defined model structure nor specific parameter settings reflecting any physical aspects of the system. Such a high fidelity nonlinear model is often required for the design and implementation of non-linear feedback controllers. The resulting non-parametric

black-box model is then subjected to several validation methods including correlation and spectral analyses. The aim of the non-parametric modelling is for the design and implementation of non-linear feedback controllers based on the identified non-parametric model.

4.2 Non-parametric modelling

Parametric and non-parametric estimations are the two major classes of system identification technique (Shaheed and Tokhi, 2002). Non-parametric identification methods are techniques to estimate model behaviour without necessarily using a given parameterised model set.

Diverse modelling techniques can be used to identify non-linear dynamic systems. These include state-output model, recurrent state model and NARMAX model. However, it is evident from the literature that if the input and output data of the plant are available, NARMAX model is a suitable choice for modelling systems with nonlinearities, using standard BP learning algorithm (Shaheed and Tokhi, 2002), which is given as:

$$\begin{aligned}\hat{y}(t) = f[(&y(t-1), y(t-2), \cdots, y(t-n_y), u(t-1), u(t-2), \cdots, u(t-n_u),\\ &e(t-1), e(t-2), \cdots, e(t-n_e)] + e(t)\end{aligned} \tag{4.1}$$

where, $\hat{y}(t)$ is the output vector determined by the past values of the system input vector, output vector and noise with maximum lags n_y, n_u and n_e, respectively. $f(.)$ is the system mapping function, constructed through an NN method with an appropriate learning algorithm. Luo and Unbehauen (1997) emphasized that if the model is good enough to identify the system without incorporating the noise term or considering the noise as additive at the output the model can be represented in a non-linear autoregressive model with exogenous inputs (NARX) form, given by:

$$\hat{y}(t) = f[(y(t-1), y(t-2), \cdots, y(t-n_y), u(t-1), u(t-2), \cdots, u(t-n_u)] + e(t) \tag{4.2}$$

where, $\hat{y}(t)$ is the output, $u(t)$ is the input and $e(t)$ accounts for uncertainties, possible noise, unmodelled dynamics, etc. n_y and n_u are the maximum lags in the output and

input vectors. *e(t)* is assumed to be a zero mean white noise sequence and *f(.)* is some vector valued nonlinear function of *y(t)* and *u(t)*. The NARX model is also referred to in the literature by various other names such as one-step ahead (OSA) predictor or as series-parallel model. Because the system noise *e(t)* is generally unobserved, it can be replaced by the prediction error or residual $\varepsilon(t)$, and equation (4.2) can be re-written as:

$$\hat{y}(t) = f[(y(t-1), y(t-2), \cdots, y(t-n_y), u(t-1), u(t-2), \cdots, u(t-n_u)] + \varepsilon(t) \qquad (4.3)$$

where, the residual is defined as:

$$\varepsilon(t) = y(t) - \hat{y}(t) \qquad (4.4)$$

where, *y(t)* is the actual output and $\hat{y}(t)$ is the model predicted output.

4.3 Neural networks

Artificial neural networks (ANNs) constitute one of the potential tools employed in intelligent control applications. Intelligent control is a control technology that replaces the human mind in making decisions, planning control strategies, self-organizing, and adaptation and learning new functions whenever the environment does not allow or does not justify the presence of a human operator (Lin and Su, 2000).

The application of NNs has attracted significant attention in several disciplines, such as signal processing, identification and control. NNs possess an inherent nonlinear structure suitable for mapping complex characteristics, learning and optimization (Hornik *et al.*, 1989; Rumelhart and McClelland, 1986; Widrow and Laher, 1990). These features have recently been shown to have considerable potential for the modelling and control of nonlinear dynamic systems (Miller *et al.*, 1990; Narendra and Parthasarathy, 1990, 1991). This fundamental link of NNs to nonlinear system representation, together with the availability of reliable and inexpensive computing hardware, has resulted in a tremendous growth of research and development in the area. The limitation of many of the conventional control

schemes for nonlinear systems is another important reason for the interest in neural designs (Miller *et al.*, 1990).

The first application of NNs to control systems was developed in the mid-1980s. Models of dynamic systems and their inverses have immediate utility in control. In the literature on NNs, architectures for the control and identification of a large number of control structures have been proposed and used (Miller *et al.*, 1990; Narendra and Parthasarathy, 1990). For network learning, error backpropagation is one of the standard methods used in these cases to adjust the weights of NNs (Narendra and Parthasarathy, 1991).

Mistry and Nair (1994) considered real-time neural identification and control designs using multiplayer feedforward networks and reported implementation results using a single-input single-output (SISO) hardware example case system with both time-varying and time-invariant load dynamics. Obtained results illustrated that neural designs are experimentally viable for on-line identification and control. Dynamic neural schemes were also found to consistently perform much better as compared to the static schemes. Reduced order linear observers were also being investigated for use in dynamic schemes for the time-invariant load case to improve convergence and learning features as compared to the static cases (Mistry *et al.*, 1996).

Henriques *et al.* (1999) applied a combination of a modified recurrent Elman network with a truncated backpropagation through time (BTT) algorithm for modeling non-linear plants. This approach is proved from the experiments on the laboratory plant, to be a feasible alternative for real-time identification. In this context, given the adaptive features revealed by the Elman networks, also implied their ability in modelling any kind of nonlinearities in the form of non-linear state space representation. Dynamic recurrent neural networks (DNNs) are bringing a valuable added-value to the control field and particularly to those strategies using an explicit model of the plant to be controlled.

Efe and Kaynak (2000) have reported identification of robotic manipulators using NNs and ANFIS. Arai *et al.* (1994) have reported modelling and trajectory control of flexible plate structures using NNs and Sharma (2000) has reported NNs for dynamic modelling and control of a flexible manipulator. Due to some clear

successes with NNs and fuzzy logic (FL) systems, there is considerable interest in examining their potential for aircraft control. To date, aircraft have shown themselves to constitute a unique and difficult application that is not amenable to most control techniques (Lin and Su, 2000). While most advanced control techniques have been demonstrated in limited fidelity simulation with an aircraft as the controlled plant, very few have been used in any way on production aircraft. One reason NN/FL technology may be right for aircraft is that it could provide a viable method for the design and implementation of true nonlinear control laws (Steinberg, 1994). A major application area for NNs based control is in the field of flight control of either manned or unmanned aerial vehicles. For these applications, the dynamics are highly nonlinear and can undergo variations due to transitions in flight conditions, initiation of highly dynamic maneuvers involving large state excursions from trim flight conditions, or due to failures in actuators and damage to the airframe.

Artificial NNs, which have the ability to approximate general continuous nonlinear functions, are ideal for the adaptive flight control application (Hornik *et al.*, 1989; Sanner and Slotine, 1992). One advantage of the NN over simple lookup table approaches is the reduced amount of memory and computation time required. In addition, the NN can provide interpolation between training points with no additional computational effort. Furthermore, experience has shown that NNs function as highly nonlinear adaptive control elements and offer distinct advantages over more conventional linear parameter adaptive controllers in achieving desired performance. The literature includes numerous applications of NNs to flight control systems. Applications in which NNs are used to control super-manoeuvrable aircraft are described by Baker and Farrel (1991), and by Steck and Rokhaz (1992). Survey papers commenting on the role of NN technology in flight control system design have been contributed by Werbos (1995) and Steinberg (1994). Examples of applications to helicopters and tilt-rotors aircraft may be found in (Jiang *et al.*, 1996; Leitner *et al.*, 1997; Rysdyk and Calise, 1998; Rysdyk *et al.*, 1997).

Baker and Farrel (1991) motivated and described an approach for the design and development of a learning augmented flight control system for high performance aircraft. Troudet *et al.* (1991) designed a model following neurocontroller for integrated airframe/propulsion linearized model of a modern fighter aircraft.

Calise (1996) presented an on-line adaptive architecture that employed NN to compensate for inversion error present when feedback linearization methods are employed to control a dynamic process (fighter aircraft). A stable weight adjustment rule for the NN was presented, and the used on-line adaptation approach employed concepts from (Sanner and Slotine, 1992), wherein the dynamics are linear in the control variable.

Kaneshige and Gundy-Burlet (2001) presented an Integrated Neural Flight and Propulsion Control System (INFPCS), which used a NN based approach for applying alternate sources of control power in the presence of damage or failures. Under normal operating conditions, the system utilized conventional flight control surfaces. Neural networks were used to provide consistent handling qualities across flight conditions and for different aircraft configurations. Under damage or failure conditions, the system utilized unconventional flight control surface allocations, along with integrated propulsion control, when additional control power was necessary for achieving desired flight control performance. In that case, NNs were used to adapt to changes in aircraft dynamics and control allocation schemes.

The neural flight control architecture was based upon the augmented model inversion controller, developed by Rysdyk and Calise (1998). This direct adaptive tracking dynamic inverse controller integrates feedback linearization theory with both pre-trained and on-line learning NNs. Piloted simulation studies were performed at NASA Ames Research Center on a commercial transport aircraft simulator. The obtained results demonstrated the potential for improving handling qualities and significantly increasing survivability rates under various simulated failure conditions. Of significant importance here is the fact that this system can operate without emergency or backup flight control mode operations. An additional advantage is that this system can utilize, but does not require, fault detection and isolation information or explicit parameter identification.

4.3.1 Multi-layer perceptron neural network

In developing a NN model, the structure/topology of the network must first be declared. The most popular neural architecture is the multi-layer perceptron (MLP), deployed in this work for developing a non-linear non-parametric model of the

TRMS in hovering mode. MLPNNs are widely used in many applications including pattern recognition, fault detection, system identification, prediction, control system design, speech and natural language processing (Tokhi *et al.*, 2000). This network consists of an input layer, one or more hidden layers and output layer as shown in Figure 4.1. Each layer consists of computing elements called neurons. The input layer usually acts as an input data holder, which distributes inputs into the first hidden layer. Usually all the nodes in a layer are fully connected to the nodes in the adjacent/following layer, but there is no connection between nodes within the same layer and no direct connection between the bridging layers. Data flows through the MLP network in one direction only, from input to output layers, thus, it is referred to as a feedforward network. An important feature of MLPNN is that this network can accurately represent any continuous non-linear function relating the inputs and outputs (Funahashi, 1989). This feature makes MLPNN an attractive topology for many applications, including modelling and control of non-linear systems.

An MLPNN network can be made up of any number of layers with reasonable number of neurons in each layer, based on the nature of the application. The layer to which the input data is supplied, is called the input layer and the layer from which the output is taken is known as the output layer. All other intermediate layers are called hidden layers. The layers are fully interconnected which means that each processing unit or neuron is connected to every neuron in the previous and succeeding layers. However, the neurons in the same layer are not connected to each other.

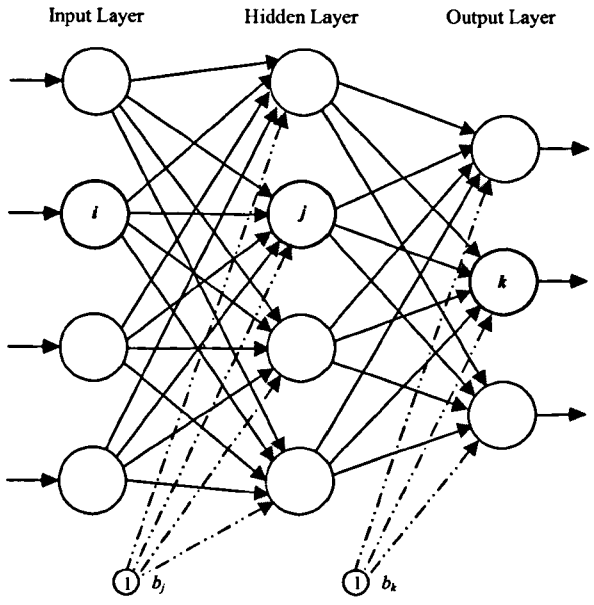

Figure 4.1: Architecture of multi-layer perceptron neural network (MLPNN)

An MLP is an adaptive network whose nodes or neurons perform the same function on incoming signals; this node function is usually a composite of the weighted sum and a differentiable non-linear activation function, also known as transfer function (Jang *et al.*, 1997). Figure 4.2 shows a structure of a neuron in an MLP network. All neurons, except those in the input layer, perform two functions. They act as a summing point for the input signals as well as propagating the input through a non-linear processing function.

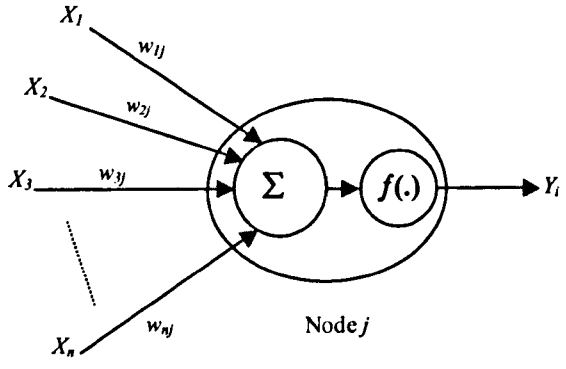

Figure 4.2: Node j of an MLPNN

In this investigation a supervised learning process, depicted in Figure 4.3, is adopted where the network is trained based on a comparison of the network output with the target till the error between them is minimized to a pre-specified tolerance level. $u(t)$ and $y(t)$ represent the observed input and output signals, respectively. While, $\hat{y}(t)$ and $\varepsilon(t)$ represent the network predicted output and the error signal, respectively The learning rule specifies how the parameters should be updated to minimize a prescribed error measure. The task is to find an appropriate NN architecture and a set of parameters which can best model an unknown target system that is described by a set of input-output data pairs (Jang *et al.*, 1997).

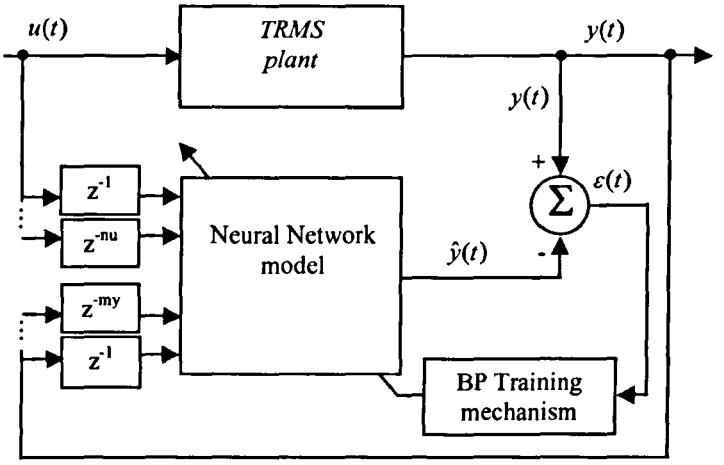

Figure 4.3: Neural network training process

4.3.2 Back-propagation learning algorithm

Once the network topology is specified, the network is trained using a minimization procedure. The training method used is a form of back-propagation of the error at the output of the network (gradient descent on the squared error at the output). This training method, Back-propagation (BP), is a steepest descent type algorithm and nowadays has become a well-known learning algorithm for feedforward NNs. It was first proposed by Werbos (1974) and further developed by Rumelhart and McClelland (1986).

The NN is trained by presenting it with a multitude of training pairs. Each pair consists of input data for the network and correct network output obtained from

the actual system. Comparison is made between the correct outputs and the network-generated outputs to determine the ability of the network to learn the required control. Sufficient training is achieved when the difference between the two sets of output becomes smaller than a predetermined tolerance. Thus, the final network architecture will be arrived at by a process of starting with a small network and increasing its size until it models the data with a sufficiently small error.

Back propagation has become popular on grounds of simplicity and its capability to learn sequentially from training instances. The derivation, implementation and properties of this algorithm have been reported by Billings *et al.* (1991, 1992). It is a particular case of mapping NNs in which the information processing operation in an approximation to some function from vectors to vectors $\left(f\colon R^n \rightarrow R^m\right)$. Nevertheless, it has many difficulties that need to be overcome, such as; how the learning algorithm escapes from trapping in local minima in the learning process? How many neurons are needed in a particular hidden layer as well as hidden layers in the whole network?

MLP networks with BP learning algorithm are the most prevalent NN architectures for modelling and control applications because they have the capability to 'learn' system characteristics through non-linear mapping. Their learning and update procedure is intuitively appealing because it is based on a relatively simple concept- if the network gives the wrong answer, the weights are corrected so that the error is reduced and as a result, future responses of the network are more likely to be corrected. When the network is given an input, the updating of activation value propagates forward from the input layer of processing units through each internal layer, to the output layer of processing units. The output units then provide the network's response. When the network corrects its internal parameters, the correction mechanism starts with the output units and propagates backward through each internal layer to the input layer. The governing equations for an MLP network with BP learning algorithm are described here.

Let O_i, O_j and O_k represent the output values of neurons i, j and k at the input, hidden and output layers, respectively. w_{ij} a connection weight from node i at the input layer to node j at the hidden layer. Similarly, w_{jk} a connection weight from neuron j at the hidden layer to neuron k at the output layer. b_j and b_k as the biases

added at the hidden and output layers, respectively. The neurons in the input layer simply store the input values. All neurons in both the hidden layer and output layer carry out two functions:

(1) They multiply all inputs and bias (bias = 1) by a weight and they sum the result as:

$$S_j = \sum_{i=1}^{N} w_{ij} O_i + b_j \tag{4.5}$$

(2) The output of the neuron O_j is calculated as a function $f(x)$ of S_j, given by:

$$O_j = f(S_j) \tag{4.6}$$

where, $f(x)$ is an activation function. Three most commonly used activation functions in MLP network with BP learning algorithm are:

- Logistic or sigmoid function: $f(x) = \dfrac{1}{1+e^{-x}}$
- Hyperbolic tangent function: $f(x) = \tanh\left(\dfrac{x}{2}\right) = \dfrac{1-e^{-x}}{1+e^{-x}}$
- Identity function: $f(x) = x$

An MLP network can consist of combinations of any of the above activation functions with linear or identity function normally used in the output layer, and sigmoid or hyperbolic tangent functions used in the hidden or input layers. The connection weights between the layers of the MLP network are adapted in accordance with the following rules:

$$\Delta w_{ij} = \eta \delta_j O_i \tag{4.7}$$

$$\Delta w_{jk} = \eta \delta_k O_j \tag{4.8}$$

where, η is the learning rate and for sigmoid function,

$$\delta_k = O_k(1-O_k)(\tau_k - O_k) \tag{4.9}$$

$$\delta_j = O_j(1-O_j)\sum_{j=1}^{N}\delta_j w_{ij} \tag{4.10}$$

and for tansigmoid function,

$$\delta_k = O_k(1-O_k^2)(\tau_k - O_k) \tag{4.11}$$

$$\delta_j = O_j(1-O_j^2)\sum_{j=1}^{N}\delta_j w_{ij} \tag{4.12}$$

The NN training may get stuck in a shallow local minimum with standard backpropagation (Shaheed, 2000). In order to avoid entering the local minimum, the learning parameters, number of hidden neurons, or initial values of the connecting weights can be changed accordingly. The learning rate η is a proportional constant rate that affects the convergence speed and stability of the weights during the learning stage. The larger the learning rate, the bigger the changes in the connecting weights. Usually, η is selected as large as possible without leading to oscillations. In order to increase the learning rate, without leading to oscillation in the output response, equations (4.7) and (4.8) can be modified to include a momentum term. This can be accomplished by the rule (Omatu *et al.*, 1996):

$$\Delta w_{ij}(t+1) = \eta\delta_j O_i + \alpha\Delta w_{ij}(t) \tag{4.13}$$

$$\Delta w_{jk}(t+1) = \eta\delta_k O_j + \alpha\Delta w_{jk}(t) \tag{4.14}$$

where, t is time and α is a constant which determines the effect of past connection weight changes on the current direction of movement in the connection weights space. The shallow local minimum problem associated with the standard BP training algorithm can be solved by using the Marquard-Levenberg modified version of the BP (Marquard, 1963). Marquard-Levenberg BP algorithm is an approximation to Newton's method (Battiti, 1992).

4.4 Implementation and results

The body resonance modes of the TRMS lie in a low frequency range of 0-3 Hz, while the main rotor dynamics are at significantly higher frequencies, as shown in sections 3.4.3 and 3.4.4 earlier. The excitation signal represents voltage input to the main rotor and the output signal represents the elevation angle (pitch angle) in radians. During experimentation, yaw plane that represents the horizontal movement is physically locked, allowing only vertical plane motion.

4.4.1 Excitation signals

In this section the characteristic of the excitation signal for nonlinear identification is delineated followed by some guidelines for input-output data pre-processing before applying it to the NNs.

In nonlinear system identification, the type of input signal to be used plays a crucial role and has a direct bearing on the fidelity of the resulting identified model. The excitation signal should be able to excite all the dynamic modes of interest. The spectral content of the input signal should be rich in frequency corresponding to system bandwidth. Such a signal is referred to as *persistently exciting*. Moreover, the excitation signal should be rich in amplitude level (i.e. has different levels of input amplitudes over the whole range of operation). These conditions can generally be fulfilled by selecting an input such as sine wave, RGS, or PRBS (Billings and Voon, 1995). In order to excite the system modes of interest, two different signals; (i) PRBS and (ii) RGS are employed as input signal in this study.

The system was excited with PRBS and RGS signals of 10 Hz bandwidth and duration of 120 seconds. The two utilized excitation signals (PRBS and RGS) and their corresponding power spectral density plots are depicted in Figures 4.4 and 4.5, respectively. The magnitude of the excitation signal was selected so that it does not drive the TRMS out of its linear operating range.

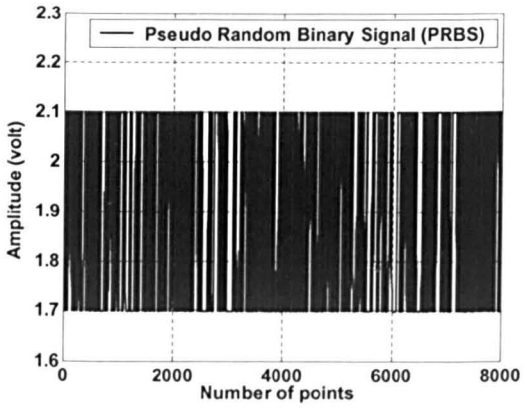

(a) Input signal (PRBS)

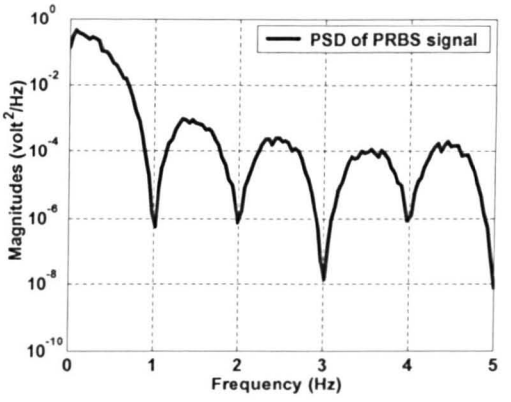

(b) Power spectral density plot of input (PRBS)

Figure 4.4: Pseudo random binary signal (PRBS)

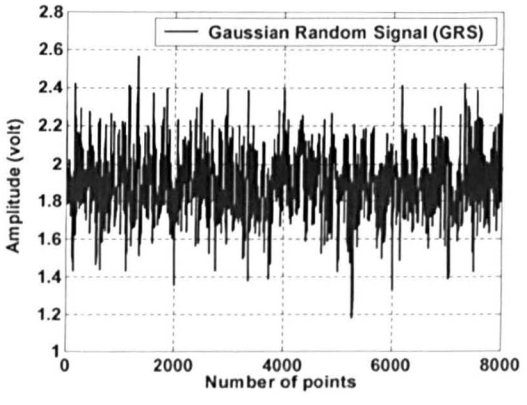

(c) Input signal (RGS)

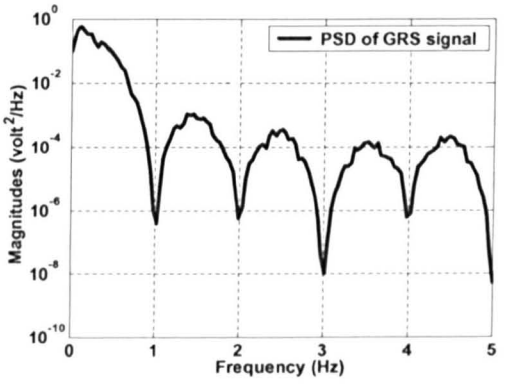

(d) Power spectral density plot of input (RGS)

Figure 4.5: Random gaussian signal (RGS)

4.4.2 Data pre-processing

Processing of the raw input-output data obtained from the experiments is recommended for system identification. Pre-processing could involve removal of outliers, stray data points and normalisation. In the case of identifying a system model using NN, it is advantageous to apply pre-processing transformations to the input data before presenting it to the network. Reducing the difference of magnitude of input variables used to train network leads to faster convergence. One of the

common methods of pre-processing is linear rescaling of the input variables. The normalised data is obtained by carrying out the following data manipulation:

$$\tilde{x}_i^n = \frac{x_i^n - \bar{x}_i}{\sigma_i} \tag{4.15}$$

where, $\bar{x}_i$ is the mean and σ_i^2 is the variance of each variable of the training set and defined as:

$$\bar{x}_i = \frac{1}{N}\sum_{n=1}^{N} x_i^n \tag{4.16}$$

$$\sigma_i^2 = \frac{1}{N-1}\sum_{n=1}^{N}(x_i^n - \bar{x}_i)^2 \tag{4.17}$$

where, $n = 1,\cdots,N$ are the number of data points or the data length. The re-scaled variables defined by $\tilde{x}_i^n$ have zero mean and unit standard deviation. The target values are also subjected to similar linear rescaling.

4.4.3 Modelling using neural network estimation

An MLPNN with standard BP learning algorithm based on OSA prediction technique is utilised for modelling the TRMS during its hovering operation. The input to the network is in a vector format consisting of several nodes of previous outputs and inputs. The network is trained to characterize the system between the detection and observation points. The network obtained, based on the minimum error produced by $\varepsilon(t) = y(t) - \hat{y}(t)$ after learning, is to be utilised as a system model.

Figures 4.6 and 4.9 show the OSA prediction of the TRMS using MLPNN approach with PRBS and RGS inputs, respectively. An MLPNN with model orders, $n_u = n_y = 4$ as the input nodes, one hidden layer with 8 tansigmoid neurons, and one output layer with linear neuron was trained to characterise the TRMS. This network structure was obtained by trial and error process for best results. 60% of the data set, which comprised 5000 data points, was used to train the network and the model was

validated with the remaining 40% of the whole data set, which comprised 3000 data points. It is observed from the prediction profiles that the model and plant outputs coincide quite well, implying good model predicting capability of the actual system's dynamics. The model reached the mean-squared error (MSE) level of 1.472746E-05 and 1.49335E-05 with PRBS and RGS inputs, respectively after 100 training passes. It is also found from the spectral density profiles that the main dominant mode of the actual system matches with its predicted model counterpart (0.35156 Hz).

Figures 4.7 and 4.9 show results of the correlation tests performed on the whole data set with PRBS and RGS inputs, respectively. In most cases, results of the correlation tests are within 95% confidence interval indicating high-level approximation of the dynamics of the TRMS system. Thus, the model validity tests corroborate that the estimated model is adequate.

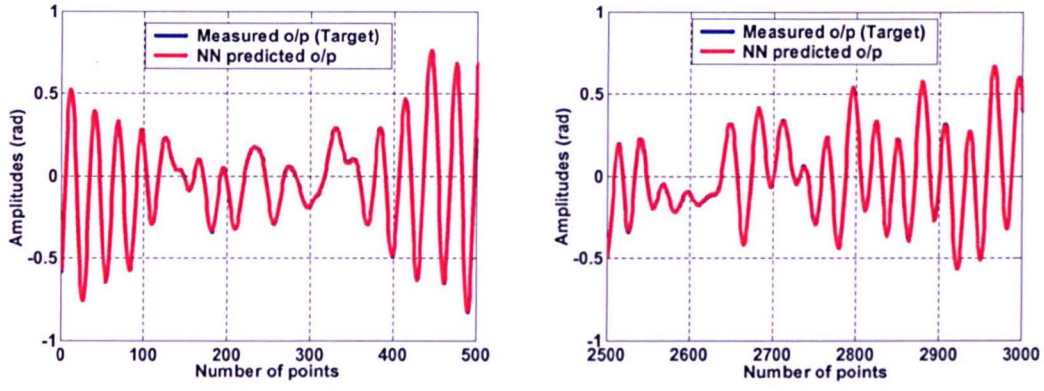

(a) Actual and predicted output (First 500 points) *(b) Actual and predicted output (Last 500 points)*

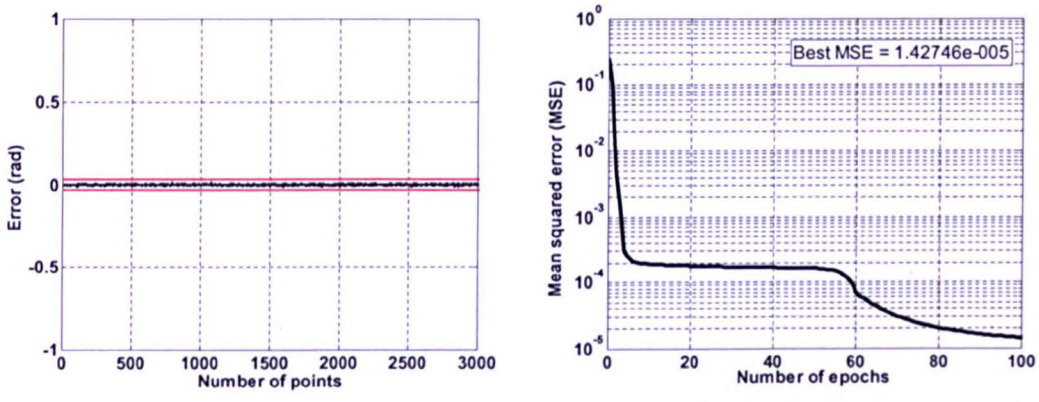

(c) Error between actual and predicted output *(d) Convergence of error*

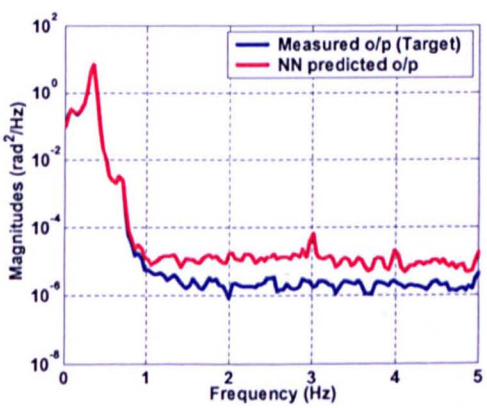

(e) Spectral density of actual and predicted output

Figure 4.6: MLPNN OSA prediction with PRBS input

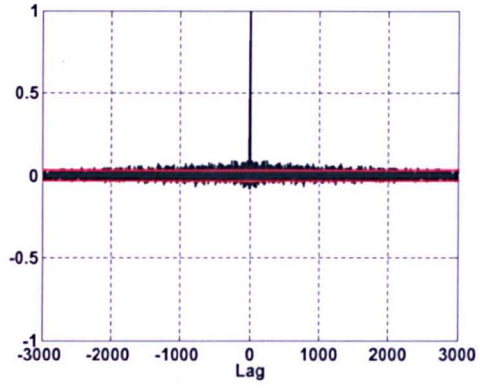

(a) Auto-correlation of residuals

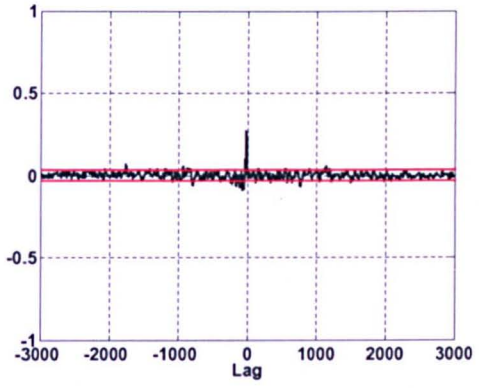

(b) Cross-correlation of input and residuals

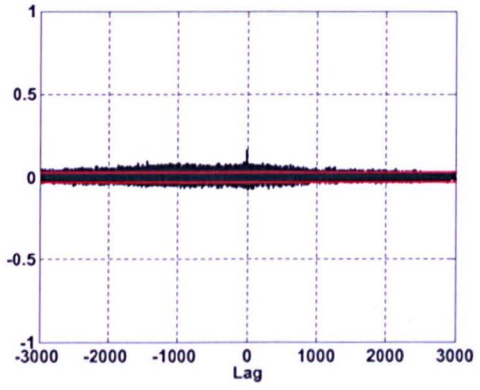

(c) Cross-correlation of input square and residuals

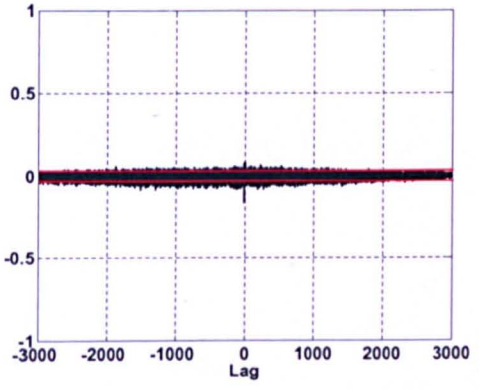

(d) Cross-correlation of input square and residuals square

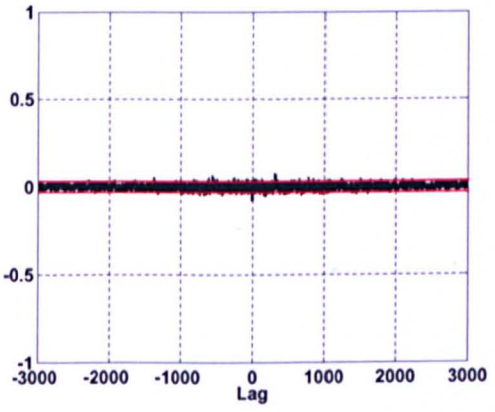

*(e) Cross-correlation of residuals and (input * residuals)*

Figure 4.7: Correlation tests of MLPNN model with PRBS input signal

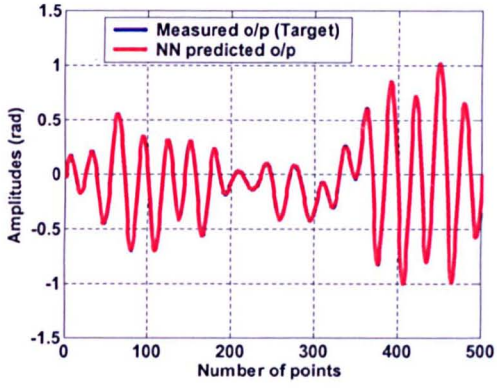

(a) Actual and predicted output (First 500 points)

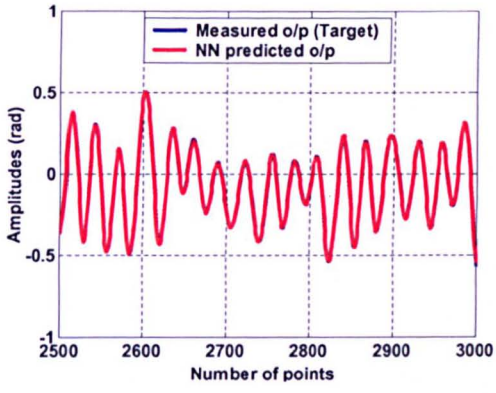

(b) Actual and predicted output (Last 500 points)

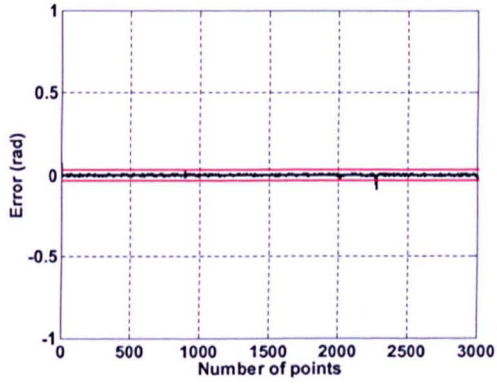

(c) Error between actual and predicted output

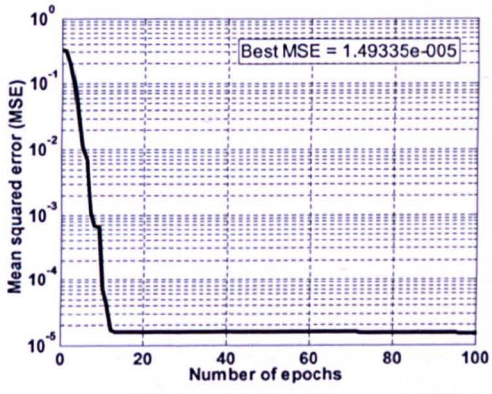

(d) Convergence of error

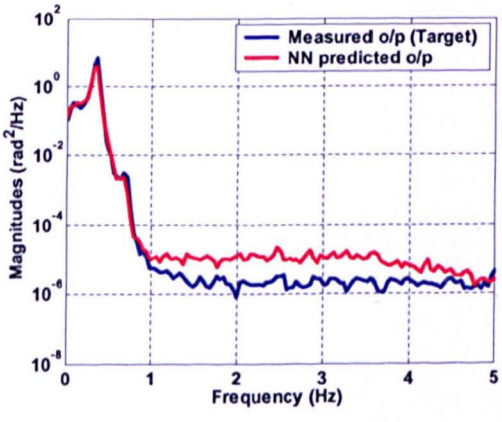

(e) Spectral density of actual and predicted output

Figure 4.8: MLPNN OSA prediction with RGS input

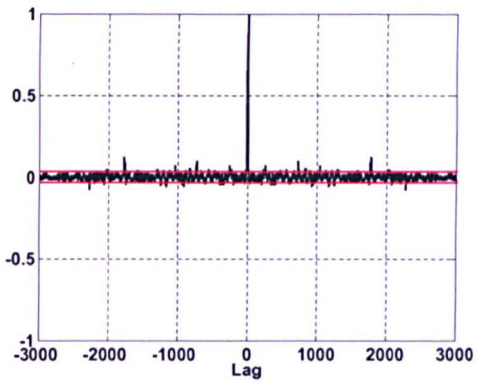

(a) Auto-correlation of residuals

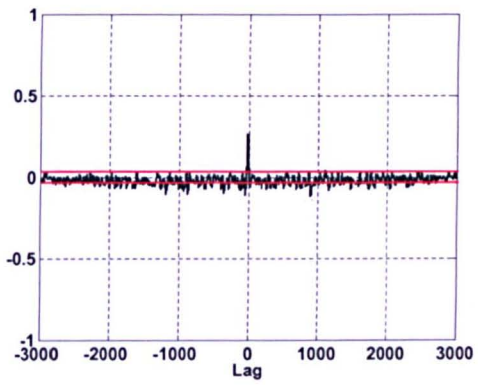

(b) Cross-correlation of input and residuals

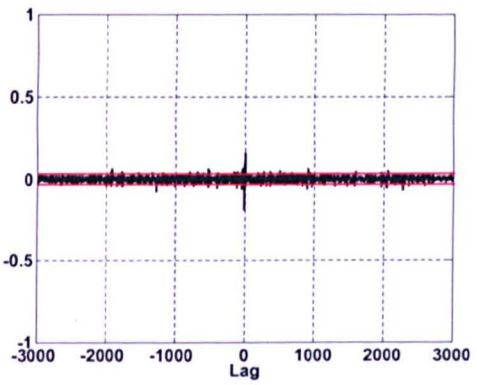

(c) Cross-correlation of input square and residuals

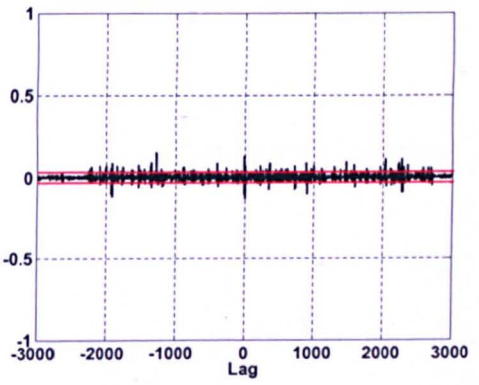

(d) Cross-correlation of input square and residuals square

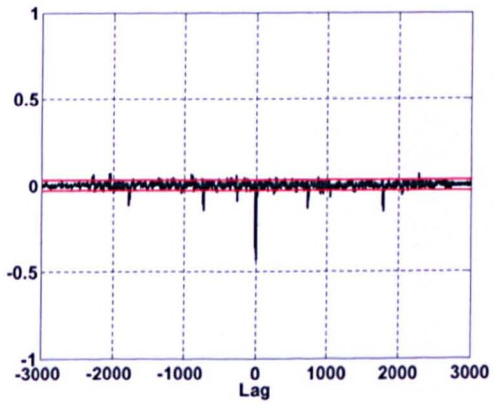

*(e) Cross-correlation of residuals and (input * residuals)*

Figure 4.9: Correlation tests of MLPNN model with RGS input

4.5 Summary

Friction, which is a nonlinear phenomenon, is the primary cause of inducing nonlinearities in a mechanical system. Thus, it can be argued that, most of the electro-mechanical systems, like the TRMS, in general are nonlinear. Hence, nonlinear modelling technique is an obvious choice to characterise such systems. MLP networks are shown to be suitable for modelling complex engineering systems, where the dynamics are not well understood or simple to establish from first principles, such as the next generation UAVs.

In this chapter, a non-linear modelling approach for characterizing the TRMS has been carried out based on MLPNN with BP learning algorithm. It is observed that MLPNN is suitable for modelling such systems. The underlying theme of this chapter has been to demonstrate the nonlinear modelling technique, which has various other applications apart from its utility as a "true" representation of the plant in a simulation environment for controller evaluation. For instance nonlinear models are essential for the design of nonlinear control laws. The MLPNN technique has performed well in approximating the system. In the time domain the developed model has predicted the system output closely and in the frequency domain the resonance frequencies of the model have matched those of the actual system very well. Thus, the developed non-parametric models of the TRMS based on MLPNN methodology will be used in subsequent investigations for the development of control strategies for vibration suppression in the TRMS.

Careful selection of the excitation signal(s) is an important part of nonlinear system identification. Without due consideration to this issue, the obtained model would not be able to capture the system dynamics, resulting in a poor model. Since no mathematical model is available, extensive model validation is imperative. This has been ensured by carrying out higher order cross-correlation tests and OSA analysis. The extracted model has predicted the system behaviour well. Such a high fidelity nonlinear model is often required for gauging the performance of control design and system analysis.

CHAPTER 5

VIBRATION CONTROL USING COMMAND SHAPING TECHNIQUES

5.1 Introduction

Control of flexible structures requires the design of a stable feedback control system. In addition to stability, certain performance measures are integrated into the design. For rapid motion of a flexible system, a satisfactory controller may prove difficult to design, due to induced undesirable residual vibration. The occurrence of any vibration after the commanded position has been reached will require additional settling time before the new maneuver can be initiated. Therefore, in order to achieve a fast and smooth system response to the command signal, it is imperative that this vibration is reduced. This feature is desirable in fast maneuvering systems, such as flexible manipulators and flexible aircraft.

Various approaches have been proposed to reduce vibration in flexible systems. They can be broadly categorized as feedforward, feedback and a combination of both methods. Vibration control of flexible maneuvering systems using feedforward methods involves the manipulation of the command signal applied to the system based on the physical and vibrational properties of the controlled system. The goal of feedforward control is to suppress the system vibration at the dominant resonance modes.

This chapter investigates the development of feedforward control method based command shaping techniques to reduce motion and uneven mass induced vibrations, produced by the main rotor during the vertical movement around the lateral axis of the TRMS. It is assumed that the motion and the rotor load are the main sources of system vibration. Thus, input profiles, which do not contain energy at system natural frequencies do not excite structural vibration and hence require no additional settling time (Ahmad *et al.*, 2002).

The remainder of this chapter highlights the fundamental concepts, design and implementation of the employed feedforward control approaches based on filtering techniques and input shaping control. The goal of the open-loop control is to shape the input signal so as to avoid excitation of residual vibrations during and at the end of the system manoeuvre.

5.2 Feedforward vibration control methods

Feedforward control methods have been considered in vibration control where the control input is developed by considering the physical and vibrational properties of the flexible system (Azad, 1994). The feedforward method employed in this chapter is called command-shaping technique, and used to reduce residual vibrations during motion in the TRMS rig. In this methodology, depicted in Figure 5.1, the desired command signal is modified so that it does not contain spectral components at the system's resonance frequencies.

The command shaping technique is widely employed in flexible aircraft (Livet *et al.*, 1996), flexible manipulators (Mohamed and Tokhi, 2002), and helicopter control (Landis *et al.*, 1996).

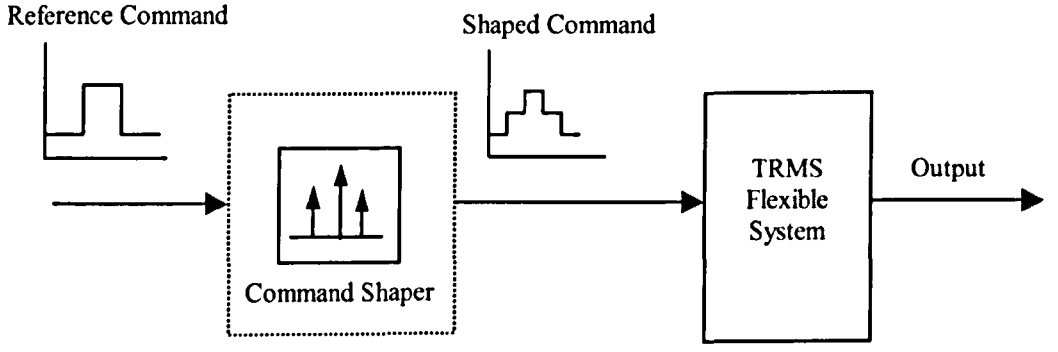

Figure 5.1: Block diagram of feedforward control configuration

5.2.1 Input shaping technique

Singer and Seering (1990), have proposed an input-shaping strategy, which has received considerable attention in vibration control (Pao, 2000; Singer and Seering, 1990; Singhose *et al.*, 1995). The popularity of input shaping is due to its simplicity and ability to be used with arbitrary actuator commands in real-time environments. Moreover, since input shaper resides outside the feedback loop, it is compatible with closed-loop vibration reduction schemes.

The method involves convolving a desired command with a sequence of impulses, as depicted in Figure 5.2, known as an input shaper (Mohamed and Tokhi, 2002; Singer and Seering, 1990). The shaped command that results from the convolution process is then used to drive the system. Design objectives are to determine the amplitude and time locations of the impulses, so that the shaped command reduces the detrimental effects of system flexibility. These parameters are obtained from the natural frequencies and damping ratios of the system. Using this method, a response without vibration can be achieved, but with a slight time delay approximately equal to the length of the impulse sequence. The method has been shown to be the most effective in reducing motion-induced vibrations (Murphy and Watanabe, 1992). With more impulses, the system becomes more robust to flexible mode parameter changes, but this will result in a longer delay in the system response.

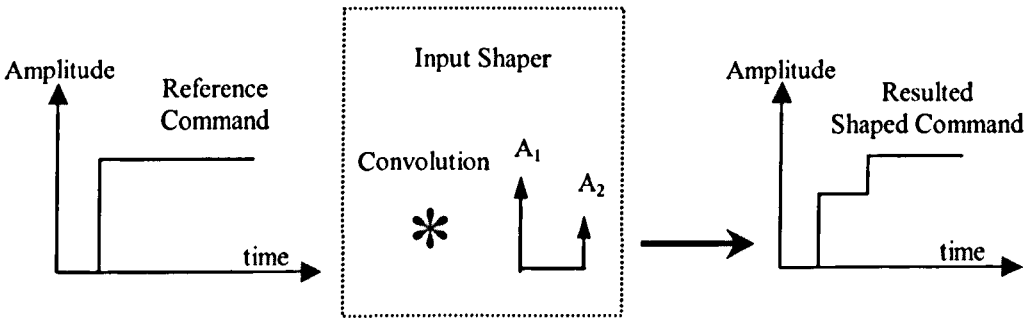

Figure 5.2: The input shaping process

A vibratory system can be modelled as a superposition of second order systems each with a transfer function given as:

$$G(s) = \frac{\omega_n^2}{s^2 + 2\zeta\omega_n s + \omega_n^2} \tag{5.1}$$

where, ω_n is the natural frequency and ζ is the damping ratio of the system. Thus, the impulse response of the system $y(t)$ at time t is:

$$y(t) = \frac{A\omega_n}{\sqrt{1-\zeta^2}} e^{-\zeta\omega_n(t-t_0)} \sin\left[\omega_n\sqrt{1-\zeta^2}(t-t_0)\right] \tag{5.2}$$

where, A and t_0 are the amplitude and time location of the impulse, respectively. Furthermore, the response to a sequence of impulses can be obtained using the superposition principle. Thus, for N impulses with damped frequency $\omega_d = \omega_n\sqrt{1-\zeta^2}$, the impulse response can be expressed as:

$$y(t) = M\sin(w_d t + \alpha) \tag{5.3}$$

where,

$$M = \sqrt{\left(\sum_{i=1}^{N} B_i \cos\phi_i\right)^2 + \left(\sum_{i=1}^{N} B_i \sin\phi_i\right)^2} \quad ,$$

$$B_i = \frac{A_i\omega_n}{\sqrt{1-\zeta^2}} e^{-\zeta\omega_n(t_N - t_i)} \quad , \quad \phi_i = \omega_d t_i \quad , \quad \alpha = \tan^{-1}\left(\sum_{i=1}^{N} \frac{B_i\cos\phi_i}{B_i\sin\phi_i}\right)$$

and A_i and t_i are the magnitudes and times at which the impulses occur. The residual single-mode vibration amplitude of the impulse response is obtained at the time of the last impulse, t_N as:

$$V = \sqrt{V_1^2 + V_2^2} \tag{5.4}$$

where, $V_1 = \sum_{i=1}^{N} \frac{A_i \omega_n}{\sqrt{1-\zeta^2}} e^{-\zeta\omega_n(t_N - t_i)} \cos(\phi_i)$, $V_2 = \sum_{i=1}^{N} \frac{A_i \omega_n}{\sqrt{1-\zeta^2}} e^{-\zeta\omega_n(t_N - t_i)} \sin(\phi_i)$

To achieve zero vibration after the last impulse, it is required that both V_1 and V_2 in equation (5.4) are independently zero. Furthermore, to ensure that the shaped command input produces the same rigid-body motion as the unshaped command, it is required that the sum of amplitudes of the impulses is unity. To avoid response delay, the first impulse is selected at time $t_1 = 0$. Hence, by setting V_1 and V_2 in equation (5.4) to zero, $\sum_{i=1}^{N} A_i = 1$ and solving yields a two-impulse sequence as shown in Figure 5.3 with a set of parameters given by:

$$t_1 = 0 \quad , \quad t_2 = \frac{\pi}{\omega_d}$$
$$A_1 = \frac{1}{1+K} \quad , \quad A_2 = \frac{K}{1+K} \tag{5.5}$$

where, $K = e^{\frac{-\zeta\pi}{\sqrt{1-\zeta^2}}}$

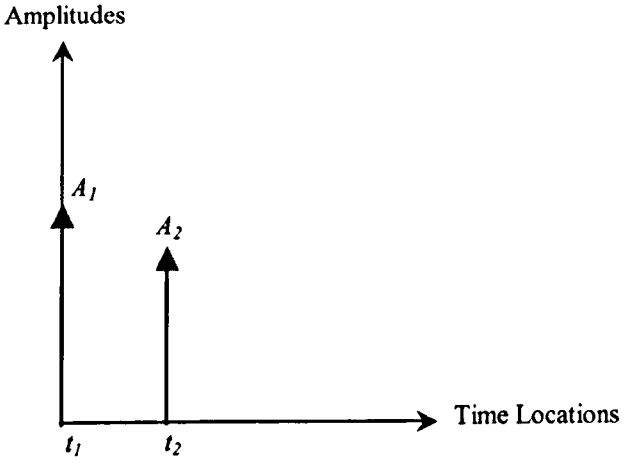

Figure 5.3: Two-impulse sequence input shaper

The robustness of the input shaper to errors in natural frequencies of the system can be increased by setting $\frac{dV}{d\omega_n} = 0$. Setting the derivative to zero is equivalent of producing small changes in vibration corresponding to natural frequency changes. By obtaining the first derivatives of V_1 and V_2 in equation (5.4) and simplifying yields (Singer and Seering, 1990):

$$\frac{dV_1}{d\omega_n} = \sum_{i=1}^{N} A_i t_i e^{-\zeta\omega_n(t_N - t_i)} \sin(\phi_i) \quad , \quad \frac{dV_2}{d\omega_n} = \sum_{i=1}^{N} A_i t_i e^{-\zeta\omega_n(t_N - t_i)} \cos(\phi_i) \tag{5.6}$$

By setting equations (5.4) and (5.6) to zero and solving yields a three-impulse sequence, as depicted in Figure 5.4, with parameters given as:

$$\begin{aligned} t_1 &= 0 \quad , \quad t_2 = \frac{\pi}{\omega_d} \quad , \quad t_3 = \frac{2\pi}{\omega_d} \\ A_1 &= \frac{1}{1+2K+K^2} \quad , \quad A_2 = \frac{2K}{1+2K+K^2} \quad , \quad A_3 = \frac{K^2}{1+2K+K^2} \end{aligned} \tag{5.7}$$

where, K is as in equation (5.5).

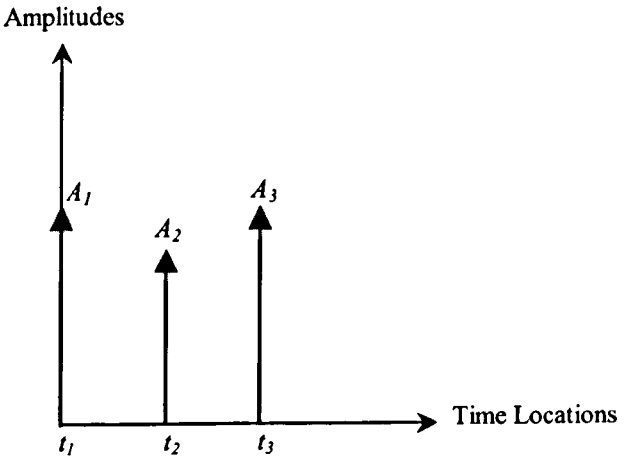

Figure 5.4: Three-impulse sequence input shaper

The robustness of the input shaper can further be increased by setting the second derivative of the vibration in equation (5.4) to zero. This yields a four-impulse sequence, as illustrated in Figure 5.5, with parameters given by:

$$t_1 = 0 \quad , \quad t_2 = \frac{\pi}{\omega_d} \quad , \quad t_3 = \frac{2\pi}{\omega_d} \quad , \quad t_4 = \frac{3\pi}{\omega_d}$$

$$A_1 = \frac{1}{1+3K+3K^2+K^3} \quad , \quad A_2 = \frac{3K}{1+3K+3K^2+K^3} \quad , \tag{5.8}$$

$$A_3 = \frac{3K^2}{1+3K+3K^2+K^3} \quad , \quad A_4 = \frac{K^3}{1+3K+3K^2+K^3}$$

where, K is as in equation (5.5).

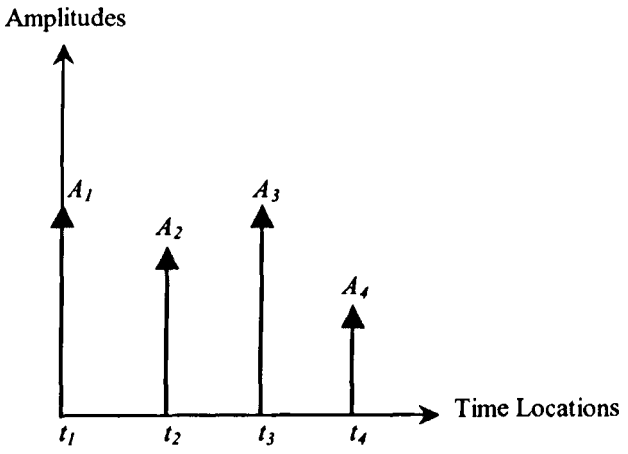

Figure 5.5: Four-impulse sequence input shaper

To handle higher vibration modes, an impulse sequence for each vibration mode can be designed independently. Then the impulse sequences can be convolved together to form a sequence of impulses that attenuate vibration at higher modes. In this manner, for a vibratory system, the vibration reduction can be accomplished by convolving a desired system input with the impulse sequence. This yields a shaped input that drives the system to a desired location with less vibration.

5.2.2 Filtering techniques

Command shaping based on filtering techniques is developed on the basis of extracting the energy around natural frequencies of the system (Mohamed and Tokhi, 2002). A significant amount of work on shaped command input based on filtering techniques has been reported. These include low-pass filters, band-stop filters and notch filters (Ahmad *et al.*, 2002; Mohamed and Tokhi, 2002; Singhose *et al.*, 1995; Tokhi *et al.*, 1995; Tokhi and Poerwanto, 1996).

The filters are used for pre-processing the input signal so that no energy is fed into the system at the natural frequencies. In this manner, the flexural modes of the system are not excited, leading to a vibration-free motion. This can be realized by employing either low-pass or band-stop filters. In the former, a low-pass filter is designed with a cut-off frequency lower than the first natural frequency of the system. In the latter case, a band-stop filter with centre frequency at the natural frequency of the system is designed.

Infinite impulse response (IIR) Butterworth low-pass and band-stop filters are used in this investigation. The Butterworth type filter is popular because of its simple design (Haykin, 1996; Jackson, 1989). The filter has only two design parameters; the order of the filter and the cut-off frequency. The Butterworth filters are also referred to as maximally flat filters because their pass-band and stop-band are without ripples (Haykin, 1996). The magnitude of the frequency response of a low-pass Butterworth filter is given as (Jackson, 1989):

$$|H(j\omega)|^2 = \frac{1}{1+\left[\frac{\omega}{\omega_c}\right]^{2m}} = \frac{1}{1+\varepsilon\left[\frac{\omega}{\omega_p}\right]^{2m}} \tag{5.9}$$

where, m is a positive integer signifying the order of the filter, ω_c is the filter cut-off frequency, ω_p is the pass-band edge frequency and $(1+\varepsilon^2)^{-1}$ is the band edge value of $|H(j\omega)|^2$. Note that $|H(j\omega)|^2$ is monotonic in both the pass-band and stop-band. The order of the filter required to yield attenuation δ_2 at a specified frequency ω_s (stop-band edge frequency) is determined from equation (5.9) as:

$$m = \frac{\log\left(\frac{1}{\delta_2^2} - 1\right)}{2\log\left(\frac{\omega_s}{\omega_c}\right)} = \frac{\log\left(\frac{\delta_1}{\varepsilon}\right)}{\log\left(\frac{\omega_s}{\omega_p}\right)} \tag{5.10}$$

where, by definition, $\delta_2 = 1/\sqrt{(1+\delta_1^2)}$. Thus, the Butterworth filter is completely characterized by the parameters m, δ_2, ε and the ratio ω_s / ω_p.

Equation (5.10) can be employed with arbitrary $\delta_1, \delta_2, \omega_c$, and ω_s to yield the required filter order m from which the filter design is readily obtained. The Butterworth approximation results from the requirement that the magnitude response be maximally flat in both the pass-band and the stop-band; i.e. the first $(2m-1)$ derivatives of $|H(j\omega)|^2$ are specified to be equal to zero at $\omega = 0$ and at $\omega = \infty$. The design relations for low-pass filters given above can be utilized in normalized form to design the corresponding band-stop filters. This involves a transformation from the low-pass to band-stop filter (Banks, 1990).

5.3 Implementation

The feedforward control techniques were designed on the basis of natural frequency and damping ratio of the TRMS system. A damping ratio of 0.0101 corresponding to the main resonance frequency mode at 0.35156 Hz was obtained analytically from the transfer function of the TRMS model, developed in Chapter 3.

Experimental study is performed on the laboratory-scale TRMS. Three forms of input shaper (with two, three and four impulse sequences) and low-pass and band-stop digital filters are designed and implemented on the TRMS rig based on the properties of the TRMS and used for pre-processing the desired input to the system. The controllers designed in this investigation are linked to the TRMS rig using MATALB/SIMULINK Real Time Workshop (RTW) described in Chapter 2. The interface system allows for online modification of certain control parameters and for online switching from one controller to another. The input signals were designed off-

line separately and then read from the workspace through the MATLAB/SIMULINK environment.

Performances of the developed controllers are assessed in terms of level of vibration reduction at the natural frequencies. This is accomplished by comparing the system response to that with the unshaped bang-bang input in simulation and real-time environments. To study the system performance, initially an unshaped bang-bang input is used to drive the main rotor of the TRMS rig, while the input to the tail rotor is kept constant. The corresponding system response is measured. The same procedure is then repeated by injecting shaped bang-bang inputs using the developed command shaping techniques to drive the real system.

5.3.1 Bang-bang input

A single-switch bang-bang input command signal referred to as unshaped input is used in this work. It represents the input voltage to the main rotor as depicted in Figure 5.6. The signal has amplitude of ± 0.3 volt, used as a desired input to the system to extract its response, and to design and evaluate the performance of the feedforward control schemes.

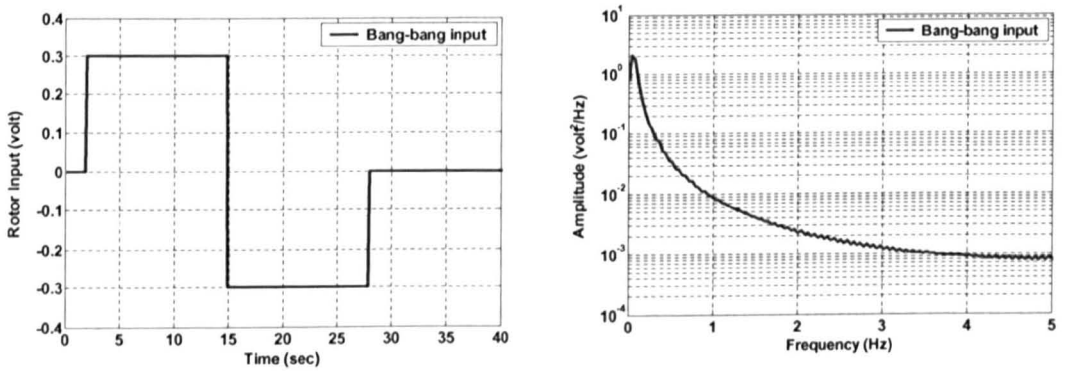

(a) Time domain *(b) Power spectral density*

Figure 5.6: Bang-bang input signal

The designed input shaper and filters were used for pre-processing the bang-bang command signal applied to the system in an open-loop configuration to reduce

the system vibration. In this process, the shaped and filtered inputs were designed with a sampling frequency of 10 Hz. Although the main resonance mode of the system is fairly low, this sampling frequency was used to cover a wider range of dynamics of the system well beyond the main resonance mode.

To verify the performance of the control techniques in vibration suppression of the TRMS rig, the results are examined in comparison to the unshaped bang-bang input for a similar input level in each case. Simulation and experimental results of the response of the system to the shaped and filtered inputs are presented in the time and frequency domains. The main objective as mentioned earlier is to suppress the system vibration at its dominant resonance mode during its operation. This is accomplished by comparing the responses to the shaped and filtered inputs with the response to the unshaped input. To illustrate the amount of vibration reduction in quantitative values, the results are presented in dB. The effect of increasing the number of impulses, in the case of input shaper, on the performance of the system is also investigated.

5.3.2 Input shaping technique

Using the natural frequency and damping ratio of the system, three input-shapers with two, three and four impulse sequences were designed and examined. The magnitude and time location of the impulses were obtained by using equations (5.5) - (5.8).

Figures 5.7, 5.8 and 5.9 show the shaped inputs and the corresponding impulse sequences for the three developed input shapers. For digital implementation of the input-shaper, locations of the impulses were selected at the nearest sample time-step. The amplitudes and corresponding time locations of impulses for the three input shaping controllers are presented in Table 5.1.

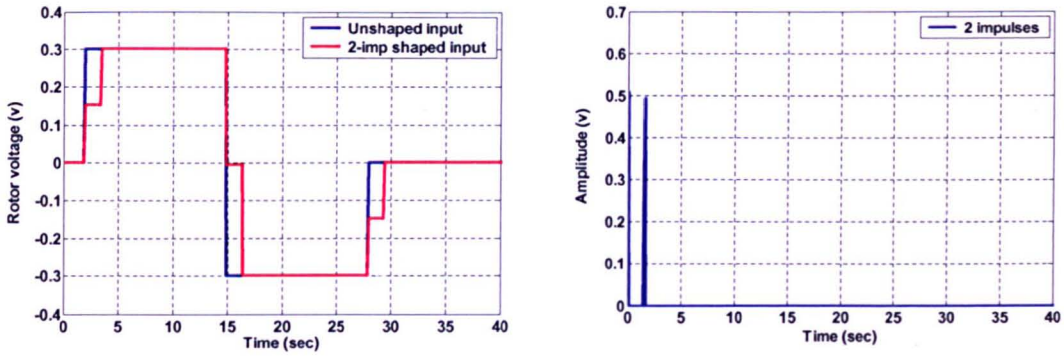

(a) System input (time domain) *(b) 2-impulse sequence*

Figure 5.7: 2-impulse input shaper

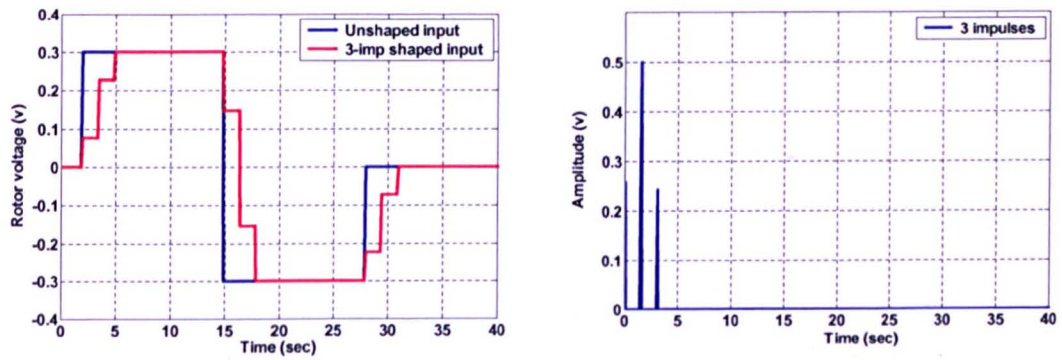

(a) System input (time domain) *(b) 3-impulse sequence*

Figure 5.8: 3-impulse input shaper

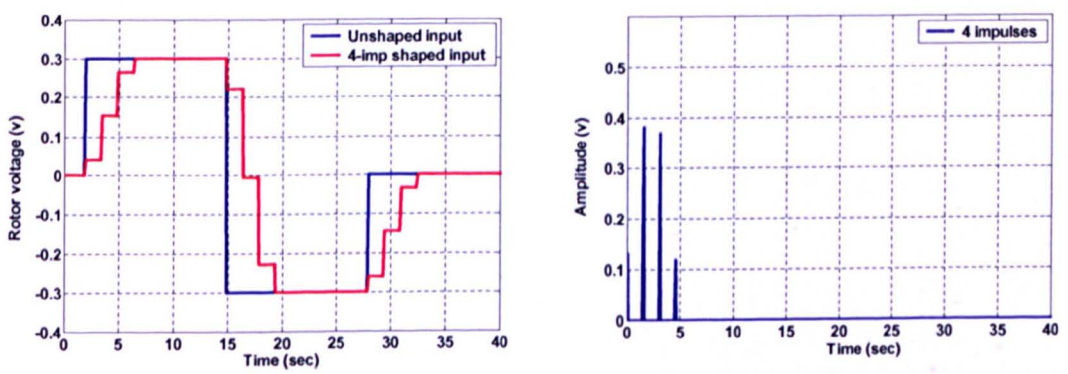

(a) System input (time domain) *(b) 4-impulse sequence*

Figure 5.9: 4-impulse input shaper

Table 5.1: Amplitudes and time locations of impulses for the developed input shapers

Input shaping technique	Impulse Number	Amplitude A_i (volt)	Time location t_i (sec)	Sample location $\left(t_i/\tau + 1\right)$
2-impulse input shaper	1	0.508	0	1
	2	0.492	1.5	16
3-impulse input shaper	1	0.258	0	1
	2	0.500	1.5	16
	3	0.242	3.0	31
4-impulse input shaper	1	0.131	0	1
	2	0.381	1.5	16
	3	0.369	3.0	31
	4	0.119	4.5	46

* τ = sampling time = 0.1 sec

5.3.3 Filtering techniques

In this study, a third-order Butterworth low-pass filter with cut-off frequency at 0.1 Hz (30% of the main vibration mode) was designed and employed for pre-processing the bang-bang input signal. Using the low-pass filter, the input energy at all frequencies above the cut-off frequency can be attenuated. Similarly, a third-order Butterworth band-stop filter with a centre frequency equal to the system's main resonance mode (0.35156 Hz) was designed and employed for pre-processing the input signal. Thus, a stop-band frequency ranging between 0.2516 to 0.4516 Hz was selected for the design of this filter. The unfiltered and filtered voltage inputs with low-pass and band-stop filters and their corresponding power spectral density plots are shown in Figures 5.10 and 5.11, respectively.

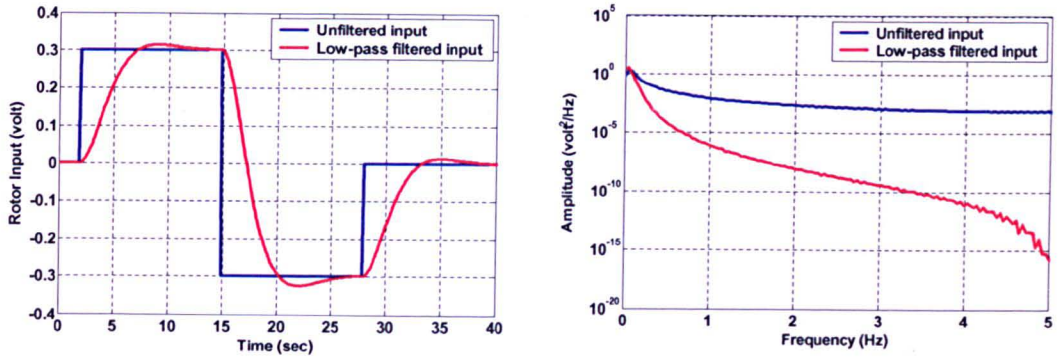

(a) System input (time domain) *(b) Power spectral density*

Figure 5.10: Filtered input with low-pass filter

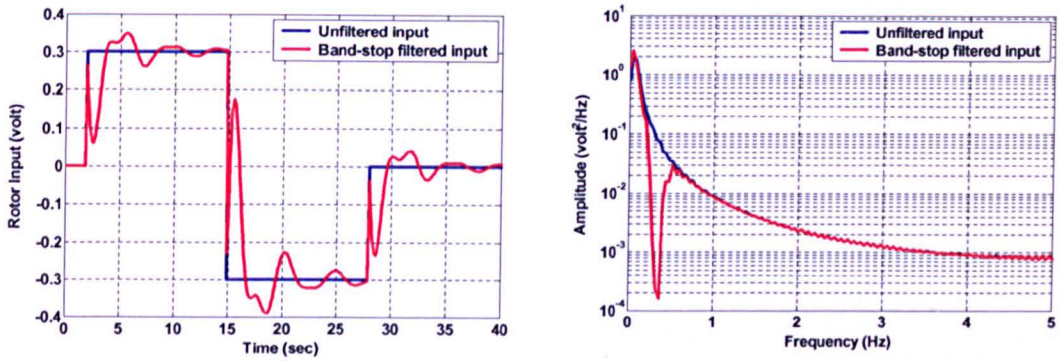

(a) System input (time domain) *(b) Power spectral density*

Figure 5.11: Filtered input with band-stop filter

5.4 Simulation results

In this section simulation results of the TRMS model response with the corresponding power spectral density (PSD) profiles to the command shaping inputs are presented and studied. In all time domain results, the system response to unshaped bang-gang input is represented by blue dashed line, which overshoots demonstrating a considerable residual vibration. Like wise, the system response to unshaped/unfiltered bang-bang input in the PSD profiles is used as a reference, represented by a blue dashed line, for comparative evaluation of the performance of the employed command shaping controllers in reducing the residual vibrations.

5.4.1 Shaped inputs

Figures 5.12 - 5.14 show the simulated responses of the TRMS model to the unshaped and shaped inputs using two, three and four-impulse sequences. It is noted in the three cases that the magnitudes of vibration at the dominant resonance mode of the system have been significantly reduced. This can be observed by comparing the system response to the unshaped input. It is also noted that the level of vibration reduction increases by increasing the number of impulses, at the expense of increase in the delay in the response of the system.

Among the three input shapers, the highest amount of vibration reduction was achieved with four-impulse input shaper (26.440 dB), followed by three-impulse input shaper that recorded 26.039 dB, and then by two-impulse input shaper of 23.884 dB.

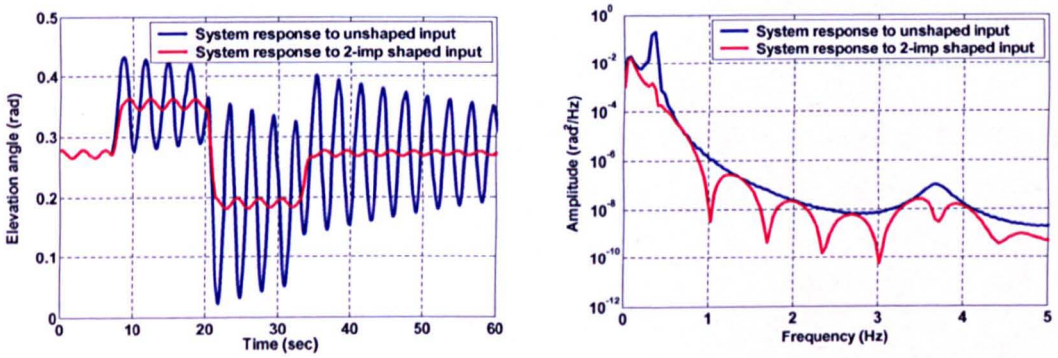

(a) Time domain (simulation) *(b) Power spectral density (simulation)*

Figure 5.12: Simulated system response to unshaped and 2-impulse shaped input

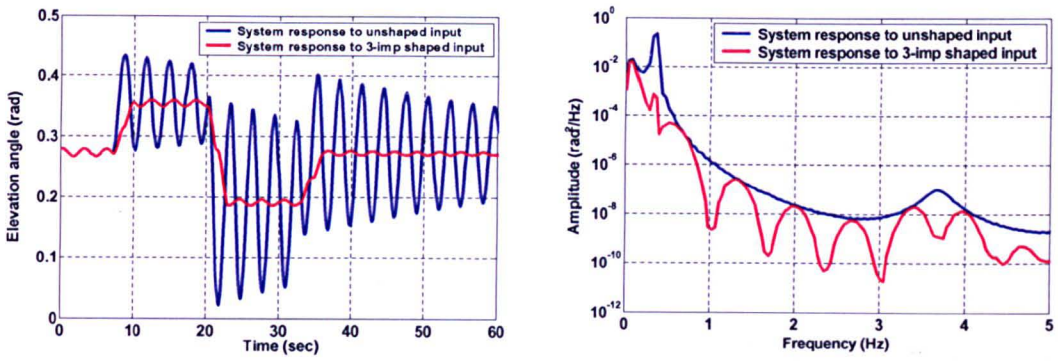

(a) Time domain (simulation) *(b) Power spectral density (simulation)*

Figure 5.13: Simulated system response to unshaped and 3-impulse shaped input

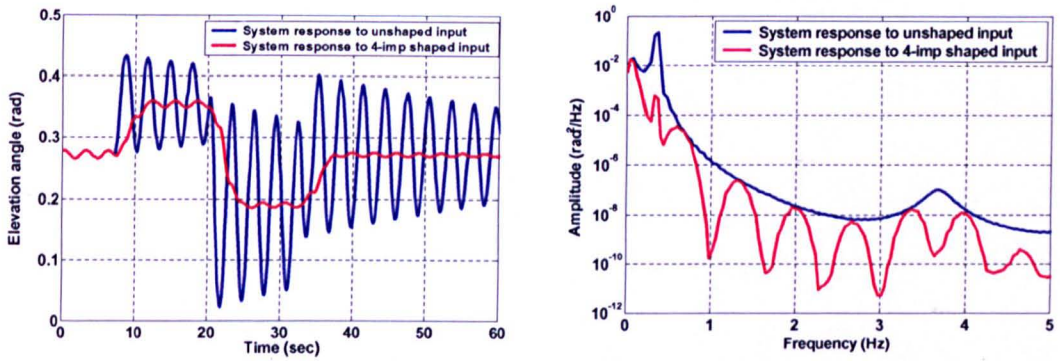

(a) Time domain (simulation) *(b) Power spectral density (simulation)*

Figure 5.14: Simulated system response to unshaped and 4-impulse shaped input

5.4.2 Filtered inputs

Figures 5.15 and 5.16 show responses of the TRMS model to the unfiltered input and filtered voltage input using third-order Butterworth low-pass (LP) and band-stop (BS) filters, respectively. It is noted that the system vibration at the resonance mode was considerably reduced in comparison to the unfiltered bang-bang voltage input.

It is noted that a higher amount of vibration reduction at the main vibration mode was achieved with the band-stop filter (24.638 dB) in comparison to that recorded with low-pass filter (18.456 dB).

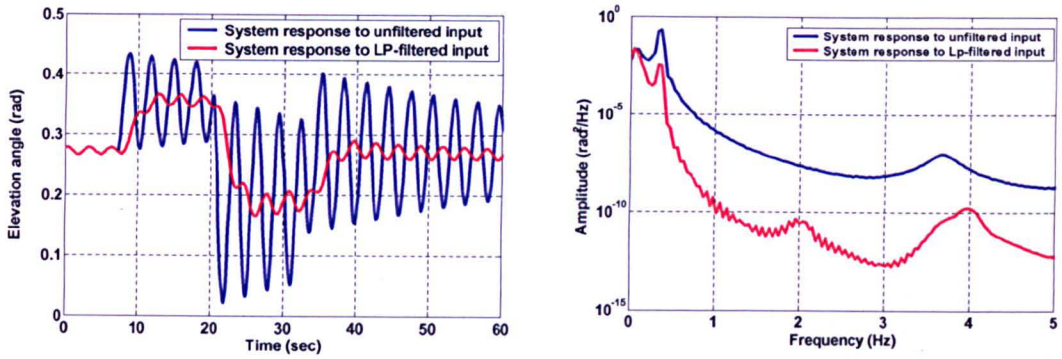

(a) Time domain (simulation) *(b) Power spectral density (simulation)*

Figure 5.15: Simulated system response to unfiltered and low-pass filtered input

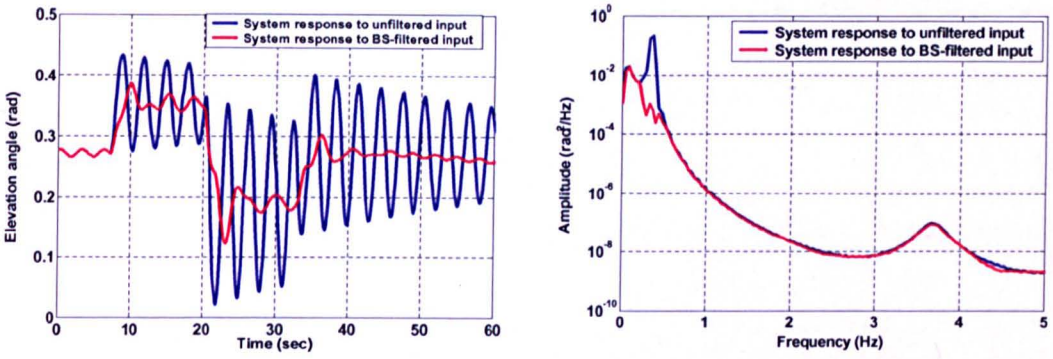

(a) Time domain (simulation) *(b) Power spectral density (simulation)*

Figure 5.16: Simulated system response to unfiltered and band-stop filtered input

5.5 Experimental results

This section presents the real-time experimental results of the TRMS response to command shaping inputs. System responses with the corresponding PSD profiles are studied. Similar to the simulation results, the system response to unshaped bang-bang input is represented by blue dashed line.

5.5.1 Shaped inputs

Figures 5.17 - 5.19 show the experimental response of the TRMS rig to the unshaped and shaped inputs using two, three and four impulse input shapers, respectively.

It is noticed from the PSD profiles that the vibration of the system has been significantly reduced at the system's resonance mode. Similar to the simulation results, the four-impulse input shaper recorded the highest amount of vibration reduction (23.096 dB), followed by three-impulse input shaper that recorded 17.317 dB, and then two-impulse input shaper of 14.073 dB. With the four-impulse sequence, the oscillations in the system response were found to have been almost reduced to zero in comparison to the system response to unshaped input.

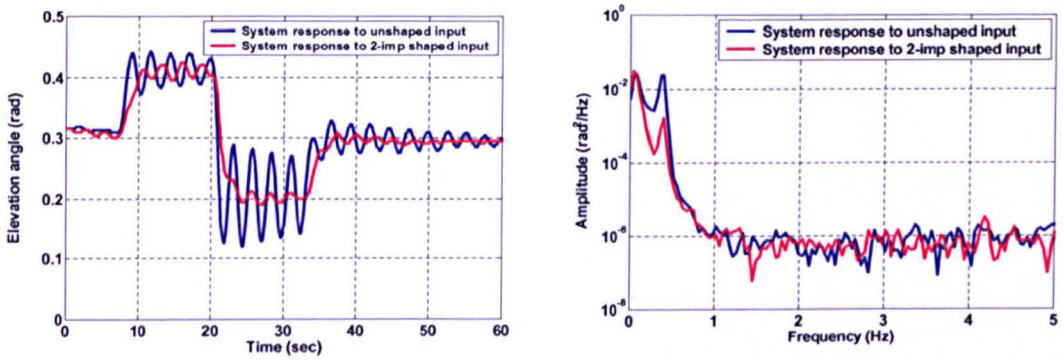

(a) Time domain (experimental) *(b) Power spectral density (experimental)*

Figure 5.17: Experimental system response to unshaped and 2-impulse shaped input

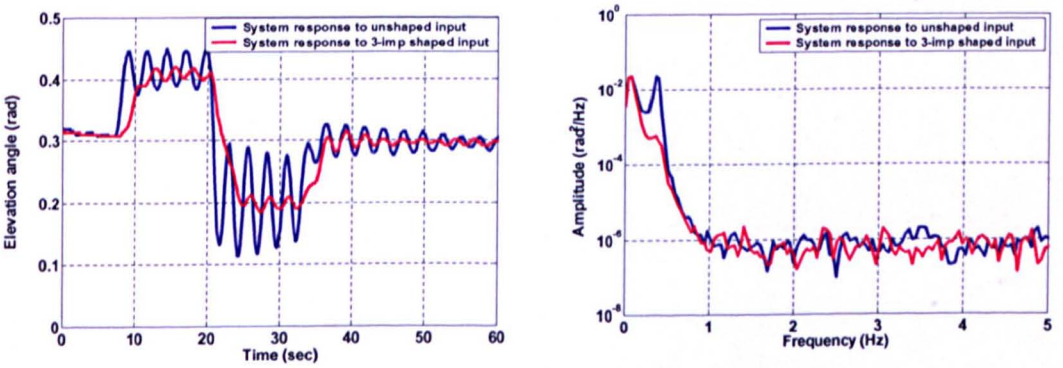

(a) Time domain (experimental) *(b) Power spectral density (experimental)*

Figure 5.18: Experimental system response to unshaped and 3-impulse shaped input

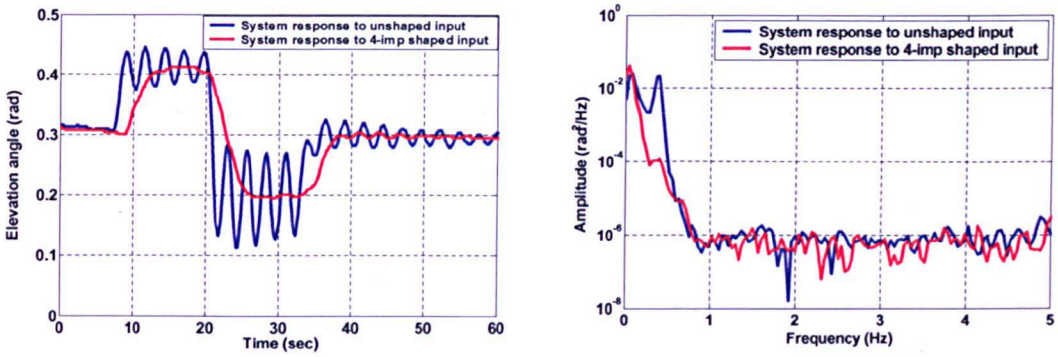

(a) Time domain (experimental) *(b) Power spectral density (experimental)*

Figure 5.19: Experimental system response to unshaped and 4-impulse shaped input

5.5.2 Filtered inputs

With the same set of parameters used in the simulation phase, third-order Butterworth low-pass and band-stop filters were designed and implemented to filter the bang-bang input signal. Figures 5.20 and 5.21 show the response of the TRMS rig to the unfiltered and filtered inputs.

The obtained experimental results revealed that a relatively small reduction in the system vibration was achieved with both filters in comparison to the input shaping techniques. In the low-pass filter case, shown in Figure 5.20, the system vibration at the natural frequency was reduced by 8.643 dB. While, in the case of band-stop filter the amount of vibration reduction was 9.863 dB.

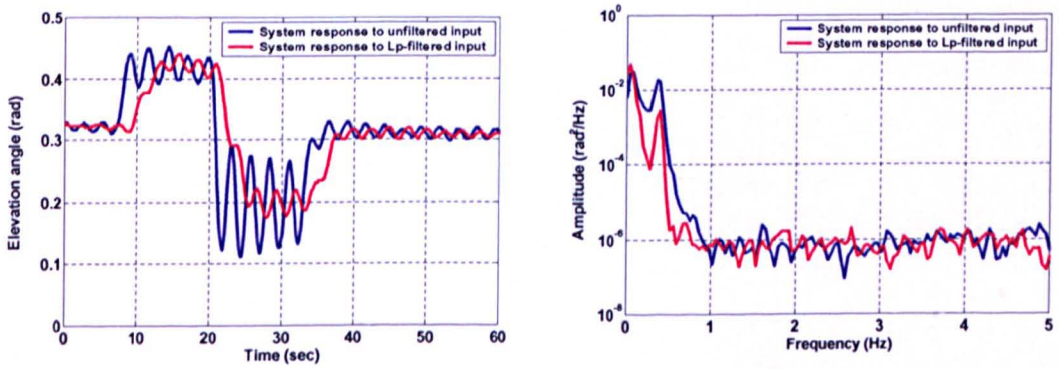

(a) Time domain (experimental) *(b) Power spectral density (experimental)*

Figure 5.20: Simulated system response to unfiltered and low-pass filtered input

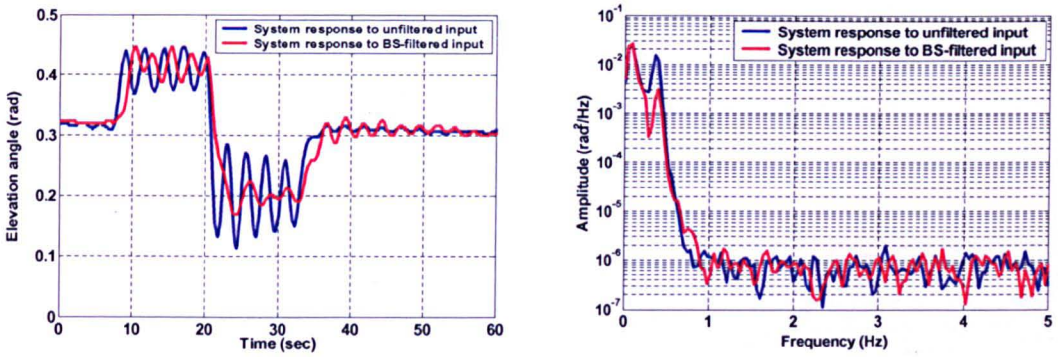

(a) Time domain (experimental) *(b) Power spectral density (experimental)*

Figure 5.21: Experimental system response to unfiltered and band-stop filtered input

5.6 Comparative performance assessment

Among the five techniques employed for vibration reduction at the resonance frequency of the system, the input-shapers have resulted in better performance than the filtering techniques. This is evidenced by the amount of vibration reduction in simulation and real-time experimental exercises, as presented in Table 5.2 and illustrated in Figure 5.22, respectively.

In the simulation phase, the highest amount of vibration reduction at the resonance mode was recorded with four-impulse input shaper, which was 26.440 dB, followed by three-impulse input shaper of 26.039 dB, followed by the band-stop filter of 24.638 dB, followed by the two-impulse input shaper of 23.884 dB, and finally the low-pass filter of 18.456 dB.

In the experimental phase, the highest amount of vibration reduction at the resonance mode was recorded with four-impulse input shaper, which was 23.096 dB, followed by the three-impulse input shaper of 17.317 dB, followed by the two-impulse input shaper of 14.073 dB, followed by the band-stop filter of 9.863 dB, and finally the low-pass filter of 8.643 dB.

Table 5.2: Amount of vibration reduction using command shaping techniques

Command shaping technique	Amount of vibration reduction (dB)	
	Simulation	Experimental
Low-pass filter	18.456	8.643
Band-stop filter	24.638	9.863
2-impulse shaper	23.884	14.073
3-impulse shaper	26.039	17.317
4-impulse shaper	26.440	23.096

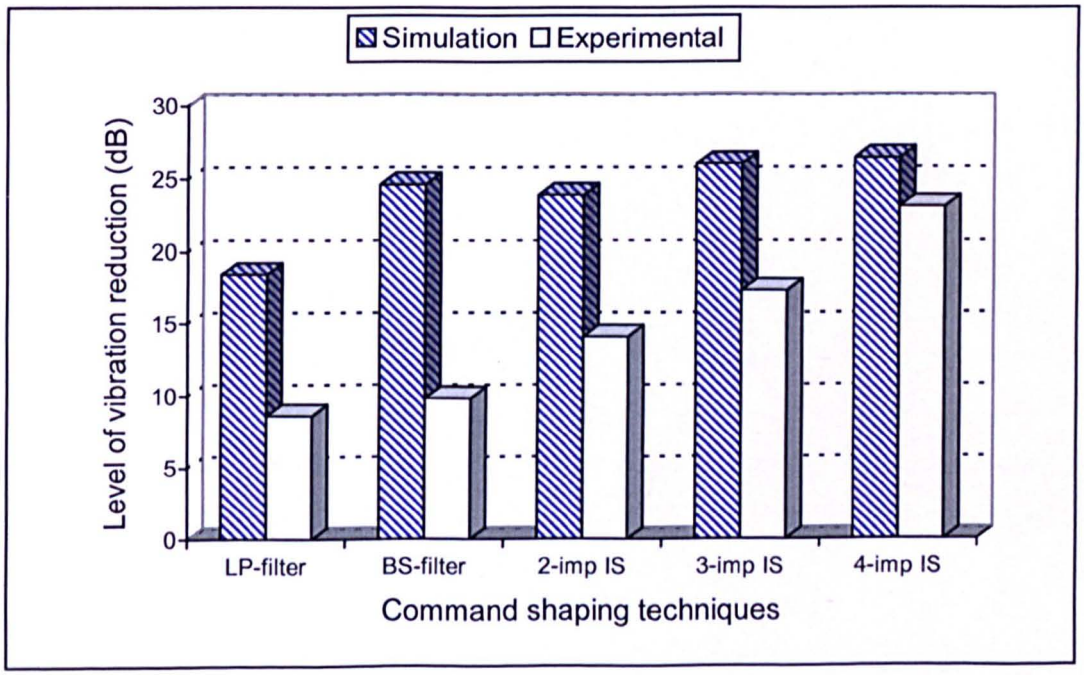

Figure 5.22: Level of vibration reduction with command shaping techniques

5.7 Summary

The development of command shaping feedforward control strategies for vibration control of the vertical movement of the TRMS rig using input shaping and filtering techniques has been presented. The residual motion (vibration) in flexible systems is normally due to their fast motion. The system response to the unshaped bang-bang input signal has been used to determine the parameters of the system for design and

evaluation of the control strategies. Performances of the techniques have been evaluated in simulation and real-time experimental environments in terms of level of vibration reduction using power spectral density profiles of the system response.

Command shaping methods developed in this investigation have been shown to be effective in reducing motion-induced vibration. A significant amount of reduction in the system vibration has been achieved with these control strategies. Among the three input shaping techniques, it was noted that the best performance in vibration reduction and time response was achieved with the input shaping technique with four impulses. With the four-impulse sequence input shaper, the oscillations in the system response were almost reduced to zero. Hence, a smoother response was achieved. However, faster system response was achieved with two-impulse input shaper, followed by three-impulse input shaper and finally four impulse input shaper. Among the two filtering techniques, band-stop filtered input resulted in better performance than the low-pass filtered input in terms of vibration reduction. Moreover, the system response with band-stop filter was faster than with low-pass filtered input.

Furthermore, with more impulses in the input shaper, a system vibration may be further reduced or even eliminated, but with a time delay approximately equal to the length of the impulse sequence. This drawback can be overcome by adding a feedback control component, which will be addressed in succeeding chapters. Investigation of open-loop control is a prelude to subsequent development of more complex feedback and augmented control laws.

CHAPTER 6

HYBRID FEEDBACK CONTROL SCHEMES FOR INPUT TRACKING PERFORMANCE

6.1 Introduction

Conventional control system design is predominantly based upon the development of mathematical models, which attempt to describe the dynamic behaviour of the system in question using typically, differential equations. Many such methods of system design have been developed over time, including three-term Proportional, Integral, Derivative control (PID-control), root-locus design, state-space, Nyquist, Bode and optimal control offering a variety of ways in which good controller design may be achieved (Passino and Yurkovich, 1998; Smuts, 2002). In practice, PID control systems, with approximately 90% of all controllers in operation, are predominately of this form (Passino and Yurkovich, 1998; Verbruggen and Brujin, 1997). The dominance of PID control may be explained by the fact that it is a long-standing, successful design technique, well understood by industrial users (Visioli, 2001).

Due to the continuously developing automation systems and more demanding control performance requirements, conventional control methods are not always adequate. On the other hand, practical control problems are usually imprecise and the input-output relations of the system may be uncertain and they can be changed by unknown external disturbances. New schemes are, thus, needed to solve such problems. Increased mathematical complexity required for conventional modelling techniques thus led to the application of fuzzy logic to control systems design in the form of fuzzy logic controllers and their use has steadily grown among industrial users (Verbruggen and Brujin, 1997). In fuzzy control, the controller can be represented with linguistic "if-then" rules. The interpretation of the controller is fuzzy but the controller is processing exact input-data and is producing exact output-data in a deterministic way. Fuzzy logic control (FLC) translates human perceptions

in the form of expert knowledge, into the numerical domain, thus facilitating suitable system controller design while avoiding the need for stringent mathematical system descriptions. Application of FLC in the domain of PID control has been, in general, used to augment existing PID controller operation or replacement of PID by fuzzy logic controller (Bandyopadhyay *et al.*, 2001). Increased technology sophistication, and use of microprocessors have enabled the development of fuzzy-PID hybrid systems, where FLC is used to adaptively tune the parameters of conventional PID controllers (Bandyopadhyay *et al.*, 2001), and replacement of PID controller with fuzzy logic controller (Karr, 1991). Visioli (2001) used FLC to implement supervisory control by auto-tuning PID controller gains in order to adapt/optimize system performance of the controller in response to changing operating conditions. Fuzzy controllers have also been used in industrial and research applications where their use has conferred improved system performance, or where a mathematical process model is intractable.

A reason for this significant role is that fuzzy logic provides a flexible and powerful alternative to construct controllers, supervisory blocks, computing units and compensation systems in different application areas (Cohen *et al.*, 2002; Jnifene and Andrews, 2005; Lai and Lin, 2003). With fuzzy sets very nonlinear control actions can be formed easily. The transparency of fuzzy rules and the locality of parameters are helpful in the design and maintenance of system (Jager, 1995). Therefore, preliminary results can be obtained within a short development period.

The fuzzy controller, however, needs more information to compensate nonlinearities when the operating conditions change. When the number of inputs of the fuzzy system is increased, the dimension of the rule base also increases. Thus, the maintenance of the rule base is more time-consuming. Another disadvantage of fuzzy controllers is the lack of systematic, effective and useful design methods, which can use a priori knowledge of the plant dynamics. Deficiencies of the PID controller and the fuzzy controller can be solved by combining them together.

This chapter presents an investigation into combining conventional compensator with fuzzy controller to form a novel nonlinear hybrid control scheme for tracking performance. The motivation of the augmentation procedure is to enhance the control performance during both the transient and steady states (i.e. overcome the drawbacks of pure PD-type and PI-type fuzzy logic controllers). Two

forms of hybrid control are developed and realized for the control of the vertical movement of the TRMS rig in hovering mode. The first proposed hybrid control scheme consists of a conventional PD controller augmented with PID compensator (PD-PID). While the second nonlinear hybrid control scheme, referred to as (FPD-PID), comprises PD-type FLC augmented with PID compensator. In both cases, the novelty is claimed based on the structure of the hybrid control scheme, which is designed in such a way that the output of the first controller (i.e. PD controller or FPD-type FLC) is fed to the proportional gain of the augmented PID compensator. The performances of the two proposed nonlinear hybrid control strategies (PD-PID and FPD-PID) are compared with PID compensator and pure PD-type and PI-type fuzzy controllers in terms of set-point tracking.

6.2 Fuzzy logic control

Most of classical design mythologies such as Nyquist, Bode, state-space, optimal control, root locus, H_∞ and μ-analysis are based on assumptions that the process is linear and stationary and hence is represented by a finite dimensional constant coefficient linear model. Hence, such methods do not suit complex systems well because few of those represent uncertainty in process knowledge or complexity in design. But, in the real world many industrial processes are highly nonlinear and complex. As the complexity of a system increases, quantitative analysis and precision become more difficult. The control of such complex and nonlinear processes has been approached in recent years using fuzzy logic techniques. During the past several years, fuzzy control has emerged as one of the most active and powerful areas of research in applications of such complex and real world systems.

Fuzzy logic control (FLC) strategies come from experience and experiments rather than from mathematical models and therefore linguistic implementations are much faster accomplished. FLC strategies involve a large number of inputs, most of which are relevant only for some special conditions. Such inputs are activated only when the related condition prevails. In this way, little additional computational overhead is required for adding extra rules. As a result, the rule base structure remains understandable, leading to efficient coding and system documentation.

Fuzzy systems are indicating good promise in consumer products, industrial and commercial systems, and decision support systems. The term "fuzzy" refers to the ability of dealing with imprecise or vague inputs. Instead of using complex mathematical equations, fuzzy logic (FL) uses linguistic descriptions to define the relationship between the input information and the output action. In engineering systems, fuzzy logic provides a convenient and user-friendly front-end to develop control programs, helping designers to concentrate on the functional objectives, not on the mathematics.

FLC has been successfully applied in the control of various physical processes (Pedrycz, 1991; Sugeno, 1985). On the other hand, their similarity with conventional control schemes is still under investigation. FL controllers use rules in the form the "IF [condition] THEN [action]" to linguistically describe the input/output relationship. The membership functions convert linguistic terms into crisp numeric values. The control method of modelling human language has many advantages, such as simple calculation, as well as high robustness, no need to find the transfer function of the system and suitability for nonlinear systems (Mudi and Pal, 1999; Verbruggen and Bruijin, 1997).

Most commercial fuzzy products are rule-based systems that receive current information in the feedback loop from the device as it operates and control the operation of a mechanical or other device (Simoes and Friedhofer, 1997; Simoes and Franceschetti, 1999). A fuzzy logic system has four blocks as shown in Figure 6.1. Crisp input information from the device is converted into fuzzy values for each input fuzzy set, using the fuzzification block. The universe of discourse of the input variables determines the required scaling for correct per unit operation. The scaling is very important because the fuzzy system can be retrofitted with other devices or ranges of operation by just changing the scaling of the input and output. The fuzzy inference, decision-making mechanism, determines how the fuzzy logic operations are performed, and together with the knowledge base (rule-base) determines the outputs of each fuzzy IF-THEN rules. Those are combined and converted to crisp values with the defuzzification block. The output crisp value can be calculated by one of the defuzzification methods, such as; centre of gravity or the weighted average.

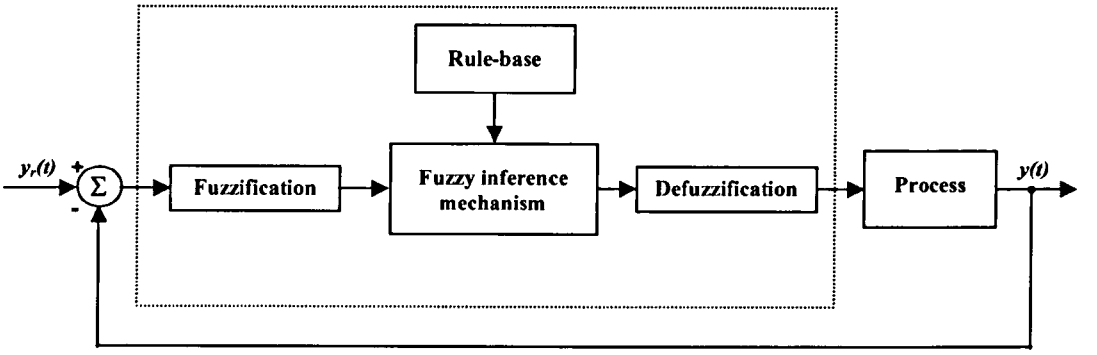

Figure 6.1: Configuration of a fuzzy logic controller

The following subsections discuss the nature of fuzziness and show how fuzzy operations are performed, and how fuzzy rules can incorporate the underlying knowledge.

6.2.1 Fuzzy sets

A fuzzy set is represented by a membership function defined on the universe of discourse. The universe of discourse is the space where the fuzzy variables are defined. The membership function gives the grade, or degree, of membership within the set of any element of the universe of discourse (Jantzen, 1998). The membership function maps the elements of the universe onto numerical values in the interval [0, 1]. A membership function value of zero implies that the corresponding element is definitely not an element of the fuzzy set, while a value of unity means that the element fully belongs to the set.

6.2.2 Fuzzification

Fuzzification is the process of decomposing a system input and output into one or more fuzzy sets. Many types of curves can be used, but triangular or trapezoidal shaped membership functions are the most common because they are easier to represent in embedded controllers. Figure 6.2 shows a system of fuzzy sets for an input with trapezoidal and triangular membership functions. Each fuzzy set spans a region of input or output value graphed with the membership. Any particular input is

interpreted from this fuzzy set and a degree of membership is interpreted. The membership functions should overlap to allow smooth mapping of the system. The process of fuzzification allows the system inputs and outputs to be expressed in linguistic terms so that rules can be applied in a simple manner to express a complex system.

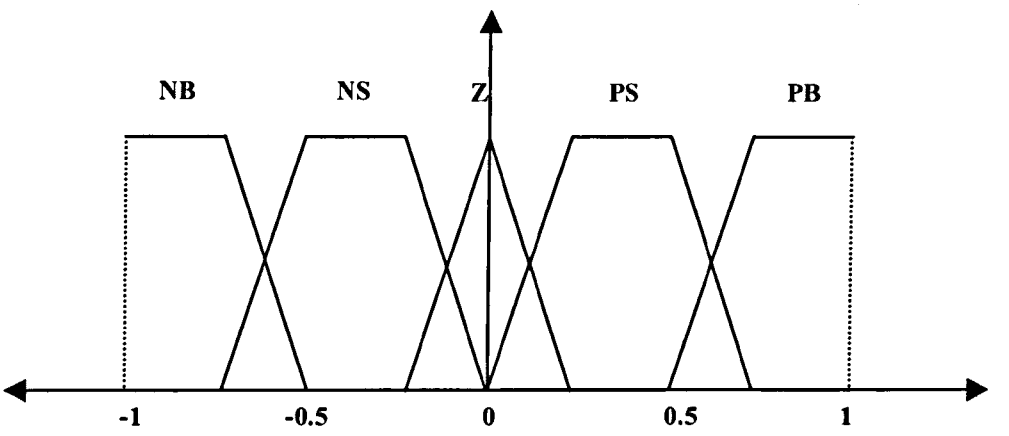

Figure 6.2: Fuzzy sets with trapezoidal and triangular membership functions

6.2.3 Fuzzy inference

Inference is the process of formulating a nonlinear mapping from a given input space to output space. The mapping then provides a basis from which decisions can be taken. The process of fuzzy inference involves all the membership functions, fuzzy logic operators and if-then rules.

There are three types of fuzzy inference models, which have been widely employed in various control applications (Passino and Yurkovich, 1998; Siddique, 2002). These fuzzy models are:

- Mamdani fuzzy models
- Sugeno fuzzy models
- Tasukamoto fuzzy models

The differences between these three fuzzy inference models lie in the consequents of their fuzzy rules, aggregations and defuzzification procedures.

6.2.4 Rule-base

A fuzzy system is characterized by a set of linguistic statements based on expert knowledge. The expert knowledge is usually in the form of *if-then* rules, which are easily implemented by fuzzy conditional statements in fuzzy logic. The collections of fuzzy rules are expressed as fuzzy conditional statements to form the rule base or rule set of FLC.

The natural language equivalent to the symbolic description of fuzzy inference, at each sampling time *(t)*, is read as follows:

- *IF* the value of error *e(t)* is <*linguistic value*> and
- The value of change-of-error $\Delta e(t)$ is <*linguistic value*>
- *THEN* the value of control output *u(t)* is <*linguistic value*>.

The symbolic name of a linguistic value is one of the linguistic qualifiers, determined for the proper variable: *e(t)*, $\Delta e(t)$ or *u(t)*, for example: Positive Big, Positive Small, Zero, Negative Small, Negative Big, etc. So, the rules of the PD-type fuzzy controller can be written as:

- IF error *e(t)* is *Positive Big* and $\Delta e(t)$ is *Negative Big* THEN *u(t)* is *Zero*.

It is necessary to describe the state of error signal *e(t)*, either positive or negative, since the actual output *y(t)* can either be higher or lower than the desired one $y_r(t)$. If *e(t)* is *negative* that means the current value of the actual output is higher than the desired output (i.e. *y(t)* is above the set-point). On the other hand, linguistic values of *e(t)* with a *positive* sign mean that the current value of y is below the set-point.

The change-of-error $\Delta e(t)$ with a *negative* sign means that the current value of the actual output *y(t)* has increased in comparison with its previous value $y(t-1)$, since $\Delta e(t) = e(t) - e(t-1) < 0$. While, the linguistic value of $\Delta e(t)$ with a *positive* sign means that the current value of *y(t)* has increased in comparison with its previous value $y(t-1)$.

A linguistic value of *Zero* for *e(t)* means that the actual output *y(t)* is equal to the desired one (i.e. is about the set-point). Consequently, if $\Delta e(t)$ is *Zero*, then the

current actual output $y(t)$ has not changed significantly from its previous value (i.e. $\Delta e(t) = e(t) - e(t-1) = 0$).

6.2.5 Defuzzification

After fuzzy reasoning there is a linguistic output variable, which needs to be translated into a crisp value. The objective is to derive a single crisp numeric value that best represents the inferred fuzzy values of the linguistic output variable. Defuzzification is such inverse transformation that maps the output from the fuzzy domain back into the crisp domain.

Some defuzzification methods tend to produce an integral output considering all the elements of the resulting fuzzy set with the corresponding weights. Other methods take into account just the elements corresponding to the maximum points of the resulting membership functions. The following defuzzification methods are of practical importance (Shaw, 1998):

- *Center-of-Area (CoA)*: This method is often referred to as the Center-of-Gravity (CoG) method, because it computes the centroid of the composite area representing the output fuzzy term.
- *Center-of-Maximum (CoM)*: In this method only the peaks of the membership functions are used. The defuzzified crisp compromise value is determined by finding the place where the weights are balanced. Thus the areas of the membership functions play no role and only the maxima (singleton memberships) are used. The crisp output is computed as a weighted mean of the term membership maxima, weighted by the inference results.
- *Mean-of-Maximum (MoM)*: This method is only used in some cases where the CoM approach does not work. This occurs whenever the maxima of the membership functions are not unique and the question is as to which one of the equal choices one should take.

6.2.6 Types of fuzzy controllers

There are three most popular types of FLC structure that have been studied and investigated, namely; PD-type, PI-type and PID-type fuzzy controllers. They are more robust and exhibit superior applicability to their conventional counterparts, namely PD, PI and PID compensators (Tang and Mulholland, 1987; Chou and Lu, 1993). Fuzzy type controllers are also used to achieve better performance with nonlinear processes (Driankov *et al.*, 1996). On the other hand, PD-type and PI-type FL controllers posses the same characteristics as the conventional PD and PI compensators, respectively. That is, the PD-type FLC adds damping and reliably predicts large overshoots, but does not improve the steady-state response (Chao and Teng, 1997; Chung *et al.*, 1998). The difficulty with the PID-type fuzzy control is that it needs three inputs, which will greatly increase the rule-base and make the design of the controller more complicated. In the next sub-sections, PD-type PI-type and PID-type FL controllers are discussed in more detail.

6.2.6.1 PD-type fuzzy control

PD-type fuzzy control is known to be more practical than PI-type, which is slow and gives poor performance in the system transient state for higher order processes due to the internal integration operator. Good experiences have been obtained especially with the PD-type fuzzy controllers in servo applications (Franssila and Koivo, 1992; Makkonen and Koivo, 1994). However, PD-type fuzzy control cannot eliminate the system steady-state error. The PD-type FLC, shown in Figure 6.3, generates a control action (u) from system error (e) and change of system error (Δe).

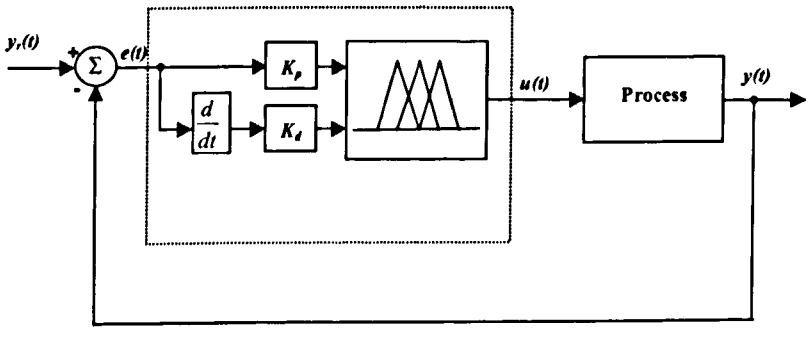

Figure 6.3: Block diagram of PD-type FLC

The output of PD-type FLC is given as:

$$u(t) = k_p e(t) + k_d \frac{d}{dt} e(t) \tag{6.1}$$

where,

$$e(t) = y_r(t) - y(t) \tag{6.2}$$

6.2.6.2 PI-type fuzzy control

It is well known that the PI-type FLC exhibits good performance at the steady state like the conventional PI controller. That is the PI-type FLC reduces the steady-state error, but yields penalized rise time and settling time (Chao and Teng, 1997). It gives inevitable overshoot when attempting to reduce the rise time, especially with high order systems (Lee, 1990). These undesirable characteristics of fuzzy PI controllers are caused by integral operation of the controller, even though the integrator is introduced to overcome the problem of steady-state error.

The PI-type FLC can be expressed in two forms. The first one is referred to as absolute PI-type controller, shown in Figure 6.4. It generates its control action $u(t)$ from error $e(t)$ and sum of error $\sum e(t)$. The absolute PI-type FL controller output is expressed as:

$$u(t) = k_p e(t) + k_i \int e(t)dt \tag{6.3}$$

where,

$$e(t) = y_r(t) - y(t) \tag{6.4}$$

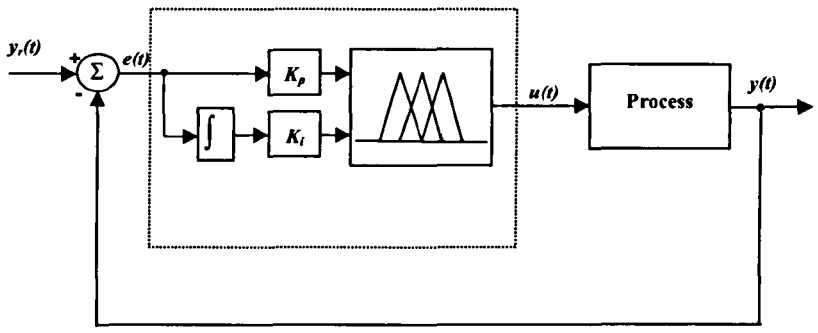

Figure 6.4: Block diagram of absolute PI-type FLC

The other form of PI-type FLC is called incremental PI-type FLC. The block diagram of the incremental PI-type FLC is shown in Figure 6.5.

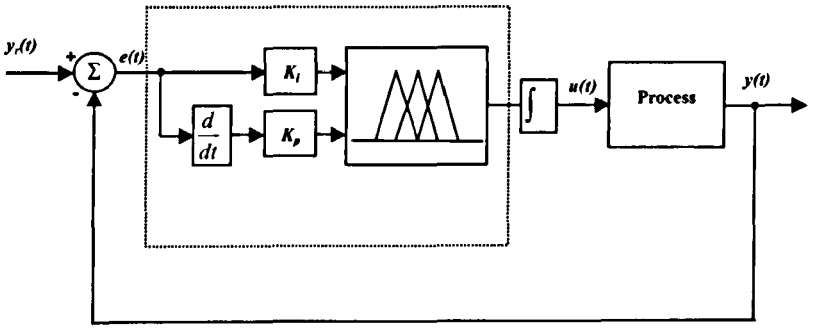

Figure 6.5: Block diagram of incremental PI-type FLC

The incremental PI-type FLC preserves all the components of PD-type FLC, yet containing one extra integral component located after the defuzzification block.

$$\frac{d}{dt}u(t) = k_p \frac{d}{dt}e(t) + k_i e(t) \tag{6.5}$$

Integrating equation (6.5), yields:

$$u(t) = k_p e(t) + k_i \int e(t)dt \tag{6.6}$$

In this case the control action and fuzzy rules, like PD-type FLC, are generated based on the error $e(t)$ and change-of-error $\Delta e(t)$. Therefore, as for the practical implementation, the second approach, i.e. incremental PI-type FLC, is adopted in this investigation.

6.2.6.3 PID-type fuzzy control

Fuzzy PID control can meet the design criteria of fast rise time, minimum overshoot, shorter settling time and zero steady sate error. However, the difficulty with the PID-type fuzzy control is that it needs three inputs, which will greatly increase the rule-base and make the design of the controller more complicated. That is because it generates its control action $u(t)$ from error $e(t)$, change-of-error $\Delta e(t)$ and sum of error $\sum e(t)$. Therefore, PID-type fuzzy controllers are rarely used. The block diagram of PID-type FLC is illustrated in Figure 6.6, and its output is given as:

$$u(t) = k_p e(t) + k_i \int e(t)dt + k_d \frac{d}{dt} e(t) \tag{6.7}$$

where,

$$e(t) = y_r(t) - y(t) \tag{6.8}$$

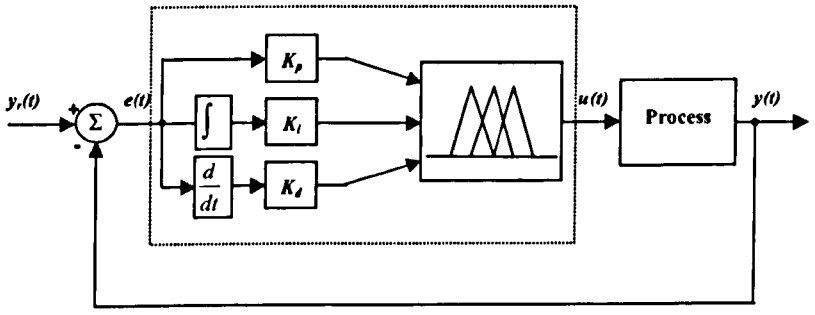

Figure 6.6: Block diagram of PID-type FLC

Theoretically, the number of rules to cover all possible input variations for PID-type FLC is $n_1 \times n_2 \times n_3$, where n_1, n_2 and n_3 are the number of linguistic labels of the three input variables ($e(t)$, $\Delta e(t)$ and $\sum e(t)$). In particular, if $n_1 = n_2 = n_3 = 5$, then the number of rules are $5 \times 5 \times 5 = 125$. In practical applications the design and implementation of such a large rule-base is a tedious task, and it will take a substantial amount of memory space and reasoning time. Due to a long reasoning time, the response of such a generic PID-type FLC will be too slow and hence not suitable for a flexible manoeuvring system such as the TRMS, where a fast response is desired.

To overcome the problems of PID-type FLC, a number of approaches have been proposed and studied. A typical method for rule reduction in PID-type FLC is to divide the three-term PID controller into two separate fuzzy PD and fuzzy PI parts (Chen and Linkens, 1998; Kwok *et al.*, 1990; Zhang and Mizumoto, 1994). This hybrid PD and PI controller with n linguistic labels in each input variable require only $n \times n + n \times n = 2n^2$ rules. For example, for $n = 5$ there will be $5 \times 5 + 5 \times 5 = 50$ rules, which are significantly smaller than n^3 ($5 \times 5 \times 5 = 125$ rules), required by the generic PID-type FLC. This number of rules, processed during the execution of generic fuzzy PID, consumes a significant amount of processing time and memory space.

A further reduction procedure is possible by using a switching mechanism between fuzzy PD and absolute fuzzy PI controllers at a specific period of time (Siddique, 2002). The switching mechanism is advocated as solutions to gain the advantages of PD-type and PI-type controllers during transient and steady-state periods as well as to reduce the size of the rule-base. In that case only one set of rules, i.e. $n \times n$ rules for each type of fuzzy controller, is executed at a time and thus the executed rules in a controller rule base are reduced to only 25 rules for $n = 5$ linguistic labels in each input variable.

6.3 Hybrid control scheme

The current study is confined to the development of two forms of hybrid control schemes that combine intelligent and conventional techniques for tracking

performance of the vertical movement in the TRMS. Controllers that combine intelligent and conventional techniques are commonly used in the intelligent control applications of complex dynamic systems. Therefore, embedded fuzzy controllers automate what has traditionally been as a human control activity. The following two sub-sections describe the two forms of hybrid control schemes.

6.3.1 Conventional PD with PID hybrid control scheme

The first hybrid control scheme comprises a conventional PD controller and PID compensator (PD-PID). The schematic diagram for this hybrid control strategy is shown in Figure 6.7.

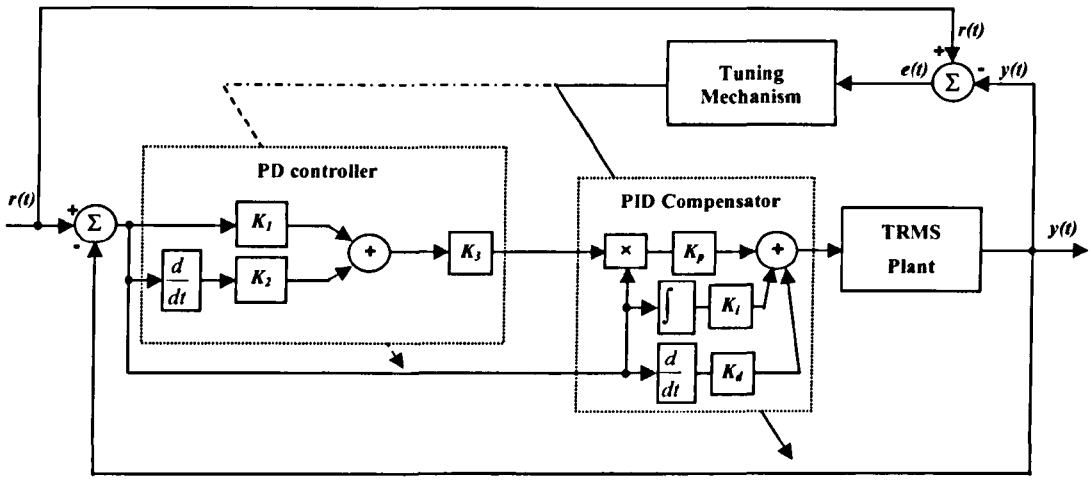

Figure 6.7: Hybrid PD with PID control scheme (PD-PID)

As can be seen from Figure 6.7, the hybrid controller is constructed in such a way that the output of the PD controller is fed into the proportional gain K_p of the PID compensator. Thus, the proportional gain component is continuously updated by the first controller's output. The other two parameters, namely integral K_i and derivative K_d, of the PID compensator are tuned using tuning mechanism explained later in section 6.4.2. The output of the hybrid controller is given as:

$$u(t) = \left\{\left[e(t)k_1 + k_2\frac{d}{dt}e(t)\right]k_3\right\}e(t)k_p + k_i\int e(t)dt + k_d\frac{d}{dt}e(t) \qquad (6.9)$$

Simplifying equation (6.9) yields:

$$u(t) = k_p e^2(t) k_1 k_3 + k_p k_2 k_3 e(t) \frac{d}{dt} e(t) + k_i \int e(t)dt + k_d \frac{d}{dt} e(t) \tag{6.10}$$

Re-arranging the terms of equation (6.10) yields:

$$u(t) = k_p k_1 k_3 e^2(t) + k_i \int e(t)dt + \left[k_d + k_p k_2 k_3 e(t)\right] \frac{d}{dt} e(t) \tag{6.11}$$

The non-linear terms on the right-hand-side of equations (6.11) will help in achieving relatively fast response during the transient-state. While the linear term will effectively take over during the steady-state and due to the integral action will reduce the steady-state error to zero.

6.3.2 Fuzzy PD with PID hybrid control scheme

The schematic diagram for the second proposed hybrid control scheme is shown in Figure 6.8. It involves PD-type FLC with PID compensator (FPD-PID).

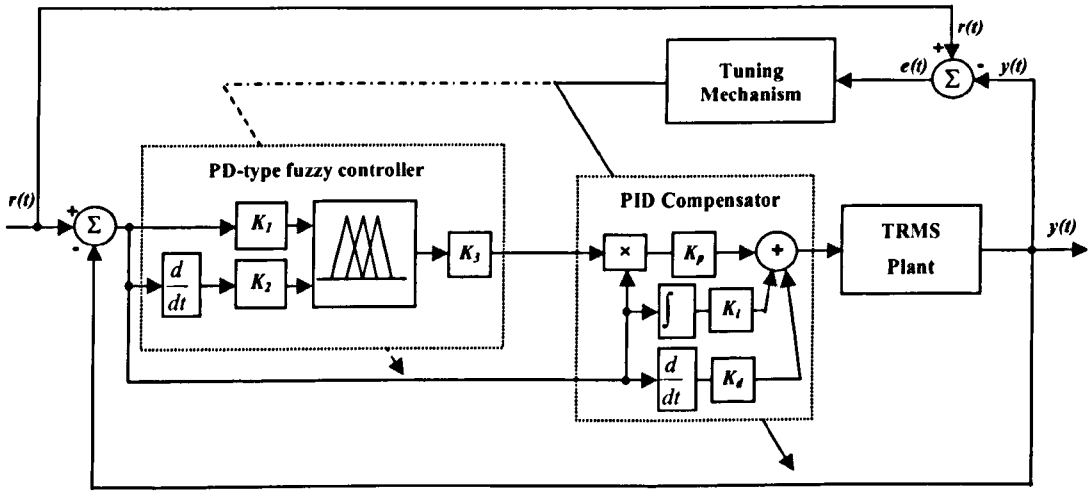

Figure 6.8: Hybrid PD-type fuzzy with PID control scheme (FPD-PID)

Since, PD-type FLC possesses the same characteristics as a conventional PD compensator, similar to the first hybrid scheme, the output of the fuzzy controller is fed into the proportional gain K_p of the PID compensator. Thus, the proportional gain component is continuously updated by the first controller's output.

6.4 Implementation

In contrast to the mathematical world, plants in the real world are ill-defined and often difficult to describe. Hence for any control paradigm, the crucial test is its implementation on the real system in the presence of real world disturbances and uncertainties. In this study, five control strategies namely; PID compensator, PD-type FLC (FPD), PI-type FLC (FPI), conventional PD controller with PID compensator (PD-PID) hybrid control scheme and PD-type FLC with PID compensator (FPD-PID) hybrid control scheme were developed and implemented within both simulation and real-time environments of the TRMS rig using the MATALB/SIMULINK Real Time Workshop (RTW) described in Chapter 2.

Essentially, the task of the developed controllers is to achieve robust tracking of commanded elevation angle by manipulating the voltage input to the main rotor. The controlled output (elevation angle) is expected to have low overshoot, quick settling time of residual oscillation and reasonably fast speed of response. Note that the operating point for this experiment is the flat horizontal main body, representing hover mode. A step input signal with a magnitude of 0.3 volt, referred as a *reference* signal, is applied to the system to extract its response. It was designed off-line separately and then read from the workspace through MATLAB/SIMULINK environment. Performances of the developed controllers are assessed in terms of set-point tracking performance.

6.4.1 Design of fuzzy controllers

An appropriate set of control rules between the two inputs and one output of the fuzzy inference system were defined based on the rule-base shown in Table 6.1. The meanings of the linguistic variables are depicted in Table 6.2.

Table 6.1: Rule-base array of the fuzzy inference system

		e				
		PB	*PS*	*Z*	*NS*	*NB*
Δe	*PB*	PVB	PB	PM	PS	Z
	PS	PB	PM	PS	Z	NS
	Z	PM	PS	Z	NS	NM
	NS	PS	Z	NS	NM	NB
	NB	Z	NS	NM	NB	NVB

Table 6.2: Meaning of the linguistic variables in the fuzzy inference system

PVB	Positive Very Big
PB	Positive Big
PM	Positive Medium
PS	Positive Small
Z	Zero
NS	Negative Small
NM	Negative Medium
NB	Negative Big
NVB	Negative Very Big

Table 6.1 represents 25 rules. For instance, the cell defined by the intersection of the first row and the first column represents the following rule:

- IF *e(t)* is *PB* and *Δe(t)* is *PB* THEN *u(t)* is *PVB*.

System stability can be predicted by observing the order in which the fuzzy rules are fired. For a stable system, *(e)* and *(Δe)* should be gradually decreased during the rule firing process. This can be noticed by drawing a trajectory and moving along it from the edges of the rule-base table towards its centre, as shown in Figure 6.9.

Δe \ *e*	*PB*	*PS*	*Z*	*NS*	*NB*
PB	PVB	PB	PM	PS	Z
PS	PB	PM	PS	Z	NS
Z	PM	PS	Z	NS	NM
NS	PS	Z	NS	NM	NB
NB	Z	NS	NM	NB	NVB

Figure 6.9: A typical trajectory for stable system rules firing

The membership functions of the two fuzzy input sets (control error and its derivative) and output (elevation angle), used for designing both PD-type and PI-type FL controllers are depicted in Figure 6.10. The input and output universes of discourse of the fuzzy controller were normalized within the range [-1, 1]. The input gains K_1 and K_2 were used to map the actual inputs (control error and its derivative) of the fuzzy system to the normalized universe of discourse [-1, 1] and are called normalizing gains. Similarly, K_3 is the output gain that scales the output of the controller. Singleton fuzzification and centre of gravity (CoG) defuzzification were used in the design of the fuzzy control system throughout this investigation.

The fuzzy controller used sigmoidal membership functions to obtain a smooth performance. As shown in Figure 6.10, the membership functions for the two fuzzy input sets are uniform. But, the membership functions for the output fuzzy set are narrower near zero. This is to decrease the gains of the controller near the set-point in order to obtain a better steady state control and avoid excessive overshoot.

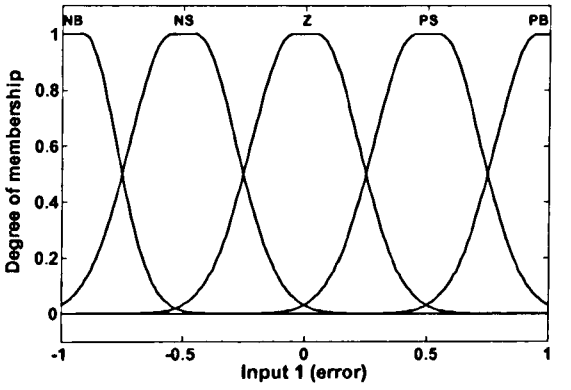

a) Membership function of Input 1

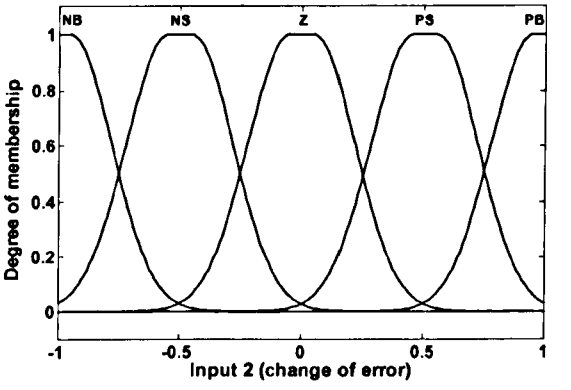

b) Membership function of Input 2

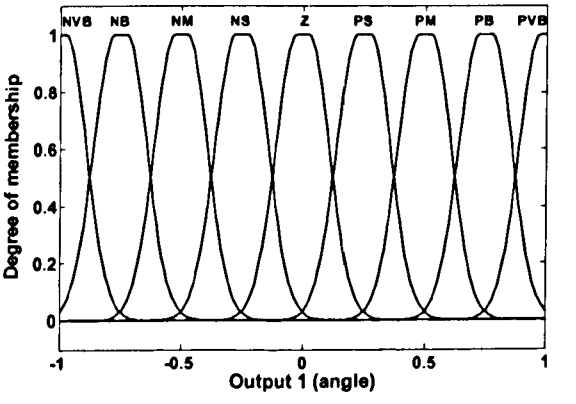

c) Membership function of the output

Figure 6.10: Membership functions of the fuzzy inference system

6.4.2 Parameter tuning mechanism

The potential of GA is utilized in this investigation as an optimization mechanism to tune the integral and derivative gains of the PID compensator within the hybrid control framework, to improve the system response. GA is a robust search technique proven to be an effective optimisation mechanism in complex search spaces (Chipperfield and Fleming, 1994; Goldberg, 1989). In control engineering, GA is usually utilized, in offline mode, to overcome the difficulty in obtaining an optimal solution when using a manual tuning of the control parameters based on a heuristic (trial-and-error) approach.

The GA-based tuning process of PID gains was accomplished offline (in the simulation phase). Then, those values are considered as a guideline for tuning process during practical implementation of the developed control strategies. Thus, the tuning process during the experimental phase was carried out based on heuristic (trial-and-error) approach. This is due to the difficulties associated with GA-based optimisation process (Fleming and Purshouse, 2002), which requires long computation time that makes it inadequate as an online tuning mechanism.

An objective function was created to tune those parameters in order to obtain a satisfactory input tracking performance in terms of overshoot, rise-time, settling-time and steady-state error. To combine all objectives (minimum overshoot, small rise and settling times and minimum steady-state error), multiple objective functions are used to minimise the output error of the controlled system.

The GA optimisation process is initialised with a random population consisting of 40 individuals. The population is represented by real valued numbers or binary strings each of 16 bits called chromosomes. Each chromosome consists of two separate strings constituting K_i and K_d terms, as defined within specific range, which can ensure stability. The integral of time-weighted absolute error (ITAE) and integral of absolute error (IAE) are used as performance measure criteria:

$$IAE = \int_0^T |y_r(t) - y(t)|dt \quad , \quad ITAE = \int_0^T t|y_r(t) - y(t)|dt \tag{6.12}$$

where, $y_r(t)$ represents the reference input and $y(t)$ represents the system response. The chromosome was assigned an overall fitness value according to the magnitude of the error; the smaller the error the larger the fitness value.

The GA optimisation process, depicted in Figure 6.11, was initialised with a random population consisting of 50 individuals. The population was represented by binary strings, each of 20 bits called chromosomes.

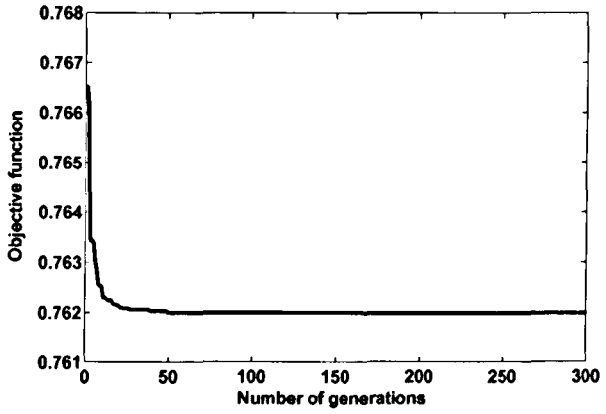

Figure 6.11: Convergence of GA objective function

6.5 Results

This section presents the obtained results of both simulation and real-time implementation of the TRMS response with the developed control strategies. The performances of the hybrid control strategies were assessed in terms of time domain specifications in comparison with PID compensator, pure PD-type and PI-type FLCs.

Figures 6.12-6.16 illustrate the system response to a step input with the five employed control strategies. The system response with the conventional PID compensator is shown in Figure 6.12, while the system responses with pure PD-type and PI-type fuzzy controllers are shown in Figures 6.13 and 6.14, respectively. It is noted that the system response with both PD and PI-type controllers were not satisfactory as compared to the system response with conventional PID compensator. The response with PI-type fuzzy controller was terribly slow, while, PD-type fuzzy

controller couldn't eliminate the steady state response error, although the response has a fast rise time. These are due to their drawbacks that were mentioned earlier.

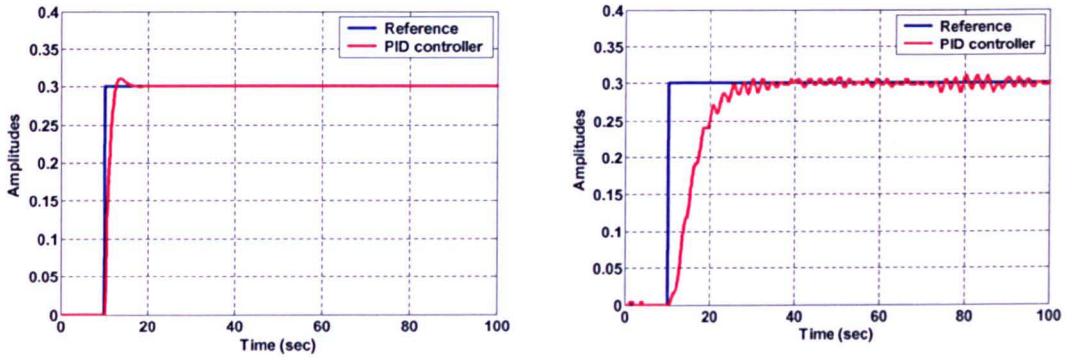

(a) Simulation *(b) Experimental*

Figure 6.12: System response with PID compensator

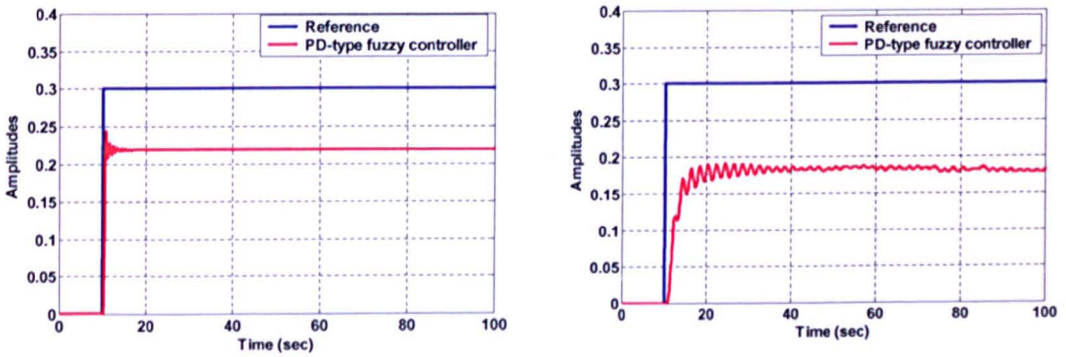

(a) Simulation *(b) Experimental*

Figure 6.13: System response with PD-type fuzzy controller

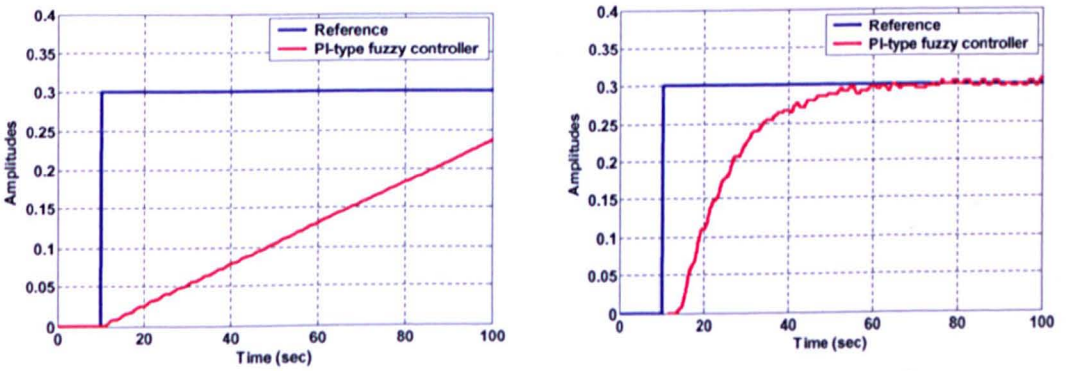

(a) Simulation *(b) Experimental*

Figure 6.14: System response with PI-type fuzzy controller

To overcome the problems associated with pure PD-type and PI-type FLCs, two forms of hybrid control schemes, namely; PD-PID and FPD-PID, were designed and implemented to improve the system response. The corresponding system responses are shown in Figures 6.15 and 6.16, respectively. The results obtained reveal that the two hybrid control schemes cope well with the complexities of the plant and demonstrated good capabilities in maintaining a better input tracking performance than the system with pure PD-type and PI-type fuzzy controllers.

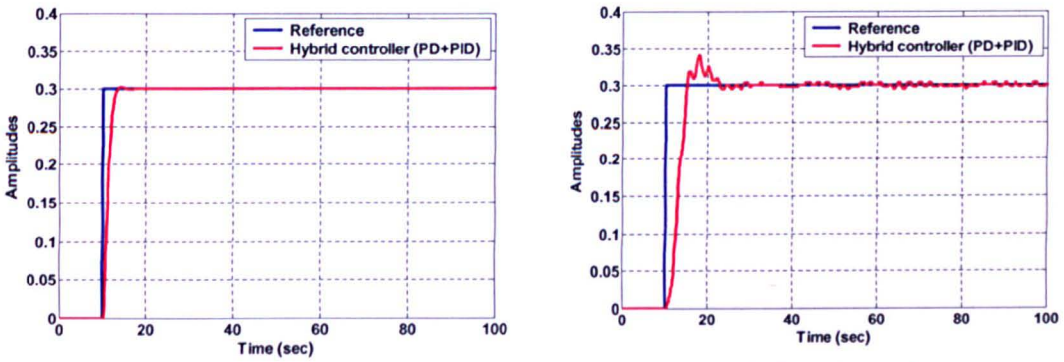

(a) Simulation *(b) Experimental*

Figure 6.15: System response with PD-PID hybrid controller

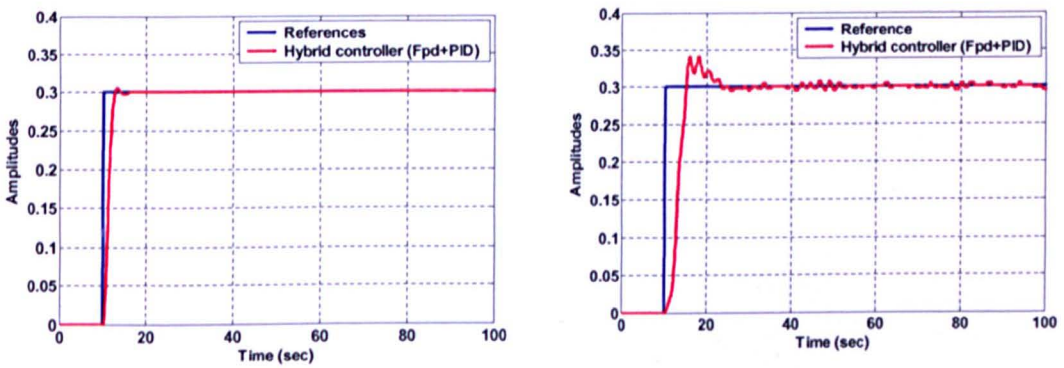

(a) Simulation *(b) Experimental*

Figure 6.16: System response with FPD-PID hybrid controller

It is noted in Figures 6.15 and 6.16 that both hybrid control schemes (PD-PID and FPD-PID) have successfully eliminated the steady-state response error and

provided satisfactory tracking performance in both steady and transient states in simulation and real-time experimentation.

6.6 Comparative performance assessment

Table 6.3 summaries the quantitative achievements of the employed controllers in terms time domain system behaviour; overshoot (OS), rise-time (RT), settling-time (ST), and steady-state error (SSE). Among the five techniques employed for set-point tracking performance, the two hybrid control schemes have resulted in better performance than the other controllers. This is evidenced in the time domain specification analysis in simulation and real-time experimental exercises, presented in Table 6.3 and illustrated in Figures 6.17 and 6.18, respectively.

Table 6.3: Performances of the employed control strategies in time domain

Control Strategy	**Time-Domain Parameters**				**Environment**
	OS %	RT sec	ST sec	SSE %	
PID compensator	3.334	1.500	4.600	0	Simulation
PD-type fuzzy controller	-	-	89.900	-27.154	
PI-type fuzzy controller	-	-	89.900	-21.450	
(PD-PID) hybrid controller	0.758	2.000	3.000	0	
(FPD-PID) hybrid controller	1.612	1.700	2.500	0	
PID compensator	3.288	10.000	82.700	0.220	Experimental
PD-type fuzzy controller	-	-	89.900	-39.254	
PI-type fuzzy controller	2.265	25.600	89.900	2.265	
(PD-PID) hybrid controller	13.515	3.100	12.400	0.220	
(FPD-PID) hybrid controller	13.515	2.800	38.900	-1.825	

OS = Overshoot RT= Rise time ST = Settling time SSE = Steady state error

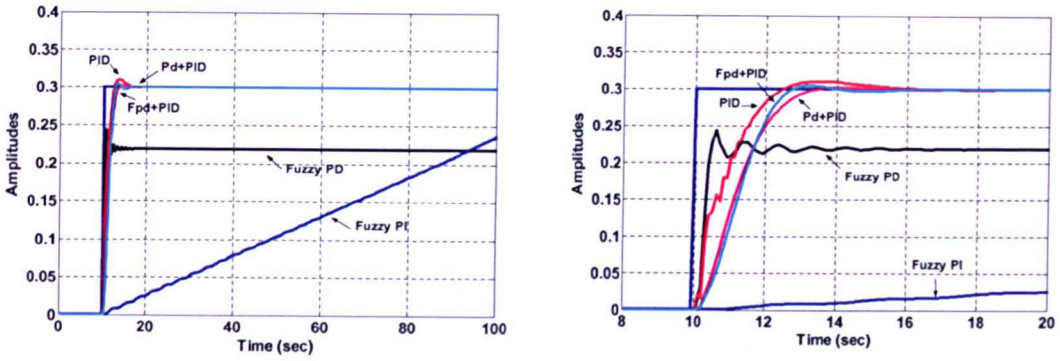

(a) All duration *(b) First 20 sec*

Figure 6.17: System response with the controllers (Simulation)

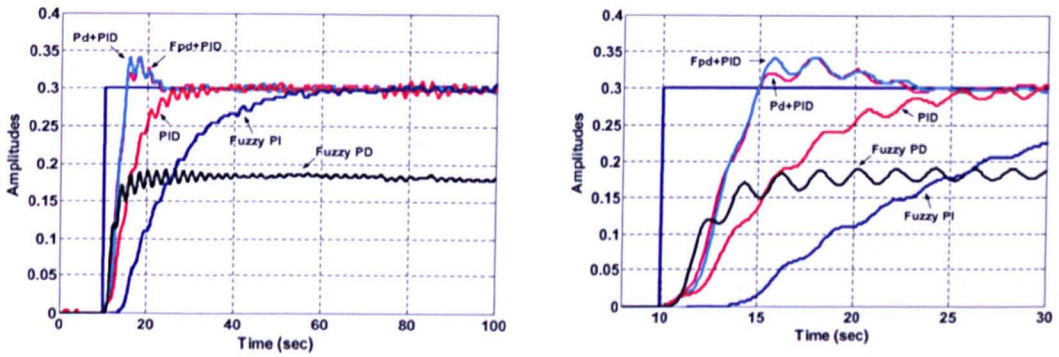

(a) All duration *(b) First 30 sec*

Figure 6.18: System response with the controllers (Experimental)

6.7 Summary

Combinations of intelligent and conventional control techniques are commonly used in control applications of complex dynamic systems. Such hybrid schemes have proved to be efficient and can overcome the deficiencies of the PID controller and intelligent controllers alone. The current study is confined to the development of two forms of hybrid control schemes that combine fuzzy control and conventional techniques for tracking performance of the vertical movement in the TRMS. The two

hybrid control strategies comprising conventional PD controller plus PID compensator and PD-type fuzzy control plus PID compensator have been developed and implemented for set-point tracking control of the vertical movement of the TRMS.

The investigation has also witnessed the ability of GA optimisation that has been introduced as a tuning mechanism for the control parameters within the hybrid scheme. The performance of hybrid control schemes have been compared with other feedback control strategies namely, PID compensator, pure PD-type and PI-type fuzzy controllers. It has been observed that the hybrid control schemes were superior in terms of time domain system behaviour; over-shoot, rise-time, settling-time and accumulated steady-state error. The obtained results also revealed that the GA technique is effective and efficient, as an offline optimization mechanism, in tuning the parameters. The GA optimization process can save time as compared with conventional trial-and-error tuning procedures.

A heuristic tuning of rule-bases and membership functions of the employed FLCs has been utilized through a trial and error mechanism. However, for increasingly larger numbers of input and output rules as well as membership functions, even with *a priori* expert knowledge, the method becomes more difficult as the number of rules rise exponentially. Therefore, intelligent techniques such as Artificial Neural Network (ANN) and GA can be advocated as solutions to this problem. ANNs can be used to learn FLC rule-bases or to tune given membership functions. Such an approach combines the learning capability of the ANN with the reasoning power of fuzzy logic. Alternatively, the search for suitable rules or membership function parameters of an FLC knowledge base can be viewed as an optimization problem to which a GA can be applied.

CHAPTER 7

AUGMENTED CONTROL SCHEME FOR INPUT TRACKING AND VIBRATION SUPPRESSION

7.1 Introduction

Following the successful implementation of command shaping techniques for vibration suppression and hybrid feedback control schemes for input tracking performance in Chapters 4 and 5 respectively, this chapter presents the development of augmented control scheme that comprises the two control methods to achieve more than one performance criteria such as robust command tracking, fast system response and vibration suppression simultaneously. The motivation for this investigation stems from the fact that for very rapid manoeuvres of a flexible system, a satisfactory feedback controller that can achieve these objectives may prove difficult to design. Moreover, the command shaping techniques are not robust to parameter changes and disturbances in the system. Therefore, in order to overcome this problem a control strategy, such as an augmented control scheme, that can provide acceptable input tracking capability and low system vibration need to be developed.

Augmenting the feedback control system with a feedforward method (Figure 7.1) can facilitate the controller design and enable the attainment of better performance (Pao, 2000). The performance of feedback methods can often be improved by adding a feedforward controller; such as an input shaping scheme. A properly designed feedforward control component can dramatically reduce the complexity of the required feedback controller for a given level of performance. Thus, the development of effective feedforward algorithms can lead to more practical and accurate control of flexible systems such as the TRMS.

This chapter presents investigations into the development of an augmented feedforward and feedback control scheme (AFFCS) for motion control of the TRMS rig. The main goal of this framework is to satisfy performance objectives in terms of

robust command tracking, fast system response and minimum residual vibration. This investigation is carried out in two stages; simulation and real-time implementation on the TRMS platform.

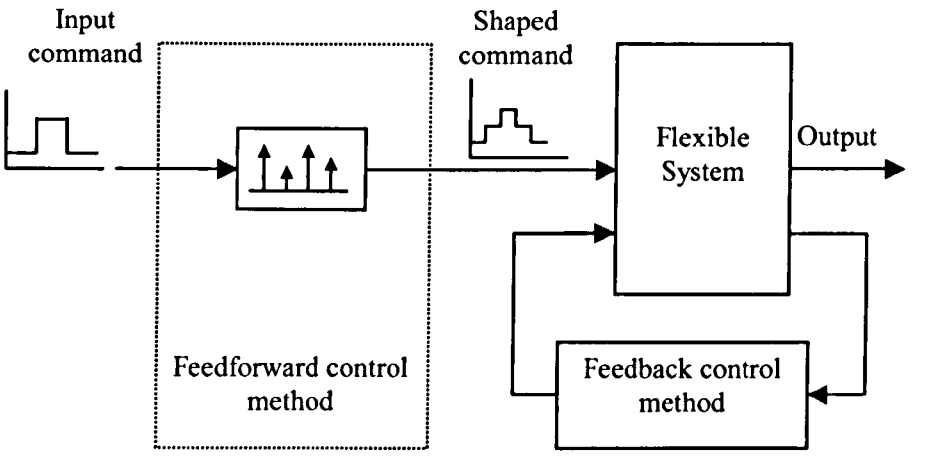

Figure 7.1: Schematic of augmented feedforward and feedback control scheme

7.2 Augmented control scheme

It is evident from the TRMS rig that structural vibrations occur due to the presence of rotor load at the end of the cantilever beam and motor torque, inducing bending movement, while in operation. These vibrations appear in the system response as oscillations with long settling times. Several different approaches have been proposed to reduce residual vibration in flexible systems. The command shaping techniques for attenuating oscillations was examined in Chapter 5, and significant reduction in the vibration of the system has been demonstrated with these techniques. However, input tracking capabilities and disturbance rejection properties of the system are unsatisfactory especially in the presence of dynamic variation.

An acceptable system tracking performance with reduced vibration that accounts for system changes can be achieved by developing an augmented control scheme (ACS) that caters for rigid body motion and vibration of the system independently. This can be realised by utilising strategies consisting of combined feedforward and feedback control methods, where the former can be used for vibration suppression and the latter for input tracking of the system.

Both feedforward and feedback control structures have been utilised in the control of flexible manoeuvring systems. A hybrid collocated and non-collocated controller has previously been proposed for control of a flexible manipulator (Tokhi and Azad, 1996). The controller design utilises end-point acceleration feedback through a proportional-integral-derivative (PID) control scheme and a proportional-derivative (PD) configuration for control of rigid body motion. Experimental investigations have shown that the control structure gives a satisfactory system response with significant vibration reduction as compared to the response with a collocated controller. A PD feedback control with a feedforward control to regulate the position of a flexible manipulator has been proposed by Shchuka and Goldenberg (1989). Simulation results have shown that although the pole-zero cancellation property of the feedforward control speeds up the system response, it increases overshoot and oscillation. A control law partitioning scheme which uses end-point sensing device has been reported by Rattan *et al.* (1990). The scheme uses end-point position signal in an outer loop to control the flexible modes, whereas the inner loop controls the rigid body motion independent of the flexible dynamics of the manipulator. Performance of the scheme has been demonstrated in both simulation and experimental trials incorporating the first two flexible modes. A combined feedforward and feedback method in which the end-point position is sensed by an accelerometer and fed back to the motor controller, operating as a velocity servo, has been proposed for the control of a flexible manipulator system (Wells and Schueller, 1990). This method uses a single mass-spring-damper system to represent the manipulator and thus the technique is not suitable for high speed operation.

Mohamed and Tokhi (2003) reported the developed of a hybrid control scheme based on feedforward with collocated feedback controllers and non-collocated with collocated feedback controllers for input tracking and end-point vibration suppression of a flexible manipulator. Initially, a fixed joint-based collocated PD controller utilising hub-angle and hub-velocity feedback was developed for control of rigid body motion. This was then extended to incorporate non-collocated and feedforward controllers for vibration suppression of the manipulator. To examine the robustness of the controllers, the control schemes were simulated with different loading conditions.

Ahmad (2001) proposed a combination of feedback mechanism referred to as Stability Augmentation System (SAS) with a command path pre-filter for tracking performance and vibration suppression control problem. The feedforward control law is based on low-pass and band-stop filtering techniques, while the feedback controller is based on a Linear Quadratic Guassian (LQG) compensator. The combined feedforward and feedback compensator was known as the Command and Stability Augmentation System (CSAS). Both SAS and CSAS control schemes have been evaluated on the TRMS test rig in simulation and real-time environments. One of the controllers failed poorly in real-time implementation as compared to the simulation runs for the SAS scheme. While the other failed due to the slow estimator poles, hence could not be evaluated.

Doughtery *et al.* (1982) and Franklin *et al.* (1988) applied classical controllers to control the vibration and attitude in space structures. The control design adopted basically treats the flexible modes as separable subsystems. Therefore, the gains originally chosen for the rigid body alone need to be decreased for lower bandwidth to assure stability when flexible modes are present. Azad (1994) demonstrated control of a single link flexible manipulator utilising a collocated PD feedback incorporating hub angle and hub velocity feedback variables. This was then extended, additionally, to incorporate non-collocated end-point acceleration feedback through a PID controller, achieving a hybrid collocated and non-collocated feedback control mechanism.

Modern control paradigms have been studied for a variety of complex systems, some of which are discussed here. Teague *et al.* (1998) developed a novel method based on linear quadratic regulator (LQR) for active control of the attitude and vibration of a flexible space structure using the Global Positioning System (GPS) as a sensor. Franklin *et al.* (1988), in addition to PD control, used modern optimal control methods to achieve command tracking and vibration suppression of a space satellite. LQR based control design for commercial aircraft control applications was investigated by Blight *et al.* (1996) to redesign an autopilot control law in order to improve stability and reduce sensitivity to plant parameter variations. An improved control law was designed and compared to classical approaches in flight tests, implemented in the autopilot of the Boeing 767 commercial transport

airplane. Their experience in implementing the LQR paradigm is documented in (Blight *et al.*, 1996).

It is apparent that performance criteria such as speed of response or manoeuvrability, flying and handling qualities, imposed on an aircraft are difficult to achieve entirely by aerodynamic means alone (i.e. using control surfaces in aircraft or rotors in the TRMS), and at the same time maintaining the dynamic stability of the airframe. This is particularly valid for highly agile new generation air vehicles, which are designed to operate over extended flight envelopes and in aerodynamically difficult flight regimes. The current investigation is confined to the development of augmented control scheme that combine feedforward control component with feedback control method for input tracking performance and vibration suppression of the vertical movement in the TRMS rig. The TRMS performance can be further enhanced by employing artificial non-aerodynamic means. This implies appending a feedforward control component based on command shaping technique to the feedback control law. The new control structure, shown in Figure 7.2, is referred to as Augmented Feedforward and Feedback Control Scheme (AFFCS).

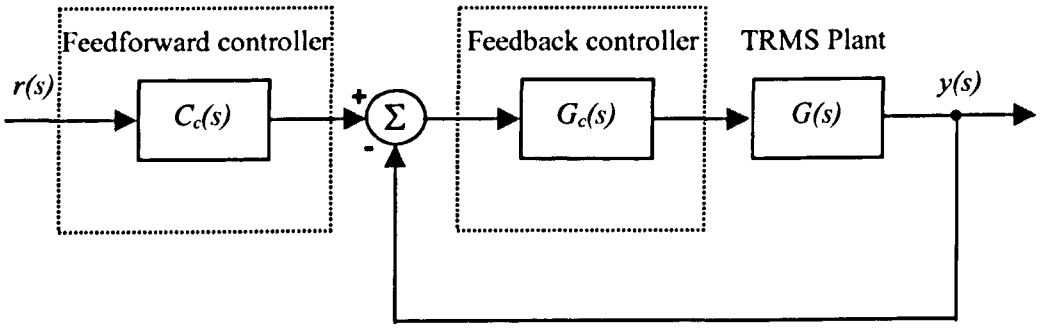

Figure 7.2: Block diagram of augmented feedforward feedback control scheme (AFFCS)

The overall closed-loop transfer function of the augmented TRMS system can be written as:

$$\frac{y(s)}{r(s)} = C_c(s)\left(\frac{G_c(s)G(s)}{1+G_c(s)G(s)}\right) \tag{7.1}$$

where, $C_c(s)$ represents that feedforward controller, while $G_c(s)$ represents the feedback control law. The reference command signal $r(s)$ is conditioned by a command control law, which determines the control and response characteristics $y(s)$ of the augmented system. The consequence of this is a shaped response and reduced control effort, which translates into reduced pilot workload and improved passenger comfort in the case of an aircraft.

It is important to note that the input shaper has no bearing on the system stability since it is outside the closed loop and does not appear in the characteristic equation of the augmented plant. By judicious choice of $C_c(s)$ and $G_c(s)$ the control engineer has considerable scope for achieving the desired stability, control and handling characteristics of the augmented system. The feedforward controller, $C_c(s)$, employed in this study comprises a 4-impulse sequence input shaper used to pre-process the reference command input applied to the TRMS plant.

7.3 Implementation

As mentioned earlier, the goal of this investigation is to develop a control method that has the ability of robust command tracking and can reduce motion and uneven mass induced vibrations in the TRMS during its operational condition, which is a flat horizontal beam, representing a hover mode. A practical way of controlling a system with resonant modes is to use a combination of feedback and feedforward controls.

A 4-impulse input shaper, representing the feedforward control component within the augmented control scheme, is designed and employed for pre-processing the command input, as described in Chapter 5. It is combined with three feedback controllers to form three different augmented control strategies named as; PID compensator with 4-impulse input shaper (PID+IS), hybrid PD-type FLC and PID with 4-impulse input shaper (FPDPID+IS) and hybrid PD controller and PID compensator with 4-impulse input shaper (PDPID+IS). The next subsections describe the designed input signal, feedforward and feedback control laws, employed in this investigation.

7.3.1 Input signal

A finite step input signal with a magnitude of 0.3 volt, depicted in Figure 7.3, referred as a *reference* signal is applied to the system to extract its response. The signal is designed off-line separately and then read from the workspace through MATLAB/SIMULINK environment to evaluate the performance of the developed controllers.

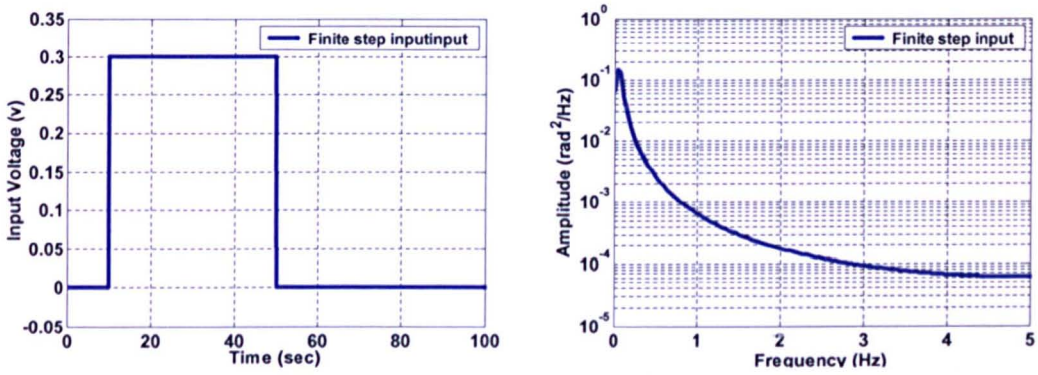

(a) Time domain *(b) Power spectral density*

Figure 7.3: Finite step input

7.3.2 4-impulse input shaper

Based on the procedure presented in Chapter 5 (sections 5.2.1 and 5.32), a four-impulse sequence input shaper, representing the feedforward controller, was designed based on the natural frequency (0.35156 Hz) and the damping ratio (0.0101) for the main dominant mode of the TRMS. The designed input shaper was then employed for pre-processing the command input in order to reduce motion and uneven mass induced vibrations in the TRMS rig during its operation.

Figure 7.4 shows the designed 4-impulse shaped input and its corresponding impulse sequence for the developed input shaper. Analogous to the analysis carried out in Chapter 5, for digital implementation of the input-shaper, locations of the impulses were selected at the nearest sample time-step. The amplitudes and corresponding time locations of the 4-impulse sequence of the designed input shaper are given in Table 7.1.

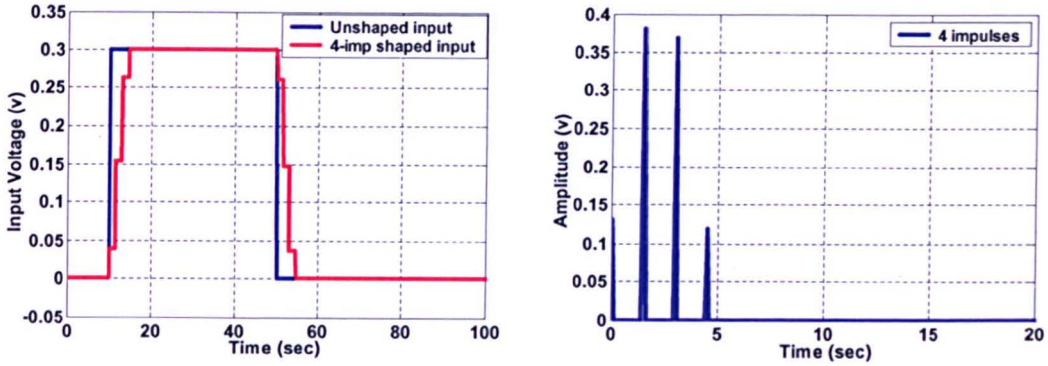

(a) System input (time domain) *(b) 4-impulse sequence*

Figure 7.4: 4-impulse input shaper

Table 7.1: Amplitudes and time locations of impulses for 4-impulse input shaper

Input shaping technique	Impulse Number	Amplitude A_i (volt)	Time location t_i (sec)	Sample location $(n+1)^*$
4-impulse input shaper	1	0.131	0	1
	2	0.381	1.5	16
	3	0.369	3.0	31
	4	0.119	4.5	46

* $n = t_i/\tau$ τ = sample period = 0.1 sec

7.3.3 Feedback control strategies

Three feedback control methods that were designed in the preceding chapter are utilized here in combination with the 4-impulse input shaper to form three different augmented control schemes. The details of the design procedure and parameter tuning mechanisms were discussed in details in Chapter 6. The first augmented control scheme comprises a conventional PID compensator with 4-impulse input shaper (PID+IS), a schematic diagram of which is shown in Figure 7.5.

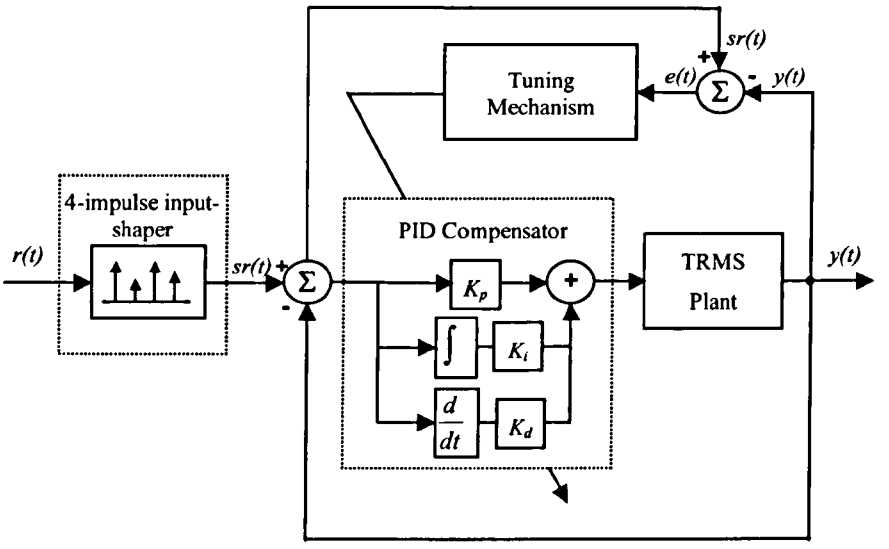

Figure 7.5: Schematic diagram of augmented (PID+IS) control scheme

Figure 7.6 shows the schematic diagram of the second augmented control scheme, which comprises a hybrid PD-type fuzzy control and PID compensator augmented with 4-impulse input shaper (FPDPID+IS).

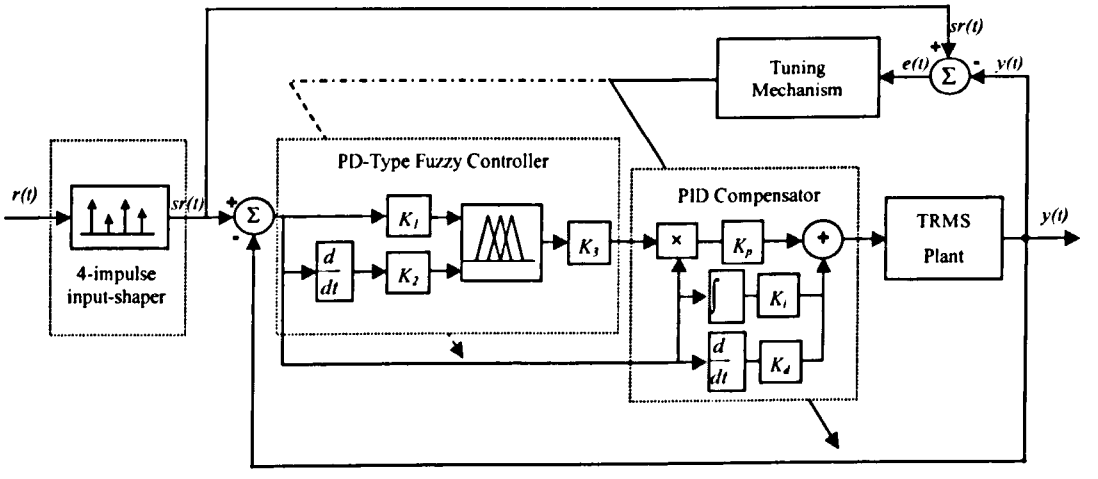

Figure 7.6: Schematic diagram of augmented (FPDPID+IS) control scheme

The third augmented control scheme comprises a hybrid PD controller and PID compensator augmented with 4-impulse input shaper (PDPID+IS), as depicted in Figure 7.7.

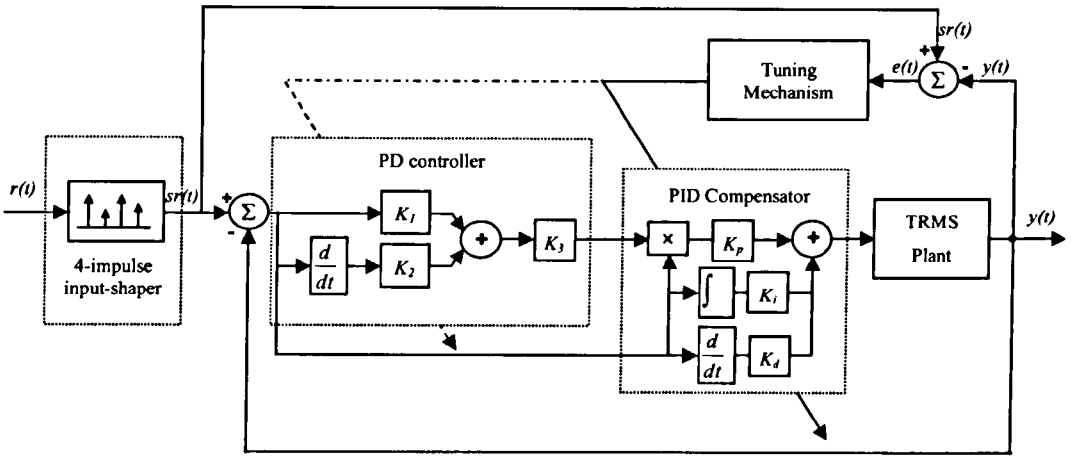

Figure 7.7: Schematic diagram of augmented (PDPID+IS) control scheme

In all three cases, the augmented controller is constructed in such way that the input shaper resides outside the feedback control loop. It is employed to pre-process the raw command signal without affecting the feedback control method. Thus, the feedback controller is used for rigid body motion (i.e. tracking performance control).

The developed control strategies were designed and implemented in both simulation and real-time environments of the TRMS rig through MATALB/SIMULINK interface, described in Chapter 2. The aim of the developed augmented controllers is to satisfy performance criteria such as command tracking, fast system response and minimum residual vibration. Therefore, the controlled output (elevation angle) is expected to have low overshoot, quick settling time of residual oscillation and reasonably fast speed of response.

7.4 Results

The proposed control schemes are implemented and tested within both simulation and real-time environments of the TRMS platform and the corresponding results are presented in the following subsections. The performances of the augmented controllers are assessed in terms of time domain performance objectives (overshoot (OS), rise-time (RT), settling-time (ST) and steady state error (SSE)) as well as level of vibration reduction in comparison to system performance in open loop without control. The level of vibration reduction is obtained from corresponding power spectral density (PSD) profiles of the system response in the frequency domain.

The obtained results revealed that the proposed augmented hybrid controllers are capable of reducing the system vibration while maintaining the input tracking performance of the TRMS rig. In both simulation and real-time experimental exercises, the three controllers demonstrated superior performances, in comparison to the system response in open loop configuration and with the feedback controllers alone (i.e. without input shaper), in tracking the reference signal. Their responses were characterised by relatively small overshoot, consistent settling time with minimum residual vibration. However, in all control cases, the system response suffers from a slow rise-time. This delay, which is equal to the length of the input shaper, is due to incorporation of the feedforward control component.

7.4.1 Simulation results

Performances of the employed control strategies within the simulation environment are summarised in Table 7.2 and illustrated in Figures 7.8 – 7.11. The controllers were evaluated in both time and frequency domains. The developed control strategies have resulted in good system performance in terms of tracking the reference command as well as attenuating the residual vibration during the TRMS movement.

Table 7.2: Performances of the employed control strategies in simulation exercises

Applied control strategy	Time-Domain Parameters			
	OS (%)	RT (sec)	ST (sec)	SSE (%)
Open loop (OL)	95.35	0.50	39.80	-41.37
Open loop with Input-shaper (OL+IS)	0	3.20	4.20	-0.91
PID (PID)	3.33	1.50	4.50	0
PID with input-shaper (PID+IS)	1.42	3.60	5.50	0
Hybrid FPDPID (FPDPID)	1.61	1.70	2.40	0
Hybrid FPDPID with input-shaper (FPDPID+IS)	0.25	3.60	6.10	0
Hybrid PDPID (PDPID)	0.76	2.00	2.90	0
Hybrid PDPID with input-shaper (PDPID+IS)	0.75	3.60	6.10	0

OS = Overshoot RT= Rise time ST = Settling time SSE = Steady state error

The TRMS model response to shaped and unshaped finite step input in open loop configuration is shown in Figure 7.8. It is noted that the performance of the model with the input shaping open loop control, denoted by red solid line, is characterised by a smooth response with a considerable rise-time of 3.2 sec, no overshoot, and settling-time of 4.2 sec, as compared with the system response without input shaper with which the response was unsatisfactory and characterised by a significant overshoot (95%) and long settling time as denoted by blue dashed line. The corresponding power spectral density (PSD) profiles also show that significant reduction of residual vibrations (54.49 dB) was recorded at the system's resonance mode, when input shaper was incorporated in the control scheme.

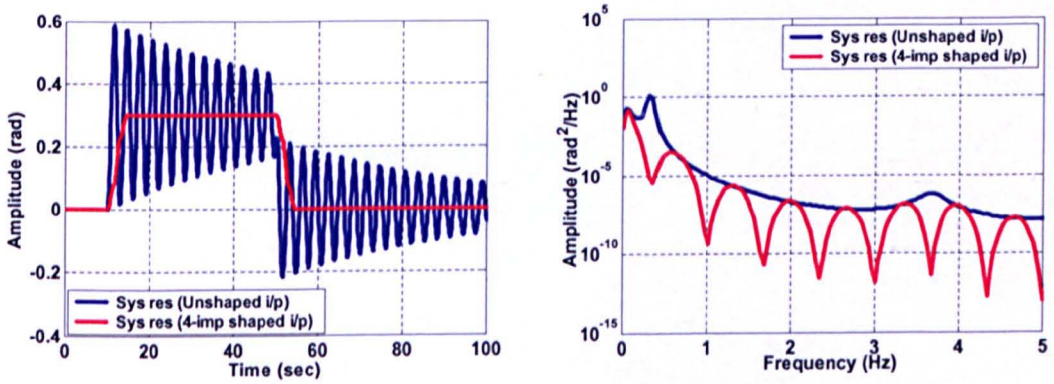

(a) System response (time domain) *(b) Power spectral density profile*

Figure 7.8: Open loop system response

The tracking capability of the three augmented control schemes in following the commanded finite-step input along with their abilities in reducing the residual vibrations are depicted in Figures 7.9, 7.10 and 7.11, respectively. Figure 7.9 shows the system response with PID+IS augmented controller. A smooth system response was observed with no significant overshoot (1.42%) and a rise-time of 3.6 sec. The system response with this controller settled within 5.50 sec. As shown in the corresponding PSD profile, a noticeable amount of vibration reduction (39.68 dB) was achieved at the system's resonance mode, when input shaper was incorporated in the control scheme.

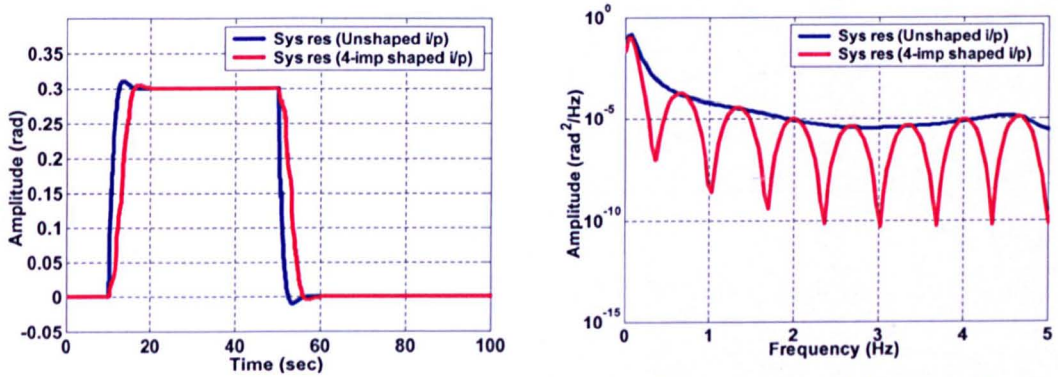

(a) System response (time domain) *(b) Power spectral density profile*

Figure 7.9: System response with augmented (PID+IS) controller

Similar to the first augmented control scheme, FPDPID+IS exhibited fairly good performance in terms of tracking the reference command and minimising the residual vibrations. This is in comparison to the system response with FPDPID feedback control method alone, as shown in Figure 7.10. With FPDPID+IS control scheme, the system response recorded a rise-time of 3.6 sec, small overshoot of 0.25% and the system response settled within 6.10 sec. A considerable amount of vibration reduction (16.20 dB) was also recorded with this controller as compared to the system response to the unshaped input.

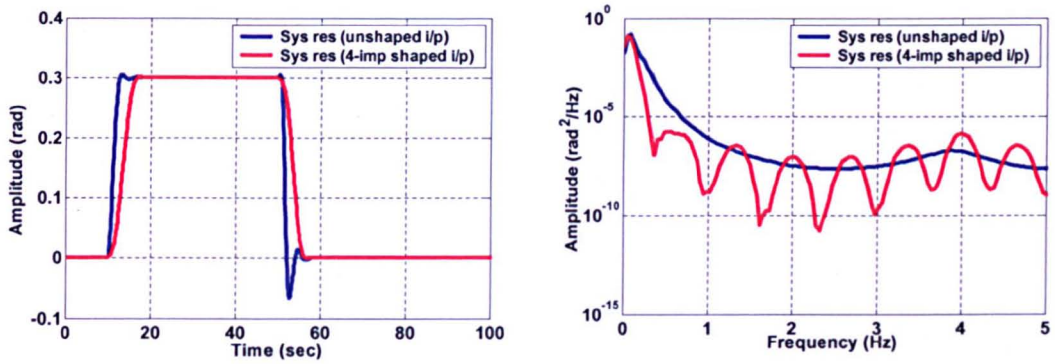

(a) System response (time domain) *(b) Power spectral density profile*

Figure 7.10: System response with augmented (FPDPID+IS) controller

The system response with the PDPID+IS augmented controller is illustrated in Figure 7.11. A closer observation reveals a very similar system response to FPDPID+IS controller, with a marginal difference. It is noted that the magnitude of vibration at the system's resonance mode was dramatically reduced by 32.77 dB, as compared to the system response without input shaper. With PDPID+IS controller, the system response recorded a rise-time of 3.6 sec with a reasonable overshoot of 0.75%, and required 6.10 sec to settle down.

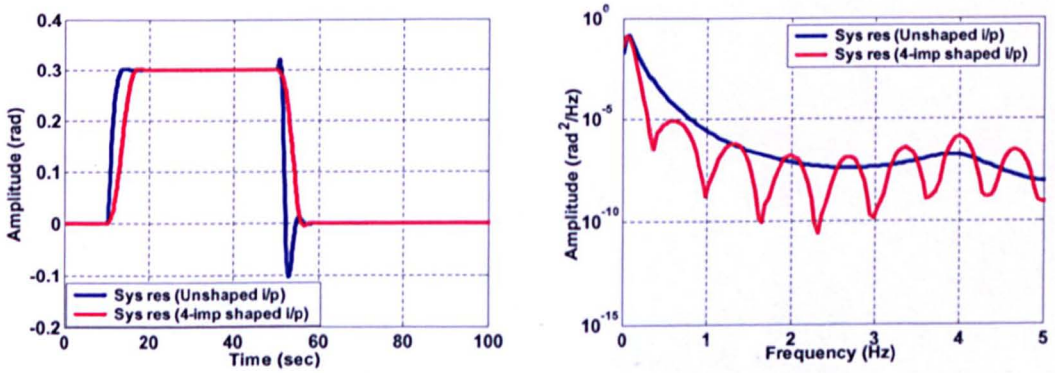

(a) System response (time domain) *(b) Power spectral density profile*

Figure 7.11: System response with augmented (PDPID+IS) controller

7.4.2 Experimental results

The crucial test for any control paradigm is when implemented on the real system in the presence of real world uncertainties and disturbances. Real-time experimental results with employed control strategies are summarised in Table 7.3 and depicted in Figures 7.12 – 7.15.

It is noted from the system responses with the employed control strategies that the input command was followed reasonably well with acceptable overshoot and also displaying a good settling time characteristic, as compared with that in open-loop configuration (without feedback control component). It is also found that there are minor oscillations in the system response that are due to inherent characteristic of the TRMS, which exhibits a minor oscillatory tendency even in the steady state. Thus, good settling behaviour is assumed.

Furthermore, by adding the feedforward control component (4-impulse input shaper), the control results in improved behaviour. This is a significant improvement over the feedback controller alone (i.e. without input shaper). However, this is at the cost of increased rise-time equal to the length of the input shaper. This problem could be tackled by further tuning of the closed-loop control gains, and then, the system response could be improved without affecting the other performance criteria, as well be demonstrated later in section 7.5.3.

Table 7.3: Performances of the employed controllers in real-time experiments

Applied control strategy	**Time-Domain Parameters**			
	OS (%)	**RT (sec)**	**ST (sec)**	**SSE (%)**
Open loop (OL)	14.54	1.20	39.30	1.24
Open loop with Input-shaper (OL+IS)	3.29	3.50	39.40	0.22
PID (PID)	2.27	10.13	39.79	2.27
PID with input-shaper (PID+IS)	2.27	10.48	37.95	0.22
Hybrid FPDPID (FPDPID)	40.10	1.37	12.73	-0.80
Hybrid FPDPID with input-shaper (FPDPID+IS)	18.63	2.49	14.68	0.22
Hybrid PDPID (PDPID)	39.08	1.39	12.95	0.22
Hybrid PDPID with input-shaper (PDPID+IS)	17.61	2.59	14.52	0.22

OS = Overshoot RT= Rise time ST = Settling time SSE = Steady state error

Figure 7.12 shows the real-time system response to the shaped and unshaped command signals, within open-loop configuration of the system along with the corresponding PSD plots. The actual TRMS response with 4-impulse input shaper resulted in a better performance than the one to the unshaped input. With the input shaping technique, the system response is characterised by a smooth response with a small overshoot of 3.29% and settled within 39.40 sec, but at the expense of a longer rise-time of 3.5 sec. This is in comparison with the system response without input shaper, which is characterised by an oscillatory response, especially at the negative cycle. Moreover, the input shaper is found to be able to handle the residual vibrations induced during the TRMS motion, as a significant reduction in system vibration was observed (22.78 dB).

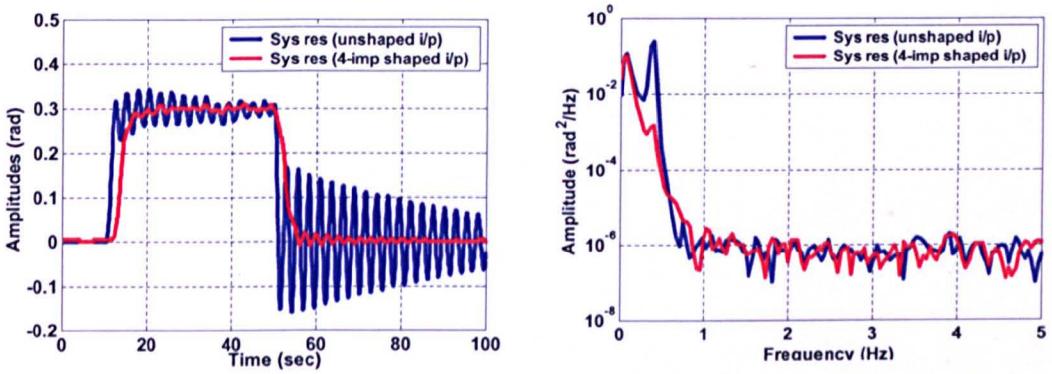

(a) System response (time domain) *(b) Power spectral density profile*

Figure 7.12: Open-loop system response

As demonstrated in Figure 7.13, the performance of the PID+IS controller at input tracking control is maintained; it recorded a rise-time of 10.48 sec and an overshoot of 2.27%. The system response with this controller needed 37.95 sec to settle down. Moreover, with this controller a significant reduction in system vibration was observed (15.93 dB).

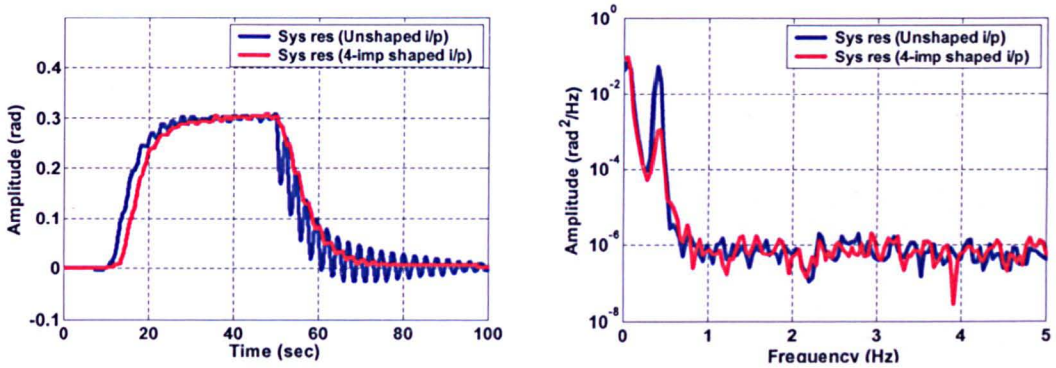

(a) System response (time domain) *(b) Power spectral density profile*

Figure 7.13: System response with augmented (PID+IS) controller

Figure 7.14 shows the system performance with FPDPID+IS augmented control. It is noted that the TRMS response recorded a rise-time of 2.49 sec and reached the desired position within 14.68 sec with a reasonable overshoot of 18.63%, in comparison to the system response with the feedback controller alone. Moreover, as expected with the FPDPID+IS, an 8.25 dB reduction in the residual vibrations of the system at the resonance mode was achieved.

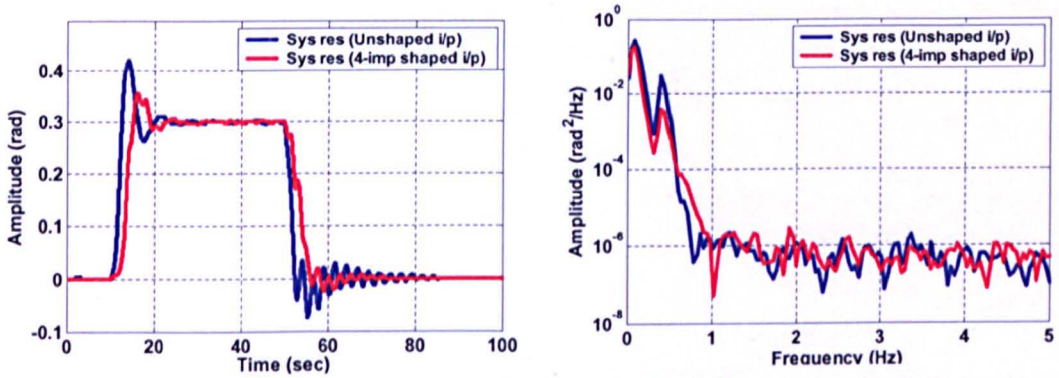

(a) System response (time domain) *(b) Power spectral density profile*

Figure 7.14: System response with augmented (FPDPID+IS) controller

For the TRMS response incorporating PDPID+IS controller, a similar trend of improvement was observed in comparison to the previous controller. Figure 7.15 shows the resulting elevation angle and its corresponding PSD profile. It is noted that a smoother system response was obtained with the augmented controller as

compared to that with the feedback control law only. With this controller, the system response recorded a rise-time of 2.59 sec, overshoot of 17.61% and settled within 14.52 sec. Furthermore, a vibration reduction of 8.83 dB was recorded with this controller at the resonance mode of the system as compared to the system response to the unshaped input.

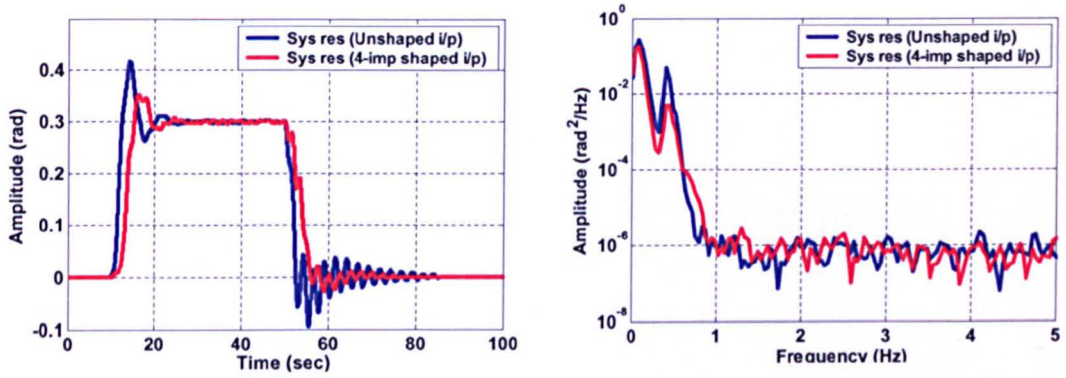

(a) System response (time domain) *(b) Power spectral density profile*

Figure 7.15: System response with augmented (PDPID+IS) controller

7.5 Comparative performance assessment

This section presents a comparative assessment of the developed control strategies in terms of input tracking performance, level of vibration suppression and improvement in system response (i.e. rise-time).

7.5.1 Input tracking performance

Table 7.4 summaries the quantitative achievements of the employed control strategies in terms time domain system behaviour; overshoot (OS), rise-time (RT), settling-time (ST), and steady-state error (SSE). Among the employed control techniques, the augmented control strategies have resulted in better performance than the other controllers. This is evidenced by the time domain specification analysis in both simulation and real-time experimental exercises.

Table 7.4: Performances of the employed control strategies in the time domain

Applied control strategy	Time-Domain Parameters				Environment
	OS (%)	RT (sec)	ST (sec)	SSE (%)	
Open loop (OL)	95.35	0.50	39.80	-41.37	Simulation
Open loop with Input-shaper (OL+IS)	0	3.20	4.20	-0.91	
PID (PID)	3.33	1.50	4.50	0	
PID with input-shaper (PID+IS)	1.42	3.60	5.50	0	
Hybrid FPDPID (FPDPID)	1.61	1.70	2.40	0	
Hybrid FPDPID with input-shaper (FPDPID+IS)	0.25	3.60	6.10	0	
Hybrid PDPID (PdPID)	0.76	2.00	2.90	0	
Hybrid PDPID with input-shaper (PDPID+IS)	0.75	3.60	6.10	0	
Open loop (OL)	14.54	1.20	39.30	1.24	Experimental
Open loop with Input-shaper (OL+IS)	3.29	3.50	39.40	0.22	
PID (PID)	2.27	10.13	39.79	2.27	
PID with input-shaper (PID+IS)	2.27	10.48	37.95	0.22	
Hybrid FPDPID (FpdPID)	40.10	1.37	12.73	-0.80	
Hybrid FPDPID with input-shaper (FPDPID+IS)	18.63	2.49	14.68	0.22	
Hybrid PDPID (PDPID)	39.08	1.39	12.95	0.22	
Hybrid PDPID with input-shaper (PDPID+IS)	17.61	2.59	14.52	0.22	

OS = Overshoot RT= Rise time ST = Settling time SSE = Steady state error

7.5.2 Level of vibration reduction

The level of vibration reduction, in both simulation and real-time exercises, achieved by the augmented control schemes is summarised in Table 7.5 and demonstrated in Figure 7.16.

The results obtained reveal that the augmented control strategies have significantly reduced the residual vibrations at the system's resonance mode. In the simulation phase, the highest level of vibration reduction (54.49 dB) was achieved by OL+IS controller, followed by PID+IS of 39.68 dB, followed by PDPID+IS of

32.77 dB, and then FPDPID of 16.20 dB. In the experimental phase, the highest amount of vibration reduction at the resonance mode was recorded with OL+IS as 22.78 dB, followed by PID+IS at 15.93 dB, followed by PDPID+IS at 8.83 dB, and finally the FPDPID+IS at 8.25 dB.

Table 7.5: Amount of vibration reduction achieved with the control strategies

Augmented Control strategy	**Amount of vibration reduction (dB)**	
	Simulation	Experimental
Open Loop with input-shaper (OL+IS)	54.49	22.78
PID compensator with input-shaper (PID+IS)	39.68	15.93
Hybrid FPDPID with input-shaper (FPDPID+IS)	16.20	8.25
Hybrid PDPID with input-shaper (PDPID+IS)	32.77	8.83

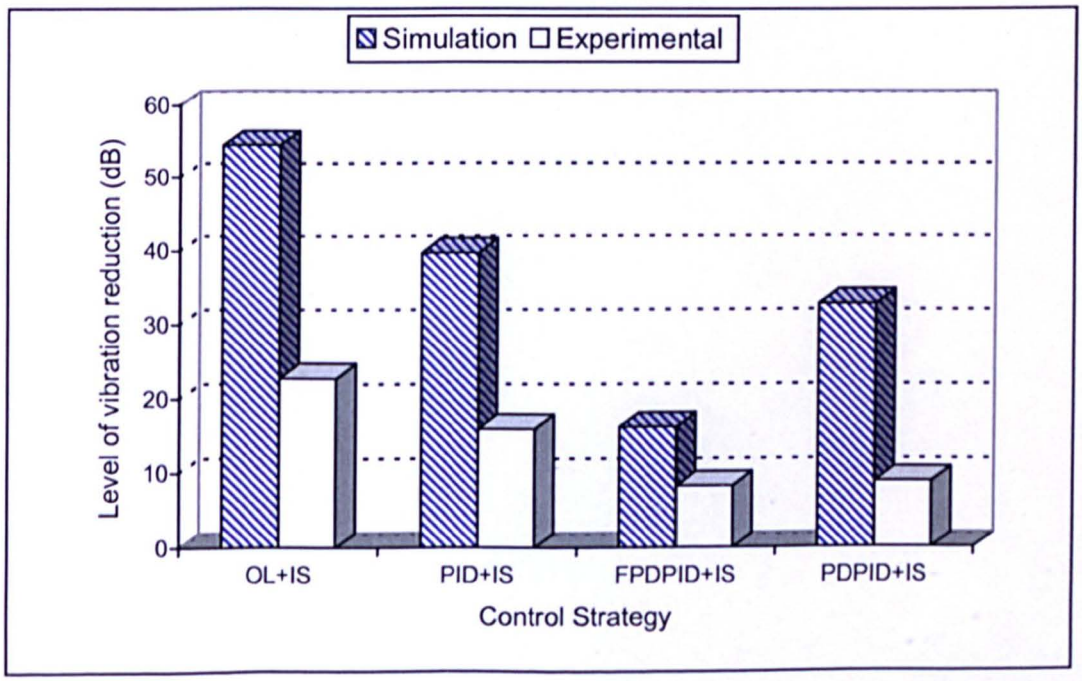

Figure 7.16: Level of vibration reduction achieved with the control strategies

7.5.3 Improvement of system response

To overcome the drawback of command shaping technique, which resulted in a delay in the system response equal to the length of the input shaper (Pao, 2000; Singhose *et al.*, 1995), the parameters of the feedback controllers were further tuned using a heuristic approach. In this investigation, the system rise-time was further accentuated by further tuning of the feedback control gains within the augmented control schemes. The obtained results, shown in Figures 7.17, 7.18 and 7.19, reveal that the system response with the augmented controllers was considerably improved, without any degradation of other performance criteria.

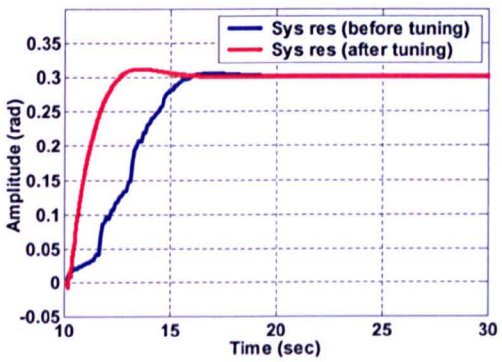

(a) Simulation

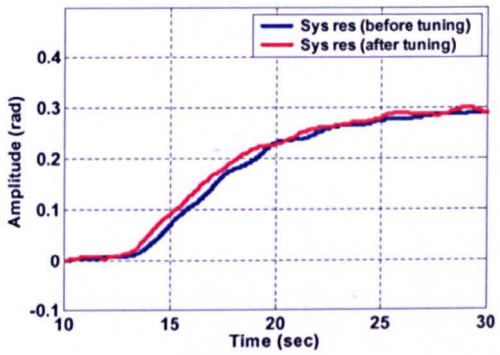

(b) Experimental

Figure 7.17: System response with augmented (PID+IS) controller

(a) Simulation

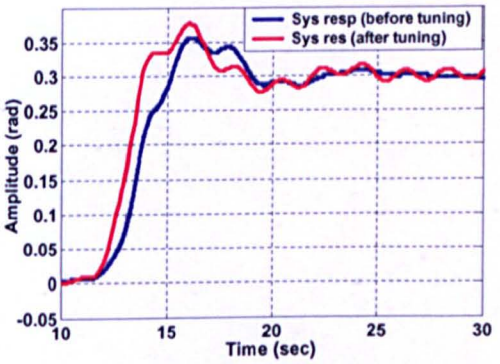

(b) Experimental

Figure 7.18: System response with augmented (FPDPID+IS) controller

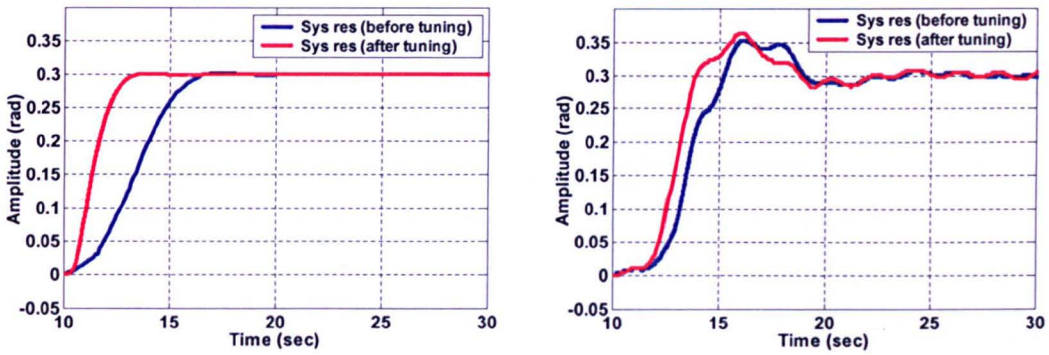

(a) Simulation *(b) Experimental*

Figure 7.19: System response with augmented (PDPID+IS) controller

The anticipated improvement in the rise time of the system performance with the augmented control schemes is evident from Table 7.6 and Figure 7.20. Among the three augmented control schemes, the fastest system response was recorded using the FPDPID+IS augmented control scheme in both simulation and real-time experimental exercises. The rise-time of the system response with this controller was decreased by 57.78% and 35.74% in the simulation and real-time experimental phases, respectively. Analogous to FPDPID+IS controller, the PDPID+IS augmented control scheme has also improved the system response in both simulation and real-time experimental exercises. After further tuning of its feedback control gains, the system response with the PDPID+IS controller was improved by 52.50% in the simulation phase and by 34.36% in the real-time experimental exercise. Finally, the rise-time of the system response with the PID+IS augmented control strategy was decreased by 55.83% in the simulation exercise, while it recorded an improvement by 4.58% in the real-time experimental phases only.

Table 7.6: Rise-time analysis after further tuning of closed loop control parameters

Control strategy	Rise-time			Environment
	Before tuning (sec)	After tuning (sec)	Improvement (%)	
PID+IS	3.60	1.59	55.83	Simulation
FPDPID+IS	3.60	1.52	57.78	
PDPID+IS	3.60	1.71	52.50	
PID+IS	10.48	10.00	4.58	Experimental
FPDPID+IS	2.49	1.60	35.74	
PDPID+IS	2.59	1.70	34.36	

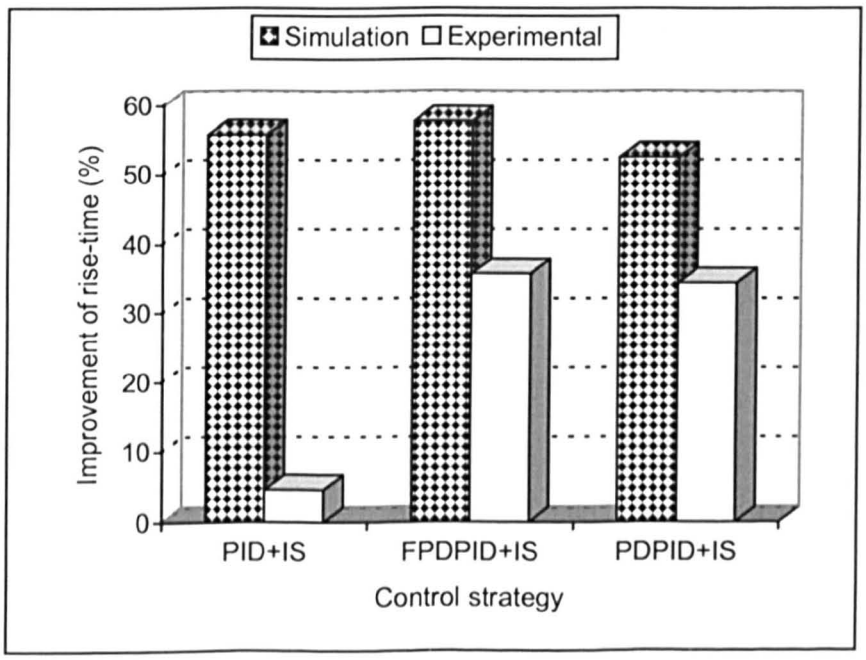

Figure 7.20: Improvement in rise-time after further tuning of closed-loop control parameters

7.6 Summary

This chapter has witnessed the design and implementation of an augmented control structure in which three forms of feedback control schemes are combined with a 4-

impulse input shaper for rigid body motion (i.e. reference command tracking performance) and vibration suppression during the TRMS operation. The developed control strategies have been designed and implemented within both simulation and real-time environments of the TRMS rig through MATALB/SIMULINK interface, described in Chapter 2.

It has been apparent from the real-time experimental results that due to very sensitive and oscillatory nature of the TRMS even in steady state mode, response profiles are found to have occasional sharp peaks and mild oscillations. Even though, the employed control strategies demonstrated acceptable performances. The obtained results have shown that much improved tracking is obtained on positive and negative cycles of the reference signal, as compared to that without any control action, implying good damping and hence tighter control. There is hardly any overshoot with smooth and acceptable settling time.

The system performance with the feedback controller was significantly improved when the feedforward control component was added. This process has resulted in a significant reduction in the system's residual vibrations. Quick elimination of residual oscillations is important for fast manoeuvring platforms, where the command signal changes rapidly. The advantage of this method is that it is not necessary to change the feedback control law in order to attenuate system's vibration.

In conclusion, an appropriately designed augmented control strategy that combines both feedforward and feedback controller is a practical approach to satisfy the design specifications and is highly desirable for fast manoeuvring systems with rapidly changing command input.

CHAPTER 8

CONCLUSION AND FUTURE WORK

8.1 Conclusion

Research interest in new generations of air vehicles such as unmanned air vehicles (UAV's) is rapidly growing. The interest stems from the fact that such air vehicles are highly agile, stealthy, multi-purpose and capable of executing different tasks such as surveillance, aerial mapping and inspection, which are beyond the domain of their conventional counterparts. These new generation air vehicles have presented a variety of unprecedented challenges and opportunities to aerodynamicists and control engineers. This research has investigated dynamic modelling and control of the vertical movement of a twin rotor multi-input multi-output system (TRMS), which is a laboratory platform representing a flexible manoeuvring structure and resembles essential characteristics of an air vehicle. Although, the TRMS does not fly, it has a striking similarity with a helicopter, such as system nonlinearities and cross-coupled modes. The TRMS, therefore, can be viewed as an unconventional and complex "air vehicle" and possesses formidable challenges in modelling, control design and analysis and implementation.

Reasonable linear system models are essential for controller design and nonlinear models for subsequent controller evaluation. In this research, a black-box system modelling was adopted to achieve a fairly good system representation. Linear models, characterising the TRMS in hovering mode, have been obtained with no *a priori* knowledge of plant model order or parameters providing any insight into physical characteristics of the plant using RLS and GA system identification approaches. The identified models have been exhaustively validated using time and frequency domain tests in order to instil confidence in the models for their subsequent use in the controller design. The modelling procedure adopted is suitable for a class of new generation air vehicles whose dynamics are not well-understood or difficult to model from first principles. The approach presented here is an important

contribution of this thesis. The identified models include the rigid as well as the flexible plant dynamics.

To study the performance of next generation air vehicles researchers are increasingly relying on nonlinear modelling and control techniques. Therefore, a nonlinear plant model is essential for predicting the system behaviour accurately in order to evaluate the controlled system performance, as well as for controlling a highly nonlinear plant by the dynamic inversion control method. In this research, neural networks were utilised to obtain the nonlinear system model. MLP based NN model was identified for the vertical movement of the TRMS. The nonlinear modelling method adopted in this work is appropriate for modelling complex new generation highly agile air platforms with significant nonlinearities. The main aim of NN based modelling has been to achieve a highly accurate model. It has been noted, however, that the nonlinear model is only slightly better than the linear model. For this reason, the nonlinear model is not incorporated in the controller evaluation; rather the linear model is used for simplicity.

Vibrations due to random excitation of structures are common phenomena experienced by large space structures with flexible appendages, ships, flexible aircraft and missiles. Although flexible structures are desirable, the vibrations are not. These vibrations may cause discomfort to passengers and degrade system performance. Vibration suppression can be accomplished via active, passive or hybrid active and passive means. Passive treatment is essential but is limited in rendering the desired accuracy. Hence, active control is needed. The modelling exercise for the TRMS revealed the presence of resonance system modes, which are responsible for inducing unwanted vibrations during and at the end of system manoeuvres.

For vibration suppression open-loop control methods have been developed on the basis of the system's vibration modes detected through the analysis of the plant spectral responses obtained during the modelling process. 2-impulse, 3-impulse and 4-impulse input shapers have been designed to pre-process the command signals. This method ensures that the system does not experience the undesirable resonance frequencies, thereby preventing the excitation of vibrational modes. The effectiveness of this concept has been demonstrated on the TRMS rig, with

significant reduction in vibration. This is evident from smooth time domain responses as well as from the attenuated resonances in the frequency domain.

In addition to vibration attenuation, it is also desirable to achieve other performance criteria such as command tracking, disturbance rejection and fast rise time. These objectives cannot be achieved by open-loop mechanisms alone, thus closed-loop strategies have also been investigated. Different forms of feedback controllers including hybrid control schemes have been designed and implemented in both simulation and real-time experimental environments for the control of TRMS rig. The developed feedback control mechanisms demonstrated satisfactory performances in terms of time domain behaviour; over-shoot, rise-time, settling-time and accumulated steady-state error. However, they have shown inadequate authority over residual system vibration. This problem was resolved by further augmenting the system with a feedforward control component based on input shaping technique.

Finally, an augmented feedforward and feedback control scheme (AFFCS) has been designed and implemented for input tracking control and vibration suppression of the system. The advantage of this method is that it is not necessary to change the feedback control law in order to attenuate system's vibration. Three forms of feedback controllers have been combined with a 4-impulse input shaper for rigid body motion control and vibration suppression during the TRMS operation. The developed control strategies were designed and implemented within both simulation and experimental environments of the TRMS rig.

Experimental and simulation results have shown that the proposed strategies are feasible, where much improved tracking responses were obtained on both positive and negative cycles of the reference signal, as compared to that without control action, implying good damping and hence tighter control. Furthermore, the system performance with the feedback controllers was significantly improved when the feedforward control component was added. This process has resulted in a significant reduction in the system's residual vibrations. Appropriately designed augmented control strategy that combines both feedforward and feedback control is a practical approach and highly desirable for fast manoeuvring systems with rapidly changing command input.

8.2 Suggestions for future work

Due to time limitations in this research work many other ideas could not be implemented. A number of investigations emanating from this research can be investigated and implemented in a future research. Some of the proposed methods and ideas are identified below:

8.2.1 Dynamic modelling and control of MIMO TRMS platform

In this research a 1DOF modelling exercise has been carried out on the elevation angle (pitch movement) of the TRMS plant. Consequently, a single-input single output (SISO) control design has been investigated. An obvious extension is, therefore, to obtain a dynamic model of 2DOF representing both yaw and pitch movements of the TRMS platform. Then, a multi-input multi-output (MIMO) controller design could be investigated. A 2DOF autopilot to control pitch and the yaw movements would involve the decoupling objective of the two channels.

8.2.2 Development of roll movement of the TRMS

An interesting development of this work would be to study the roll control of the TRMS. This is a non-trivial task that will necessitate modification of the TRMS rig to provide an additional degree of freedom for roll movement. The modified TRMS would then mimic the hover mode for a vertical take off and landing (VTOL) type aircraft. Thus, the design objectives would then be roll as well as pitch and yaw control.

8.2.3 Reconfigurable control system

Reconfiguration is highly desirable in many advanced aerospace systems such as advanced tactical fighters, adaptive structures and autonomous robots. The main motivation of reconfiguration is greater survivability and controllability, attained through the ability of the feedback system to reorganise itself in the presence of actuator/sensor failures and surface damage. The TRMS rig is an ideal platform upon which the reconfigurable control strategies can be tested.

8.2.4 Adaptive input shaping for vibration suppression

Input shaping has been shown to provide significant reduction in the residual vibration during the TRMS motion. Adaptive input shapers (AIS) would be worthy to investigate and their performances in vibration suppression of the system may be evaluated in comparison to the standard input shapers developed in this work.

8.2.5 Intelligent techniques for tuning rule-bases and membership functions of fuzzy logic controllers

A heuristic tuning of rule-bases and membership functions of the employed fuzzy logic controllers (FLCs) has been utilized through a trial and error mechanism. However, for increasingly larger numbers of input and output rules as well as membership functions, even with *a priori* expert knowledge, the method becomes more difficult as the number of rules rise exponentially. Therefore, intelligent techniques such as Artificial Neural Network (ANN) and GA can be advocated as solutions to this problem. ANNs can be used to learn FLC rule-bases or to tune given membership functions. Such an approach combines the learning capability of the ANN with the reasoning power of fuzzy logic. Alternatively, the search for suitable rules or membership function parameters of an FLC knowledge base can be viewed as an optimization problem to which a GA can be applied.

REFERENCES

Ahmad, S. M. (2001). *Modelling and control of a twin rotor multi-input multi-output system.* PhD thesis, Department of Automatic Control and Systems Engineering, University of Sheffield, UK.

Ahmad, S. M., Chipperfield, A. J. and Tokhi, M. O. (2002). Dynamic modelling and open-loop control of a twin rotor multi-input multi-output system. *Proceedings of IMechE-Part I, Journal Systems and Control Engineering*, **216**, pp. 477-496.

Astrom, K. J. and Hagglund, T. (1988). *Automatic tuning of PID controllers.* Instrument Society of America, Research Triangle Park, NC.

Astrom, K. J. and Hagglund, T. (1995). *PID controllers: Theory, design, and tuning*, 2nd Ed., International Society for Measurement and Control, NC.

Azad, A. K. M. (1994). *Analysis and design of control mechanisms for flexible manipulator systems.* PhD thesis, Department of Automatic Control and Systems Engineering, The University of Sheffield, UK.

Babuska, R. (1998). *Fuzzy modelling for control.* Kluwer Academic Publisher, Boston.

Baker, W. and Farrel, J. (1991). Learning augmented flight control for high performance aircraft. *Proceedings of AIAA on Guidance, Navigation and Control Conference*, pp. 347-358.

Bandyopadhyay, R., Chakraborty, U. K. and Patranabis, D. (2001). Autotuning a PID controller: A fuzzy-genetic approach. *Journal of Systems Architecture*, **47**, pp. 663-673.

Banks, S. (1990). *Signal processing, image processing and pattern recognition.* Prentice-Hall International, London, UK.

Billings, S. A. and Voon, W., (1986). Correlation-based model validity tests for nonlinear models. *International Journal of Control*, pp. 235-244.

Billings, S. A., Jamaluddin, H. B. and Chen, S. (1991). A comparison of the back-propagation and recursisive prediction error algorithms for training neural networks. *Mechnical Systems and Signal Processing*, **5**, pp. 233-255.

Billings, S. A., Jamaluddin, H. B. and Chen, S. (1992). Properties of neural networks with applications to modelling non-linear dynamic systems. *International Journal of Control*, **55**, (1), pp. 193-224.

Billings, S.A. and Voon, W.S.F. (1995). *Correlation based model validity tests for non-linear model.* Research report no. 285, Department of Automatic Control and Systems Engineering, The University of Sheffield, UK.

Bishop, C. M. (1995). *Neural networks for pattern recognition.* Oxford University Press, Oxford, UK.

Blight, J. D., Dailey, R. L. and Gangsaas, D. (1996). Practical control law design for aircraft using multivariable techniques. In Tischler, M. B. (Ed.). *Advances In Aircraft Flight Control*, pp. 231-267.

Bodson, M. (1998). An adaptive algorithm for the tuning of two input shaping methods. *Automatica*, **34**, (6), pp. 771-776.

Booker, L. (1987). Improving search in genetic algorithms, In Davis, L. (Ed.). *Genetic algorithms and simulated annealing*, chapter 5, pp. 61-73, Pitman Kaufmann, New York.

Calise, A. (1996). Neural networks in nonlinear aircraft flight control. *IEEE AE System Magazine*, **11**, (7), pp. 5-10.

Chipperfield A. J. and Fleming, P. J. (1994). *Parallel genetic algorithms: A survey.* Research report no. 518, Department of Automatic Control and Systems Engineering, The University of Sheffield, UK.

Chipperfield, A. J., Fleming, P. J., Pohlheim, H. and Fonseca, C. (1994). A genetic algorithm toolbox for MATLAB. *Proceedings of the International Conference on Systems Engineering*, Coventry, UK, 06-08 September 1994.

Choi, B.-J., Kwak, S.-W. and Kim, B. K. (2000). Design and stability analysis of single-input fuzzy logic controller. *IEEE Transactions on Systems, Man, and Cybernetics – Part B: Cybernetics*, **30**, (2), pp. 303-309.

Cohen, K., Yaffe, R., Weller, T. and Ben-Asher, J. Z. (2002). Experimental studies on adaptive fuzzy control of a smart structure. *Journal of Vibration Control*, **8**, (8), pp. 1071-1083.

Cutforth, C. F. and Pao, L. Y. (2000). Command shaping control for vibration reduction without lengthening the command. *Proceedings of AIAA Guidance, Navigation, and Control Conference*, Denver, CO.

Cutforth, C. F. and Pao, L. Y. (2003). Control using equal length shaped commands to reduce vibration. *IEEE Transactions on Control Systems Technology*, **11**, (1), pp. 62-72.

Demuth, H. and Beale, M., (2000). *Neural networks toolbox user's guide v.4*. The Math Works, Inc.

Donoghue, K. O. and Bruton, J. (2002). *Real-time adaptive PID control of a nonlinear process based on genetic optimization*. MSc dissertation, School of Electronic Engineering, Dublin City University, available online from: http://www.eeng.dcu.ie/~brutonj/Reports/KieranODonoghue02.pdf

Dougherty, H., Tompetrini, K., Levinthal, J. and Nurre, G. (1982). Space telescope pointing control system. *Journal of Guidance, Control, and Dynamics*, **5**, (4), pp. 403-409.

Dragan.D. K., Kuzmanovic S. B. and Emil L. (2001). Design of a PID-like compound fuzzy logic controller. *Engineering Applications of Artificial Intelligence*, **14**, pp. 785-803.

Driankov, D. Hellendoorn, H. and Reinfrank, M. (1996). *An Introduction to Fuzzy Control*, 2nd revised Ed., Springer-Verlag, Berlin.

Efe, M. O. and Kaynak, O. (2000), A comparative study of soft-computing methodologies in identification of robotic manipulators. *Robotics and Autonomous Systems*, **30**, pp. 221–230.

Elanayar, S. V. T. and Yung, C. S. (1994). Radial basis function neural network for approximation and estimation of non-linear stochastic dynamic systems. *IEEE Transaction on Neural Networks*, **5**, (4), pp. 594-603.

Farag, W. A., Quintana, V. H. and Lambert-Torres, G. (1998). A genetic-based neuro-fuzzy approach for modeling and control of dynamical systems. *IEEE Transactions on Neural Networks*, **9**, (5), pp. 756-767.

Fausett, L. (1994). *Fundamentals of Neural Networks: Architecture, algorithms, and applications*. Prentice-Hall Inc., Englewood Cliffs, NJ.

Feddema, J. T., Dohrmann, C. R., Parker, G. G., Robinett, R. D., Romero, V. J. and Schmitt, D. J. (1997). Control for Slosh-free motion of an open container. *IEEE Control System Magazine*, **17**, (1), pp. 9-36.

Feedback Instruments Ltd. (1996). *Twin rotor MIMO system,* Manual 33-007-0. Sussex, UK.

Fleming, P. J. and Purshouse, R. C. (2002). Evolutionary algorithms in control systems engineering: A survey. *Control Engineering Practice*, **10**, pp. 1223–1241.

Franklin, G. F., Powell, J. D. and Emami-Naeini, A. (1988). *Feedback control of dynamic systems*, Addison-Wesley, USA.

Franssila, J. and Koivo, H. N. (1992). Fuzzy control of an industrial robot in transputer environment. *Proceedings of IEEE International Conference on Industrial Electronics, Control, Instrumentation and Automation IECON'92*, San Diego, USA, pp. 624-629.

Funahashi, K. (1989). On the approximate realization of continuous mappings by neural networks. *Neural Networks*, **2**, pp. 303-314.

Goldberg, D. E. (1989). *Genetic algorithms in search, optimisation and machine learning*. Addison Wesley Longman, Publishing Co. Inc., New York.

Gorzalczany, M. B. and Gluszek, A. (2000). Neuro-fuzzy networks in time series modelling. *Proceedings of the Fourth International Conference on Knowledge Based Intelligent Engineering Systems and Allied Technologies*, Brighton, UK, 30 August – September 2000, **1**, pp. 450-453.

Grefenstette, J. J. and Baker, J. E. (1989). How genetic algorithms work: a critical look at implicit parallelism. *Proceedings of the 3rd International Conference on Genetic Algorithms.*

Griffin and Bruton, J. (2003). *Online PID controller tuning using genetic algorithms.* MSc dissertation, School of Electronic Engineering, Dublin City University, available online from: http://www.eeng.dcu.ie/~brutonj/Reports/IGriffin_MEng_03.pdf.

Gurocak, H. B. (1999). A genetic algorithm method for tuning fuzzy logic controllers. *Fuzzy Sets and Systems*, **108**, pp. 305-316.

Ha, C. M. (1995). Neural networks approaches to AIAA aircraft control design challenge. *Journal of Guidance, Control, and Dynamics*, **18**, (4), pp. 731-739.

Hagan, M. T. and Demuth, H. B. (1999). Neutral Networks for Control. *Proceedings of the 1999 American Control Conference*, San Diego, Ca, pp. 1083 – 1112.

Hagan, M. T. and Menhaj, M. B. (1994). Training feedforward networks with Marquardt algorithm. *IEEE Transactions on Neural Networks*, **5**, (6), pp. 989-993.

Harris, C. J. (1994). Introduction to intelligent control, In Harris, C. J. (Ed.). *Advances in intelligent control*, Taylor and Francis Inc., USA.

Harvey, B. (1997). Micro unmanned aerial vehicles, *Intelligent Automation Inc.* SA.

Haykin, S. (1986). *Adaptive filter theory*, Prentice-Hall, Englewood Cliffs, NJ.

Haykin, S. (1998). *Neural networks, a comprehensive foundation.* (2nd Ed.), Upper Saddle River, NJ, Prentice-Hall.

Haykin, S. S. (1996). *Adaptive Filter Theory.* Prentice-Hall Inc., NJ, USA.

Henriques, J., Gil, P., Dourado, A. and Duarte-Ramos, H. (1999). Application of a recurrent neural network in online modelling of real-time systems. *European Symposium on Intelligent Techniques ESIT '99*, Orthodox Academy of Crete, Greece.

Hillsley, K. L. and Yurkovich, S. (1993). Vibration control of a two-link flexible robot arm. *Journal Dynamics and Control*, **3**, pp. 261-280.

Holland, J. H. (1975). *Adaptation in natural and artificial systems.* University of Michigan Press, Ann Arbor MI, University Michigan Press.

Hornik, K., Stinchombe, M. and White, H. (1989). Multilayer feedforward networks are universal approximators. *Neural Networks*, **2**, (5), pp. 359-366.

Hossain, M. A., Tokhi, M. O., Chipperfield, A. J., Fonseca, C. M. and Dakev, N. V. (1995). Adaptive active vibration control using genetic algorithms. *The 1st IEE/IEEE International Conference on GAs in Engineering Systems: Innovations and Applications*, Sheffield, UK, pp. 175-180.

Hu, B.-G., Mann, G. I. and Gosine, R G. (2001). A systematic study of fuzzy PID controllers – Function-based evaluation approach. *IEEE Transactions on Fuzzy Systems*, **9**, (5), pp. 699-712.

Hunt, K. J., Sbardato, D., Zbikowski, R. and Gawthrop, P. J. (1992). Neural networks for control systems - A survey. *Automatica*, **28**, (6), pp.1083-1112.

Hush, D. R. and Horne, B. G. (1993). Progress supervised neural networks. *IEEE Signal Processing Magazine*, **10**, (1), pp. 8-39.

Hyun-Joon, C., Kwang-Bo, C. and Bo-Hyeun, W. (1997). Fuzzy-PID hybrid control: Automatic rule generation using genetic algorithms. *Fuzzy Sets and Systems*, **92**, pp. 305-316.

Jackson, L. B. (1989). *Digital Filters and Signal Processing.* Kluwer Academic Publishers, London, UK.

Jager, R. (1995). *Fuzzy Logic in Control.* PhD Thesis, Technical University of Delft, The Netherlands.

Jain, L. C., Johnson, R. P., Takefuji, Y. and Zadeh, L. A. (1999). *Knowledge-based intelligent techniques in industry*, CRC Press, Boca Raton, FL.

Jang, J.-S. R., Sun, C.-T. and Mizutani, E. (1997). *Neuro-fuzzy and soft computing.* Prentice Hall, Upper Saddle River, NJ.

Jantzen, J. (1998). *Tutorial on fuzzy logic.* Technical report no. 98-E 868, Department of Automation, Technical University of Denmark.

Jantzen, J. (1998). *Tuning of fuzzy PID controllers.* Technical report no. 98-H 871, Department of Automation, Technical University of Denmark.

Jiang, T., Prasad, J. and Calise, A. (1996). Adaptive fuzzy logic flight controller for rotorcraft. *Proceedings of AIAA Guidance, Navigation, and Control Conference*, AIAA 96-35729.

Jones, S. D. and Ulsoy, A.G. (1994). Control input shaping for coordinate measuring machines. *Proceedigns of American Control Conference*, Baltimore, MD, **3**, pp. 2899-2903.

Jnifene, A. and Andrews, W. (2005). Experimental study on active vibration control of a single-link flexible manipulator using tools of fuzzy logic and neural networks. *IEEE Transactions on Instrumentation and Measurement*, **54**, (3), pp. 1200-1208.

Kaneshige, J. and Gundy-Burlet, K. (2001). Integrated neural flight and propulsion control system. *Proceedings of AIAA Guidance, Navigation, and Control Conference and Exhibit*, Montreal, Canada, August 6-9, pp. 2001-4386.

Kantner, M., Bodenheimer, B., Bendotti, P. and Murray, R. M. (1995). An experimental comparison of controllers for a vectored thrust, ducted fan engine. *Proceedings of the American Control Conference*, Seattle, Washington, USA, June 21-23, **3**, pp. 1956-1961.

Kapila, V., Tzes, A. and Yan, Q. (1999). Closed-loop input shaping for flexible structures using time-delay control. *Proceedings of The 38th Conference on Decision and Control*, Phoenix, Arizona, USA, pp. 1561-1566.

Karr, C. L. (1991). Design of an adaptive fuzzy logic controller using a genetic algorithm. *Proceedings of the 4th International Conference on Genetic Algorithms.*

Kim, B. S., Calise, A. J. (1997). Nonlinear flight control using neural networks. *Journal of Guidance, Control, and Dynamics*, **20**, (1), pp. 26-33.

Klir, G. J. (1995). *Fuzzy sets and fuzzy logic: Theory and applications*. Prentice Hall.

Kozak, K., Huey, J. and Singhose, W. (2003). Performance for input shaping. *Proceedings of IEEE Conference on Control Applications*, **2**, pp. 1227-1232.

Kristinsson, K. and Dumont, G. A. (1992). System identification and control using genetic algorithms. *IEEE Transactions on Systems, Man and Cybernetics*, **22**, (5), pp. 1032-1046.

Kumbla, K. K., and Jamshidi, M. (1994). Control of robotic manipulator using fuzzy logic. *Proceedings of The 3rd IEEE Conference on Fuzzy Systems*, **1**, pp. 518-523.

Lai, Y.-S., and Lin, J.-C. (2003). New hybrid fuzzy controller for direct torque control induction motor drives. *IEEE Transactions on Power Electronics*, **18**, (5), pp. 1211-1219.

Landis, H. K., Davis, J. M., Dabundo, C. and Keller, J. F. (1996). Advanced flight control research and development at Boeing Helicopter. In Tischler, M.B. (Ed.). *Advances in Aircraft Flight Control*, Taylor and Francis, London, pp. 103-141.

Lee, C. C. (1990). Fuzzy logic in control systems: Fuzzy logic controller- Part I&II. *IEEE Transactions on Systems, Man and Cybernetics*, **SMC-20**, (2), pp. 404-435.

Leitner, J., Calise, A. and Prasad, J. (1997). Analysis of adaptive neural networks for helicopter flight controls. *AIAA Journal of Guidance, Control, and Dynamics*, **20**, (5), pp. 972-979.

Leshno, M., Lin V. Y., Pinkus A. and Schocken, S. (1993). Multilayer feed forward networks with a non-polynomial activation function can approximate any function. *Neural Networks*, **6**, pp. 861-867.

Li, W. (1998). Design of a hybrid fuzzy logic proportional plus conventional integral-derivative controller. *IEEE Transactions on Fuzzy Systems*, **6**, (4), pp. 449-463.

Lin, C. L. and Su, H. W. (2000). Intelligent control theory in guidance and control system design: An overview. *Proceedings of the National Science Council, Rupublic of China ROC(A)*, **24**, (1), pp. 15-30.

Lin, C.-T. and Lee, C. S. G. (1996). *Neural Fuzzy Systems*, Prentice Hall.

Linkens, D. and Nyongesa, Y. (1996). Learning system in intelligent control: an appraisal of fuzzy, neural and genetic algorithm control applications. *IEE Proceedings of Control Theory Application*, **134**, (4), pp. 367-365.

Linse, D. and Stengel, R. (1992). Identification of aerodynamic coefficients using computational neural networks. *Proceedings of the AIAA Aerospace Design Conference*, Irvine, CA.

Liu, Q. and Wie, B. (1992). Robust time-optimal control of uncertain flexible spacecraft. *Journal of Guidance, Control, and Dynamics*, **15**, pp. 597-604.

Ljung, L. (1987). *System Identification: Theory for the user.* Prentice-Hall, Englewood Cliffs, NJ.

Ljung, L. and Sjöberg, J. (1992). A system identification perspective on neural networks. *Neural Networks for Signal Processing II-Proceedings of the IEEE-SP Workshop,* Helsingoer, Denmark, pp. 423-435.

Ljung, L. and Söderström, T. (1983). *Theory and practice of recursive identification.* MIT press, Cambridge, USA.

Long, M. E. (1999). Mars on earth, *National Geographic*, USA, July, pp. 36-51.

Lopez-Toribio, C. J., Patton, R. J. and Daley, S. (2000). Takagi–Sugeno Fuzzy Fault-Tolerant Control of an Induction Motor. *Neural Computing & Applications*, **9**, pp. 19-28.

Luo, F-L. and Unbehuen, R. (1997). *Applied neural networks for signal processing.* Cambridge University Press, Cambridge, New York.

Magee, D. P. and Book, W. J. (1995). Filtering micro-manipulator wrist commands to prevent flexible base motion. *Proceedings of American Control Conference*, Seattle, WA.

Makkonen, A. and Koivo, H. N. (1994). Fuzzy control of a nonlinear servomotor model. *3rd International Workshop on Advanced Motion Control*, Berkeley, CA, USA, pp. 833-841.

Mamdani, E. H. (1974). Application of fuzzy algorithms for control of simple dynamic plant. *Proceedings of IEEE*, **121**, (12), pp. 1585-1588.

Man, K. F., Tang, K. S. and Kwong, S. (1996). Genetic algorithms: concepts and applications. *IEEE Transactions on Industrial Electronics*. **43**, (5), pp. 519-533.

MathWorks Inc. (1995). *Fuzzy logic toolbox – User guide for use with MATLAB.*

Miller, W., Sutton, R. and Werbos, P. (1990). *Neural Networks for Control.* Cambridge MA, MIT Press.

Mistry, S. and Nair, S. (1994). Identification and control experiments using neural networks. *IEEE Control Systems*, **14**, (3), pp. 48-57.

Mistry, S., Chang, S. and Nair, S. (1996). Indirect control of a class of nonlinear dynamic systems. *IEEE Transactions on Neural Networks*, **7**, (4), pp. 1015-1023.

Mohamed, Z. and Tokhi, M. O. (2002). Vibration control of a single-link flexible manipulator using command shaping techniques. *Proceedings of IMechE-I: Journal of Systems and Control Engineering*, **216**, pp. 191-210.

Mohamed, Z. and Tokhi, M. O. (2003). Hybrid control schemes for input tracking and vibration suppression of a flexible manipulator. *Proceedings of IMechE-I: Journal of Systems and Control Engineering*, **217**, (1), pp. 23-34.

Morris, J. C., Van Nieuwstadt, M. J. and Pascale, B. (1994). Identification and control of a model helicopter in hover. *Proceedings of the American Control Conference*, Baltimore, 29 June – 1 July, **2**, pp.1238-1242.

Mudi, R. K. and Pal, N. R. (1999). A robust self-tuning scheme for PI and PD-type fuzzy controllers. *IEEE Transactions on Fuzzy Systems*, **7**, (1), pp. 2-16.

Murphy, B. R. and Watanabe, I. (1992). Digital shaping filters for reducing machine vibration. *IEEE Transactions on Robotics and Automation*, **8**, (2), pp. 285-289.

Napolitano, M. R., Casdorph, V., Neppach, C. and Naylor, S. (1996). On-line learning neural architectures and cross-correlation analysis for actuator failure detection and identification. *International Journal of Control*, **63**, (3), pp. 433-455.

Narendra, K. and Parthasarathy, K. (1990). Identification and control of dynamical systems using neural networks. *IEEE Transactions on Neural Networks*, **1**, (1), pp. 4-27.

Narendra, K. and Parthasarathy, K. (1991). Gradient Methods for The Optimization of Dynamical Systems Containing Neural Networks. *IEEE Transactions on Neural Networks*, **2**, (2), pp. 252-262.

Narendra, K. S. and Mukhopadhyay, S. (1997). Adaptive control using neutral networks and approximate models. *IEEE Transactions on Neural Networks*, **8**, pp. 475-485.

Nauck, D., Klawonn, F. and Kruse, R. (1992). Fuzzy sets, fuzzy controllers and neural networks. *Proceedings of Physiological Aspects of Regulation between Chaos and Reflex*, Potsdam, Germany.

Nørgaard, M., Ravn, O., Poulsen, N. K. and Hansen, L. K. (2000). *Neural Networks for Modelling and Control of Dynamic Systems*. Springer, London.

Oliveira, P., Sequeira, J. and Sentieiro, J. (1991). Selection of controller parameters using genetic algorithms. In Tzafestas, S. G. (Ed.). *Engineering Systems with Intelligence: Concepts, Tools, and Applications*, pp. 431–438, Dordrecht: Kluer.

Omatu, S., Khalid, M. and Yusof, R. (1996). *Neuro-control and its applications*. Springer, London.

Omerdic, E. and Roberts, G. N. (2003). A fuzzy track-keeping autopilot for ship steering. *Journal of Marine Engineering and Technology*, **A2**, pp. 23-35.

Onnen, C., Babuska, R., Kaymak, U., Sousa, J. M., Verbruggen, H. B. and Isermann, R. (1997). Genetic algorithms for optimization in predictive control. *Control Engineering Practice*, **5**, (10), pp. 1363–1372.

Pao, L. Y. and Singhose, W. E. (1995). A comparison of constant and variable amplitude command shaping techniques for vibration reduction. *Proceedings of The 4th IEEE Conference on Control Applications*, Albany, NY, pp. 875-881.

Pao, L. Y. and Lau, M. A. (2000). Robust input shaper control design for parameter variations in flexible structures. *Journal of Dynamic Systems, Measurement and Control*, **122**, pp. 63-70.

Pao, L. Y. (2000). Strategies for shaping commands in the control state of flexible structures. *Proceedings of Japan–USA–Vietnam Workshop on Research and*

Education in Systems, Computation and Control Engineering, Vietnam, pp. 309-318.

Parnichkum, M. and Ngaecharoenkul, C. (2000). Hybrid of fuzzy and PID in kinematics control of a pneumatic system. *IEEE International Conference on Industrial Electronics, Control and Instrumentation*, Nagoya, pp.1485-1490.

Passino, K. M. and Yurkovich, S. (1998). *Fuzzy Control*, Addison-Wesley.

Patterson, D. W. (1996). *Artificial Neural Networks: theory and applications*. Simon and Schuster, Singapore.

Pedrycz, W. (1991). Fuzzy modelling: fundamentals, construction, and evaluation. *Fuzzy Sets and Systems*, **41**, (1), pp. 1-15.

Porter, B. and Jones, A. H. (1992). Genetic tuning of digital PID controllers. *Electronics Letters*, **28**, (9), pp. 843-844.

Rappole, B. W., Singer, N. C. and Seering, W. P. (1994). Multiple-mode impulse shaping sequences for reducing residual vibrations. *23rd Biennial Mechanisms Conference*, Minneapolis, MN, DE-71, pp. 11-16.

Rattan, K. S., Feliu, V. and Brown, H. B. (1990). Tip position control of flexible arms using control law partitioning scheme. *Proceedings of the 1990 IEEE International Conference on Robotics and Automation (ICRA '90)*, May 1990, **3**, pp. 1803-1808, Honolulu, USA.

Richard, C. D. and Bishop, R. H. (2001). *Modern Control Systems*. 9th Ed., Upper Saddle River: Prentice Hall Inc., New Jersey.

Roberts, G. N., Sutton, R., Zirilli, A. and Tiano, A. (2003). Intelligent ship autopilots – A historical perspective. *Mechatronics Journal*, **13**, (10), pp. 1091-1103.

Roth, G. and Levine, M. D. (1994). Geometric primitive extraction using a genetic algorithm. *IEEE Transaction on Pattern Analysis and Machine Intelligence*, **16**, pp. 901-905.

Rumelhart, D. and McClelland, J. (1986). *Parallel distributed processing I.* Cambridge MA: MIT Press.

Rumelhart, D. E., Hilton G. E. and Williams, R. J. (1986). Learning representations by back-propagating errors. *Nature*, **323**, pp. 533-536.

Rysdyk, R. and Calise, A. (1998). Fault tolerant flight control via adaptive neural network augmentation. *AIAA Guidance, Navigation and Control Conference and Exhibit AIAA 98-4483*, 10-12 August, pp. 1722-1728, Boston, MA, USA

Rysdyk, R., Calise, A. and Chen, R. (1997). Nonlinear adaptive control of tiltrotor aircraft using neural networks. *Proceedings of AIAA/SAE World Aviation Congress*, Anaheim, CA.

Sahinkaya, M. N. (2001). Input shaping for vibration-free positioning of flexible systems. *Proceedings of IMechE-I: Journal of Systems and Control Engineering*, **215**, (1), pp. 467-481.

Sanner, R and Slotine, J. (1992). Gaussian networks for direct adaptive control. *IEEE Transactions on Neural Networks*, **3**, (6), pp. 837-863.

Sastry, P. S., Santharam, G. and Unnikrishnan, K. P. (1994). Memory neuron networks for identification and control of dynamic systems. *IEEE Transaction on Neural Networks*, **5**, (2), pp. 306-319.

Seth, N., Rattan, K. S. and Brandstetter, R. W. (1993). Vibration control of a coordinate measuring machine. *IEEE Conference on Control Applications*, Dayton, OH, pp. 368-373.

Shaheed, M. H. (2000). *Neural and genetic modelling, control and real-time finite element simulation of flexible manipulators.* PhD thesis, Department of Automatic Control and System Engineering, The University of Sheffield, Sheffield, UK.

Shaheed, M. H. and Tokhi, M.O. (2002). Dynamic modelling of a single-link flexible manipulator: parametric and non-parametric approaches. *Robotica*, **20**, pp. 93–109.

Shan, J., Liu, H.-T. and Sun, D. (2005). Modified input shaping for a rotating single-link flexible manipulator. *Journal of Sound and Vibration*, **285**, pp. 187-207.

Shaw, I. S. (1998). *Fuzzy control of industrial systems: Theory and applications.* Kluwer Academic Publishers.

Shchuka, A. and Goldenberg, A. A. (1989). Tip control of a single-link flexible arm using feedforward technique. *Mechanical Machine Theory*, **24**, pp. 439-455.

Shi, Y., Eberhart, R. and Chen, Y. (1999). Implementation of evolutionary fuzzy systems. *IEEE Transactions on Fuzzy Systems*, **7**, (2), pp. 109-119.

Siddique, M. N. H. (2002). *Intelligent control of flexible-link manipulator system.* PhD Thesis, Department of Automatic Control and Systems Engineering, The University of Sheffield, UK.

Simoes, M. G. and Franceschetti, N. N. (1999). Fuzzy optimisation based control of a solar array system. *IEE Proceedings - Electric Power Applications*, **146**, (5), pp. 552-558.

Simoes, M. G. and Friedhofer, M. (1997). An implementation methodology of a fuzzy based decision support algorithm. *International Journal of Knowledge-Based Intelligent Engineering Systems*, **1**, (4), pp. 267-275.

Simpson, P. K., (1990). *Artificial Neural Systems: Foundations, Paradigms, Applications, and Implementations.* Pergamon Press, New York.

Singer, N. C. and Seering, W. P. (1990). Preshaping command inputs to reduce system vibration. *ASME Journal on Dynamic Systems, Measurement and Control*, **112**, (1), pp. 76-82.

Singer, N. C. and Seering, W. P. (1992). An extension of command shaping methods for controlling residual vibration using frequency sampling. *IEEE International Conference on Robotics and Automation*, Nice, France, **1**, pp. 800-805.

Singer, N., Singhose, W. and Kriikku, E. (1997). An input shaping controller enabling cranes to move without sway. *ANS 7th Topical Meeting on Robotics and Remote Systems*, Augusta, GE.

Singh, T. and Vadali, S. R. (1995). Robust time-delay control of multimode systems. *International Journal of Control*, **62**, pp. 1319-1339.

Singhose, W. and Pao, L. (1997). A comparison of input shaping and time optimal flexible body control. *Journal of Control Engineering Practice*, **5**, (4), pp. 459-467.

Singhose, W. E., Singer, N. C. and Seering, W. P. (1995). Comparison of command shaping methods for reducing residual vibration. *Proceedings of European Control Conference*, Rome, pp. 1126-1131.

Singhose, W., Derezinski, S. and Singer, N. (1996a). Extra-insensitive input shapers for controlling flexible spacecraft. *Journal of Guidance, Control, and Dynamics*, **19**, pp. 385-391.

Singhose, W., Seering, W. and Singer, N. (1994). Residual vibration reduction using vector diagrams to generate shaped inputs. *Journal of Mechanical Design*, **116**, pp. 654-659.

Singhose, W., Singer, N. and Seering, W. (1996b). Improving repeatability of coordinate measuring machines with shaped command signals. *Precision Engineering*, **18**, pp. 138-146.

Sivashankar, N., Kaminer, I. and Kuechenmeister, D. (1994). Design, analysis and hardware-in-the-loop simulation of MIMO controller for a VTOL unmanned aerial vehicle using synthesis. *Proceedings of the American Control Conference*, 29 June – 1 July 1994, Baltimoore, Maryland, USA, **3**, pp. 2506-2510.

Smith, J. Y., Kozak, K. and Singhose, W. E. (2002). Input shaping for a simple nonlinear system. *Proceedings of the American Control Conference*, Anchorage, AK, pp. 821-826.

Smith, O. J. M. (1958). *Feedback Control Systems*. McGraw-Hill, pp. 331-345.

Smuts, J. (2002). PID explained. *Canadian Process Equipment and Control News*.

Söderström, T. and Stoica, P. (1989). *System identification*. New York; London: Prentice Hall.

Song, Y. H. and Johns, A. T. (1999). Applications of fuzzy logic in power systems - Part 3: Example applications. *Power Engineering Journal*, **13**, (2), pp. 97-103.

Sowerby, N. W. A., Omerdic, E. and Roberts, G. N. (2005). System identification and fault accommodation for thruster propelled UUVs. *IMarEST Proceedings: Journal of Marine Engineering and Technology*, **A7**, pp. 41-50.

Steck, J. and Rokhasz, K. (1992). Use of neural networks in control of high alpha maneuvers. *30th AIAA Aerospace Sciences Meeting and Exhibit*, Reno, NV.

Steinberg M., (1994). An initial assessment of neural network and fuzzy logic technology for flight control systems. *Proceedings of the American Control Conference*, pp. 173-177.

Sugeno, M. (Ed.) (1985). *Industrial Applications of Fuzzy Control*. Elsevier Science, North-Holland, Amsterdam.

Sze, T. L. (1995). *System identification using radial basis neural networks*. PhD thesis, Department of Automatic Control and Systems Engineering, The University of Sheffield, Sheffield, UK.

Teague, E. H., How, J. P. and Parkinson, B. W. (1998). Control of flexible structures using GPS: methods and experimental results. *Journal of Guidance, Control, and Dynamics*, **21**, (5), pp.673-683.

Tokhi, M. O. and Azad, A. K. M. (1995). Active vibration suppression of flexible manipulator systems: open-loop control methods. *International Journal of Active Control*, **1**, (1), pp. 15-43.

Tokhi, M. O. and Azad, A. K. M. (1996). Control of flexible manipulator systems. *Proceedings of IMechE-I: Journal of Systems and Control Engineering*, **210**, pp. 113-130.

Tokhi, M. O. and Leitch, R. R. (1992). *Active noise control.* Clarendon Press, Oxford.

Tokhi, M. O. and Poerwanto, H. (1996). Control of vibration of flexible manipulators using filtered command inputs. *Proceedings of International Congress on Sound and Vibration*, St. Petersburg, Russia, pp. 1019-1026.

Tokhi, M. O., Shaheed, M. H. and Poerwanto, H. (2000). Adaptive neuro-inverse-dynamic active vibration control of a flexible manipulator. *Proceedings of the Mechatronics-2000,* Atlanta, USA.

Tokhi, M. O. and Veres, S. M. (2002). *Active sound and vibration control: Theory and applications*. Institution of Electrical Engineers, London.

Troudet, T., Garg, S. and Merrill, W. (1991). Neural network application to aircraft control system design. *Proceedings of AIAA on Guidance, Navigation and Control Conference*, New Orleans, LA, pp. 993-1009.

Tuttle, T. D. and Seering, W. P. (1996). Vibration reduction in flexible space structures using input shaping on MACE: Mission results. *IFAC World Congress*. San Francisco, CA.

Van Nieuwstadt, M. J. and Murray, R. M. (1998). Rapid hover-to-forward-flight transitions for a thrust-vectored aircraft. *AIAA Journal of Guidance, Control, and Dynamics,* **21**, pp. 93-100.

Vandersteen, G., Rolain, Y., Schoukens, J. and Pintelon, R. (1996). On the use of system identification for accurate parametric modelling of nonlinear systems using noisy measurements. *IEEE Transactions on Instrumentation and Measurement*, **45**, (2), pp. 605-609.

Verbruggen, H. B. and Bruijin, P. M. (1997). Fuzzy control and conventional control: what is (and can be) the real contribution of fuzzy systems? *Fuzzy Sets and Systems*, **90**, pp. 151-160.

Visioli, A. (2001). Tuning of PID controllers with fuzzy logic. *IEEE Proceedings - Control Theory Applications*, **148**, (1), pp. 1-8.

Vlachos, C., Williams, D. and Gomm, J. B. (1999). Genetic approach to decentralised PI controller tuning for multivariable processes. *IEE Proceedings of Control Theory and Applications*, **146**, (1), pp. 58-64.

Von Altrock, C. (1995). *Fuzzy logic and neuro-fuzzy applications explained.* Prentice Hall, Upper Saddle River, NJ.

Wang, P. and Kowk, D. P. (1994). Optimal design of PID process controllers based on genetic algorithms. *Control Engineering Practice*, **2**, (4), pp. 641-648.

Warwick, G. (2000). Agents for change. *Flight International*, UK, July 2000, pp. 151-153.

Wells, R. L. and Schueller, J. K. (1990). Feedforward and feedback control of a flexible manipulator. *IEEE Control System Magazine*, **10**, pp. 9-15.

Werbos, P. (1995). Neural networks and flight control: Overview of capabilities and emerging applications. *Proceedings of the AIAA Guidance, Navigation, and Control Conference*, pp. 912-919.

Werner, H. and Meister, T. (1999). Robust control of a laboratory aircraft model via fast output sampling. *Control Engineering Practice,* **7**, pp. 305-313.

Whitley, D. (1994). A genetic algorithm tutorial. *Statistics and Computing*, **4**, pp. 65-85.

Widrow, B. and Laher, M. (1990). 30 years of adaptive neural networks: Perceptron, madaline, and backpropagation. *Proceedings of IEEE*, **78**, (9), pp. 1415-1441.

Zadeh, L. A. (1965). Fuzzy sets. *Information and Control*, **8**, pp. 338-353.

Zadeh, L. A. (1968). Fuzzy algorithms. *Information and Control*, **12**, pp. 94-102.

Zadeh, L. A. (1973). Outline of a new approach to the analysis of complex systems and decision process. *IEEE Transaction on Systems, Man and Cybernetics (SMC)*, **3**, pp. 28-44.